

**STATIN FOR THE PREVENTION OF OSTEOARTHRITIS – A CLINICAL
COHORT STUDY AND ITS CELLULAR MECHANISMS**

by

Mengxi Lv

A dissertation submitted to the Faculty of the University of Delaware in partial fulfillment of the requirements for the degree of Doctor of Philosophy in Bioinformatics and Systems Biology

Spring 2019

© 2019 Mengxi Lv
All Rights Reserved

**STATIN FOR THE PREVENTION OF OSTEOARTHRITIS – A CLINICAL
COHORT STUDY AND ITS CELLULAR MECHANISMS**

by

Mengxi Lv

Approved: _____
Cathy H. Wu, Ph.D.
Chair of the Center for Bioinformatics & Computational Biology

Approved: _____
Levi T. Thompson, Ph.D.
Dean of the College of Engineering

Approved: _____
Douglas J. Doren, Ph.D.
Interim Vice Provost for Graduate and Professional Education

I certify that I have read this dissertation and that in my opinion it meets the academic and professional standard required by the University as a dissertation for the degree of Doctor of Philosophy.

Signed:

X. Lucas Lu, Ph.D.
Professor in charge of dissertation

I certify that I have read this dissertation and that in my opinion it meets the academic and professional standard required by the University as a dissertation for the degree of Doctor of Philosophy.

Signed:

Cathy H. Wu, Ph.D.
Member of dissertation committee

I certify that I have read this dissertation and that in my opinion it meets the academic and professional standard required by the University as a dissertation for the degree of Doctor of Philosophy.

Signed:

Liyun Wang, Ph.D.
Member of dissertation committee

I certify that I have read this dissertation and that in my opinion it meets the academic and professional standard required by the University as a dissertation for the degree of Doctor of Philosophy.

Signed:

Shawn W. Polson, Ph.D.
Member of dissertation committee

I certify that I have read this dissertation and that in my opinion it meets the academic and professional standard required by the University as a dissertation for the degree of Doctor of Philosophy.

Signed:

Zugui Zhang, Ph.D.
Member of dissertation committee

ACKNOWLEDGMENTS

First and foremost, I would like to sincerely thank my esteemed mentor, Dr. X. Lucas Lu. I always feel grateful to be a student of Dr. Lu. Working together with Lucas during my past five-year Ph.D. study, I deeply appreciate his tireless guidance, support, and encouragement. Under his advisory, I have avoided many potential pitfalls in my research projects. With a systematic understanding of cartilage bioengineering, he offers me great guidance in stepping into the area of orthopedic research. As a result, so far we have more than 20 abstracts presented as poster or podium in academic conferences, and 6 journal manuscripts published or under review. I could not have accomplished this thesis work without his guidance and support. Most importantly, I learned from Lucas on how to be a good scientist – think creatively, plan carefully, and cooperate openly with others.

I would also like to thank my committee members, Drs. Zugui Zhang, Cathy H. Wu, Liyun Wang and Shawn W. Polson. They have been the model roles of my life. Their life stories motivate me to work diligently; and their advice on my career development inspires me to think openly. I am also very grateful for their continuous support and intellectual advice throughout my Ph.D. research.

I thank my fellow colleagues, Drs. Yilu Zhou, Shongshan Fan, Tong Li, and Miri Park. Without them, I would not have been achieved so much during my time in this lab. I also would like to acknowledge the undergraduates Tiange Zhang, Kalani Picho, Raina Coflin, and Olivia Smith for their excellent work on data processing. In

addition, I am grateful for lab members from Dr. Wang's lab: Shaopeng Pei and Ashutosh Parajuli for their generous help with my experiments.

Finally, I would like to acknowledge my beloved parents and family for their unconditional love. I want to thank my husband Mr. Xingyu Chen, for his accompany and support. Without him, I couldn't achieve these.

TABLE OF CONTENTS

LIST OF TABLES	xi
LIST OF FIGURES	xii
ABSTRACT	xix

Chapter

1	LITERATURE REVIEW	1
1.1	Articular Cartilage	1
1.1.1	Ultra-structure of Articular Cartilage	2
1.1.2	Chondrocytes	4
1.1.3	Extracellular Matrix.....	7
1.1.3.1	Water	8
1.1.3.2	Collagens	8
1.1.3.3	Proteoglycans	9
1.1.3.4	Non-collagenous Proteins and Glycoproteins	10
1.2	Osteoarthritis	11
1.2.1	Posttraumatic OA Development Stages	12
1.2.2	Phenotypic Shift of Chondrocytes in Posttraumatic Cartilage	14
1.2.3	Signaling Molecules in the Pathogenesis of OA	17
1.2.3.1	Inflammatory Cytokines	18
1.2.3.2	ECM-degrading Enzymes	20
1.2.3.3	Rho GTPase Family Proteins	22
1.2.4	Existing and Potential Preventions and Treatments of PTOA	25
1.2.4.1	Current Treatments for PTOA Patients	25
1.2.4.2	Emerging Pharmacological Treatment Options	27
1.3	Bisphosphonate and Statins	29

2	THE ROLE OF CALCIUM SIGNALING IN MECHANOTRANSDUCTION OF IN SITU CHONDROCYTES UNDER COMPRESSEION.....	33
2.1	Abstract.....	34
2.2	Introduction	35
2.3	Materials and Methods	37
2.3.1	Cartilage Explant.....	37
2.3.2	Mechanical Loading and Calcium Imaging	38
2.3.3	Calcium Signaling Pathways	40
2.3.4	Data Analysis and Statistics	41
2.4	Results	42
2.4.1	Mechanical Loading Enhanced $[Ca^{2+}]_i$ Signaling	42
2.4.2	Extracellular Calcium Influx	45
2.4.3	Roles of ER Calcium Store.....	46
2.4.4	Ion Channels on Plasma Membrane	47
2.5	Discussion.....	49
3	IDENTIFICATION OF CHONDROCYTE GENES AND SIGNALING PATHWAYS IN RESPONSE TO ACUTE JOINT INFLAMMATION.....	57
3.1	Abstract.....	58
3.2	Introduction	59
3.3	Materials and Methods	60
3.3.1	Effects of IL-1 β on Cartilage Matrix and Chondrocytes.....	60
3.3.2	RNA Sequencing Analysis and qRT-PCR of IL-1 β Treated Cartilage	62
3.3.3	Calcium Signaling of Chondrocytes.....	64
3.3.4	Statistical Analysis	64
3.4	Results	65
3.4.1	Cartilage Degradation Induced by IL-1 β	65
3.4.2	Differentially Expressed Genes (DEGs)	68
3.4.3	Matrix Protein Related DEGs.....	71
3.4.4	Enrichment Analysis of Gene Ontology and Pathway	73
3.4.5	Intracellular Calcium Signaling.....	77
3.5	Discussion.....	83

4	STATIN PROTECTS THE CARTILAGE FROM INFLAMMATORY ATTACK BY INHIBITING THE RHO-GTPASES SIGNALING PATHWAY IN CHONDROCYTES	89
4.1	Introduction	89
4.2	Materials and Methods	92
4.2.1	Cartilage Explant Culture	92
4.2.2	Biochemical Assay and Mechanical Test of Cartilage Explant ..	93
4.2.3	RNA sequencing.....	94
4.2.4	Morphology Evaluation of in-situ Chondrocyte.....	95
4.3	Results	95
4.3.1	Statins Protect Cartilage Explant from Inflammatory Attack	95
4.3.2	Protective Effects of Statin is Dependent on Rho Activities.....	99
4.3.3	Statin Can Directly Regulate the Expression of Rho GTPase-related Genes in Chondrocytes	103
4.3.4	Another Mevalonate Inhibitor, Bisphosphonate, Presented Similar Chondro-protective Effects as Statins Did	106
4.4	Discussion.....	109
5	STATIN USE AND REDUCED RISK OF OSTEOARTHRITIS FOR DELAWARE POPULATION: A RETROSPECTIVE COHORT STUDY WITH PROPENSITY SCORE-MATCHING.....	117
5.1	Introduction	117
5.2	Materials and Methods	119
5.2.1	Cohort Population.....	119
5.2.2	Definition of OA Case and Statin User	120
5.2.3	Baseline Covariates	120
5.2.4	Propensity Score Estimation.....	121
5.2.5	Statistical Analysis:	122
5.3	Results	123
5.3.1	Cohort Population.....	123
5.3.2	Propensity Score Methods to Reduce Confounding Effects	127
5.3.3	Survival Analysis by Cox Proportional Hazard Model	128
5.3.4	Association between Statin use and Other Common Joint Diseases	131
5.3.5	Artificial Intelligence for Cohort Analysis.....	132

5.4	Discussion.....	136
6	SUMMARY AND FUTURE WORK	141
6.1	Summary.....	141
6.2	Future Directions	143
	REFERENCES	145
Appendix		
A	PERMISSION FOR USING COPYRIGHTED MATERIALS	167

LIST OF TABLES

Table 2.1	Number of the Total Cartilage Explants and Chondrocytes Analyzed in $[Ca^{2+}]_i$ Signaling for Seven Pathways	42
Table 3.1	Pathway enrichment analysis identified 20 child pathways (sub level 2 to 3) that are significantly changed by IL-1 β . The child pathways of FDR < 0.1 were selected and grouped together if belonging to one parent (top-level, left column) pathway.	72
Table 3.2	Summary of key genes involved in six calcium-related pathways. The “-” represents downregulation, and “+” represents upregulation. The RPKM was calculated to assess the abundance of transcript of each gene, which is correlated positively to the gene expression level.	77
Table 3.3	Major catabolic and anabolic genes in DEGs, including MMP- and ADAMTS-, collagen-, proteoglycan-family genes. The “-” in front of the fold change value represents downregulation of expression, and “+” represents upregulation of expression after IL-1 β treatment.	82
Table 4.1	Summary of statins’ effects on the cartilage: clinical cohort studies. ...	115
Table 4.2	Summary of statins’ effects on the cartilage: animal studies.	116
Table 5.1	The baseline characteristics between statin users and non-users for raw and propensity score matched cohort. * office visit denotes total number of hospital office visits in 10 years, and drug count denotes total number of prescribed drug in 10 years.	134
Table 5.2	Association between statin initiation and OA occurrence according to different populations.	135

LIST OF FIGURES

- Figure 1.1 Articular cartilage structure. (a) H&E staining of bovine cartilage explant cultured in our Cartilage Bioengineering Lab, at University of Delaware. Schematic representation of (b) chondrocytes morphology, (c) Collagen organization, and (d) matrix composition of hyaline cartilage. SZ, superficial zone; MZ, middle zone; DZ, deep zone; CZ, calcified zone; SB, subchondral bone. Picture is used with permission from *J Cytochem Biochem*⁷. 4
- Figure 1.2 A schematic drawing of the calcium signaling pathways in chondrocytes. The cytoplasm calcium can exchange with extracellular calcium source in medium and intracellular calcium store in ER. Voltage-gated calcium channels, P2 receptor, TRPV4, mechanosensitive ion channels can transfer Ca²⁺ between intra- and extracellular environments. The calcium store in ER can be released by activation of IP3 receptors on ER membrane. Picture generated by M. Lv in Dr. X. Lucas Lu's lab. 7
- Figure 1.3 Extracellular matrix of cartilage. Three classes of proteins exist in articular cartilage: collagens, proteoglycans, other noncollagenous proteins, and the smaller proteoglycans. The interaction between highly negatively charged cartilage proteoglycans and typed II collagen fibrils is responsible for the compressive and tensile strength of the tissue, which resists load *in vivo*. This figure is used from *R&D Systems Inc*³⁸ with permission. 11
- Figure 1.4 Timeline of the pathogenic processes following joint injury. After the immediate consequences of injury, mechanobiological, molecular and cellular changes in cartilage and other joint structures slowly progress into an acute post-traumatic phase. This acute phase can spontaneously resolve after a couple of months or persist through a long latency period without clinically symptom. The chronic phase last years and may eventually lead to chronic OA. Picture was regenerated by M Lv with permission from *BMJ*⁴⁷. 14

Figure 1.5	Molecular mediators involved in OA-related hypertrophic-like changes of chondrocytes. During hypertrophy-like shift, a number of transcription factors regulate the differentiation from a normal articular chondrocyte to a terminal differentiated chondrocyte. Meanwhile, chondrocytes produce many proteins that are regulating cartilage ECM remodeling and calcification. Picture is obtained with permission from <i>J Osteoarthritis and Cartilage</i> ⁵³	17
Figure 1.6	Schematic representation of the Mevalonate pathway. The inhibitory effects of statins and Nitrogen-containing Bisphosphonates (N-BPs) are indicated.	32
Figure 2.1	A bidirectional microscopy loading device for cartilage explant. (A) A schematic illustration of the device. Cartilage sample is placed in an imaging chamber and submerged in medium. Two parallel loading platens on both sides of the sample are driven by two coaxial motors, respectively. Load cell can record the responding force from cartilage. All components are fixed on a based plate, which itself can be mounted on the X-Y stage of a microscope. (B) A picture of the loading device mounted on a confocal microscope (Zeiss LSM510). (C) Loading profile during the calcium imaging of the cartilage sample. Tissue was compressed at 0.2 $\mu\text{m/s}$ for 1,000 seconds (~10% compression of the cartilage explant). (D) A typical force response curve of the cartilage sample under the compressive loading. Due to the slow loading rate, increase of responding force is close to a linear curve.	39
Figure 2.2	[Ca ²⁺] _i responses of <i>in situ</i> chondrocytes in a loaded cartilage explant. (A) Calcium images of the chondrocytes stained with Fluo 8 AM at five different time points taken by confocal microscope. White arrows highlight cells with oscillating [Ca ²⁺] _i concentration. Some cells showed multiple calcium peaks. Scales bars = 50 μm . (B) A typical [Ca ²⁺] _i transient of chondrocyte in cartilage. The characteristic temporal parameters are defined. t ₁ denotes the time from baseline to the maximum value of the peak. t ₂ is the time from peak value to the 50% relaxation. t ₃ is the time interval between two neighboring peaks..	44

- Figure 2.3 Comparison of $[Ca^{2+}]_i$ signaling of *in situ* chondrocytes in the loaded and unloaded cartilage explants. (A) Typical $[Ca^{2+}]_i$ intensity curves of chondrocytes in 1,000 seconds from the loaded and unloaded groups. Each curve represents the calcium transient of a single cell. A large number of chondrocytes can release multiple $[Ca^{2+}]_i$ peaks in 1,000 seconds. (B) Percentage of chondrocytes showed $[Ca^{2+}]_i$ peaks in loaded cartilage is significantly higher than the unloaded sample, while the average number of peaks in each responsive cell had no difference. Temporal parameters of $[Ca^{2+}]_i$ peaks, including time to reach a peak, peak relaxation time, and time between two peaks are compared between two groups. *: P value < 0.05; and **: P value < 0.01. 45
- Figure 2.4 Role of extracellular Ca^{2+} source in the $[Ca^{2+}]_i$ responses of *in situ* chondrocytes in loaded cartilage explants. Few chondrocytes can have $[Ca^{2+}]_i$ transients after the depletion of extracellular Ca^{2+} in the medium. No responsive cells can have multiple $[Ca^{2+}]_i$ peaks (time between peaks not showing). Time to reach a peak and peak relaxation time of responsive cells have no difference between the two groups. ***: P value < 0.001. 46
- Figure 2.5 Role of P2 receptors and intracellular ER calcium release in the $[Ca^{2+}]_i$ responses of *in situ* chondrocytes. Cartilage explants are loaded in both control and chemical treated groups. (A) $[Ca^{2+}]_i$ responses after the ER calcium store was depleted by thapsigargin. (B) $[Ca^{2+}]_i$ responses with inhibited PLC-IP₃ activities by neomycin. (C) $[Ca^{2+}]_i$ responses with the presence of PPADS, a P2 receptor inhibitor. *: P value < 0.05; and **: P value < 0.01; and ***: P value < 0.001. 47
- Figure 2.6 Role of three nonselective ion channels in the $[Ca^{2+}]_i$ responses of *in situ* chondrocytes. Cartilage explants are loaded in both control and chemical treated groups. (A) $[Ca^{2+}]_i$ responses with the mechanosensitive channels blocked by gadolinium. (B) $[Ca^{2+}]_i$ responses with the T-type VGCCs blocked by NNC55-0396. (C) $[Ca^{2+}]_i$ responses with the TRPV4 channel blocked by GSK205. *: P value ≤ 0.05; and **: P value ≤ 0.01; and ***: P value < 0.001. 49

Figure 3.1 Effects of IL-1 β during the long-term *in vitro* culture of cartilage explants. (a) Schematic diagram of experimental design. Cylindrical cartilage explants (diameter = 3 mm, thickness = 2 mm) were harvested from the central region of femoral condyle head of bovine knee joint using a biopsy punch. (b) Accumulative loss of sGAG content from cartilage explants during 8-day treatment of different doses of IL-1 β . The accumulative sGAG loss was defined as the total sGAG released into the culture medium divided by total sGAG content in explant and culture medium. (c) Accumulative collagen loss from cartilage explant in 24-day treatment of 1 ng/mL IL-1 β . (d) The total sGAG content of cartilage explants, which includes the sGAG released into medium (white bar) and sGAG left in explants (grey bar) at the end of 8-day culture. (e) The total collagen content and distribution of collagen in medium and explant after 24-day culture. (f) Safranin O staining of the superficial zone of cartilage explant after 2- and 8-day culture. Scale bar = 200 μ m. (g) Mechanical properties of cartilage explants after 8-day IL-1 β treatment, including equilibrium Young's modulus, dynamic modulus, and permeability. All data were shown as mean \pm 95% confidence intervals. *: vs control, $p < 0.001$ if otherwise marked. 68

Figure 3.2 Summary statistics of RNA sequencing data. (a) Unsupervised hierarchical clustering was performed for differentially expressed genes (absolute value of fold change > 2 and FDR < 0.05) in the IL-1 β treated cartilage explants. (b) Distribution of gene expression fold changes according to log₂ transformation. (c) Validation of RNAseq results with qRT-PCR. Seven selected genes were tested and correlated with the Pearson's correlation analysis. (d) Enrichment analysis of the protein family classification and Gene Ontology annotations in terms of (e) molecular functions and (f) biological processes..... 70

Figure 3.3 Chondrocyte swelling and proliferation. (a) H&E staining of cartilage explants after 2- and 8-day IL-1 β treatment. Cell swelling, also termed as fattening, and proliferation can be observed after 8-day IL-1 β culture. Scale bar = 200 μ m. (b) Cell volume of chondrocytes in cartilage explants measured by 3D confocal imaging. Scale bar = 30 μ m. (c) Cell proliferation rate determined by MTT assay. (d) Visualization of Ras superfamily signaling pathway regulated by IL-1 β -treatment. Flowchart was plotted using RNAseq data in Pathview (version 3.6). Each node represented a gene, and the associated node color represented the expression changes in log2 ratios. For better readability, multiple genes with similar or redundant functional roles were pooled together as a single node. Absolute value of the maximum of expression changes of these genes was reflected by the node color. All data were shown as mean \pm 95% CI. 75

Figure 3.4 Calcium signaling of chondrocytes in cartilage explants. (a) Visualization of calcium signaling pathway regulated by IL-1 β . (b) Illustration of calcium signaling. Half cartilage explant was dyed with fluorescent indicator and imaged on a confocal microscope for 15 minutes. Due to the fluctuation of [Ca²⁺]_i concentration, image intensity of chondrocyte oscillates in recorded video. (c) Definition of spatiotemporal parameters of [Ca²⁺]_i peaks. (d) Representative [Ca²⁺]_i curves of *in situ* chondrocytes from the control group and IL-1 β treated group. (e) Parameters of [Ca²⁺]_i peaks, including the average number of [Ca²⁺]_i peaks, magnitude of peaks, time to reach a peak, and time between neighboring peaks. All data were shown as mean \pm 95% CI. *: vs control, p < 0.05 if otherwise marked. 81

Figure 4.1 Protective effects of statins on IL-1 β treated cartilage explant. (a) cartilage explant harvest and *in vitro* culture. (b) 1ng/mL IL-1 β was supplemented into the culture medium to mimic a moderate inflammatory attack to cartilage explant. (c) Simvastatin treatment preserved the mechanical function of cartilage explant with the presence of IL-1 β . All three types of statins prevented the (e) loss of GAG and (f) loss of collagen contents from cartilage explants during *in vitro* culture. IL-1 β -induced collagen loss was completely abolished by statins treatment. (g) Simvastatin treatment mainly suppressed the GAG loss from the surface of cartilage explant (Safranin O staining) and the phenotypic shift of chondrocytes (H&E staining). Scale bar = 200 μ m. Statin prevents chondrocyte phenotypic shift in terms of (g) cell volume and (h) cell proliferation rate by MTT. All data were shown as mean \pm 95% CI. * vs IL-1 β : p value < 0.01, and ** vs IL-1 β : p value < 0.001. 99

- Figure 4.2. Chondro-protective effects of statins are related to the inhibition of Rho activities. (a) Illustration of mevalonate pathway and its related inhibitors. (b) A mevalonate pathway derivative GGOH which is required for Rho GTPase proteins geranylgeranylation abolished the chondro-protective effects of statin. (c) A downstream mevalonate inhibitor GGTI298 which can inhibit the geranylgeranylated Rho GTPase proteins showed similar protective effects as statin. (d) Specific inhibitors of Rho GTPases also prevented the IL-1 β -induced collagen loss. (e) Illustration of the regulatory role of Rho GTPases in cytoskeleton and gene expression. * vs IL-1 β : p value < 0.01, ** vs IL-1 β : p value < 0.001; and \$ vs IL-1 β + simvastatin: p value < 0.01.. 102
- Figure 4.3 RNA sequencing analysis. (a) Total number of Differentially Expressed Genes (DEGs, absolute fold change > 1.5 and FDR < 0.05). (b) Expression changes of well-studied anabolic genes and catabolic genes in chondrocytes treated by IL-1 β + simvastatin compared to that of IL-1 β alone group. (c) Enrichment analysis using DEGs for identifying significantly altered pathways (FDR < 0.05). (d) Overrepresented biological processes in the simvastatin-treated cartilage (FDR < 0.05). The pathways denoted by red star are involved in the regulation of chondrocytes phenotype stability..... 106
- Figure 4.4 Zoledronic acid, another mevalonate inhibitor, presented similar protective effects on cartilage explants as statins did. (a) Osteoclasts mediated bone resorption is inhibited by bisphosphonates and undergo apoptosis. ZA treatment suppressed the (b) loss of GAG and (c) catabolic gene expression of IL-1 β -treated cartilage explant. (d) Safranin O histological and immune-histological staining of sGAG and type II collagen respectively. (e) Mechanical property of cartilage explant was preserved by ZA treatment after 8-day culture. (f) Serum damaged cartilage explant model. ZA treatment rescued the cartilage explant in terms of (g) ECM content and (h) mechanical property. Co-treatment of ZA and GGOH overrides the beneficial effects of ZA. All data were shown as mean \pm 95% CI. * vs IL-1 β : p value < 0.01, ** vs IL-1 β : p value < 0.001; and \$ vs IL-1 β + simvastatin: p value < 0.01.. 109
- Figure 4.5 Statins and bisphosphonates inhibit the Rho activities in chondrocytes and prevent the aberrant phenotypic shift of chondrocytes under catabolic stimuli. 114

Figure 5.1	The cohort information. (a) Collecting of patients with CVD during the observation window from January 1, 2008 to December 31, 2015. (b) Demographic information including age, gender, CVD type, and race. (C) The geographic information. (d) The definition of OA case and censored patients within our observation winder.	124
Figure 5.2	The baseline characteristics of 53,452 patients in the raw cohort. The baseline difference between statin-users and non-users on (a) The continuous variates, and (b) the categorical variates.....	126
Figure 5.3	The propensity score matching process. (a) The matching criterial. (b) The propensity score distribution of statin-users and non-users before and after matching. (c) The Standardized Mean Difference between statin-users and non-users.	128
Figure 5.4	Cox proportional hazard model analysis. (a) Correlation of the covariates for the raw and propensity score-matched data. Time to OA for the (b) propensity score-matched and (c) raw patients. (d) The hazard ratio for OA occurrence in statin users compared to non-users.	130
Figure 5.5	Logistic regression analysis. (a) Top eight common musculoskeletal disorders in the cohort of our study. (b) The odds ratio for specific joint disease in statin user population compared to the non-user population.....	131
Figure 5.6	The Artificial Intelligence model. (a) The artificial neuron network (ANN) with the optimized number of nodes as 10 and the decay as 15. (b) The ordered importance score of all covariates. (c) Correlation between the importance score determined by ANN and the coefficient determined by logistic regression model.....	134

ABSTRACT

Osteoarthritis, also known as OA, is a leading cause of disability in United States, which affects over 30 million adults and leads to more than \$128 billion financial burden. One of the important factors that can increase the risk of OA is traumatic joint injury, *e.g.*, meniscus or ligament tears in the knee joint, commonly affecting younger population including athletes and military service. Traumatic events often cause physical injury of cartilage and render the chondrocytes under OA-inducing stimulations, such as inflammation, bleeding, and altered loading patterns. These stimulations significantly accelerate the OA development, however there is no existing treatment that can effectively prevent disease initiation. Thus, a significant unmet clinical need exists for preventing early initiation of OA after joint injuries. This dissertation highlights a potential biologically-driven solution using a statin therapy.

Statins are an FDA-approved class of drugs prescribed to over 40 million U.S. people to control the cholesterol levels. In this thesis, using the patient database at Christiana Health Care System, I investigated the impact of statin use on the clinically defined OA occurrence in the Delaware population. It's shown that the use of statin was associated with significantly lower occurrence of OA and other common musculoskeletal disorders, *e.g.* joint pain and low back pain. Furthermore, integrating experimental and bioinformatics data, my thesis revealed that the joint-favoring effects of statins were through inhibiting a fundamental metabolic pathway called mevalonate pathways and its downstream Rho GTPase signaling in chondrocytes. Rho GTPase

proteins play essential roles in regulating aberrant phenotypic shift and catabolic activities of chondrocytes under OA-inducing stimulations. Statins can directly inhibit the activation of Rho GTPase proteins and prevent the chondrocytes from entering a degradative state, therefore protecting the cartilage from degeneration.

Taken together, this thesis involves interdisciplinary approaches and contributes to the discovery of potential treatments of OA. The mevalonate pathway and its downstream Rho GTPases in chondrocytes could be a new target for cartilage protection. Repurposing of statins might represent a new pharmaceutical solution for OA prevention. More importantly, the finding that statin use is associated with significant OA reduction in Delaware population could increase the prescription adherence of current statin users, especially those at high risk of OA development due to joint injury histories.

Chapter 1

LITERATURE REVIEW

In this chapter, I review the basics of articular cartilage and chondrocyte, including the ultrastructure and composition of articular cartilage and the fundamental cellular activities of chondrocyte. Then, I give an introduction of osteoarthritis, especially posttraumatic osteoarthritis, in terms of the chondrocyte phenotypic shift, signaling molecules, and current and emerging pharmacological treatments for this joint degenerative disease. Finally, I reviewed the current knowledge of two FDA-approved drugs, statins and bisphosphonates, including their historical clinical application and recently discovered chondro-protective mechanism on cartilage. This chapter 1 will provide necessary background knowledge and introduction for my thesis work.

1.1 Articular Cartilage

Articular cartilage is a soft, connective tissue covering the articulating surface of long bones in the diarthrodial joints. The principal function of articular cartilage is to provide the joint with essential biomechanical functions, such as shock absorption, wear resistance, and load bearing for the whole life ¹.

Articular cartilage, in 2 - 4 mm thickness, is hyaline cartilage. Unlike most tissues, articular cartilage is devoid of blood vessels, nerves, or lymphatics ². The two major components of this tissue include a dense extracellular matrix (ECM) and a sparsely distributed cell population called chondrocytes. The ECM is principally

composed of water, collagen, and proteoglycans, with other noncollagenous proteins and glycoproteins present in lesser amounts³. Together, these components help to retain water within the ECM, which is critical to maintain its unique mechanical properties³.

1.1.1 Ultra-structure of Articular Cartilage

The ECM ultrastructure of cartilage varies along with depth from the articular surface. To facilitate the research, people usually classify articular cartilage into 4 zones - the superficial zone, the middle zone, the deep zone, and the calcified zone⁴. Within each zone, the organization and degree of alignment of the collagen fibres have unique features, and thus determining the zonal distinction in biomechanical behaviors and functions (Fig. 1.1).

The superficial zone is thin, accounts for 10 ~ 20% of total articular cartilage thickness, which is in contact with synovial fluid. This zone is featured with the highest water content (75% ~ 80%) and highest collagen content (85% dry weight), while the lowest aggrecan level⁵. The collagen fibers of this zone are packed tightly and aligned parallel to the articular surface (Fig. 1.1). This zone is mainly responsible for the tensile properties of cartilage, enabling it to resist the shear, tensile, and compressive forces imposed by articulation⁶.

Immediately deep to the superficial zone is the middle zone, which serves as the first line of resistance to compressive forces⁶. The middle zone represents 40% ~ 60% of the total cartilage volume, and it contains proteoglycans and thicker collagen fibrils. In this layer, the collagen is organized obliquely. This zone is an anatomic and functional bridge connecting the superficial and deep zones.

The deep zone represents approximately 30% of articular cartilage volume, which contains the largest diameter collagen fibrils in a radial disposition, the highest proteoglycan content, and the lowest water concentration. The deep zone is responsible for providing the greatest resistance to compressive forces, given the high proteoglycan content and perpendicularly arranged collagen fibrils ⁶.

The tide mark distinguishes the deep zone from the calcified cartilage. The deep zone is responsible for providing the greatest amount of resistance to compressive forces, given the high proteoglycan content. Of note, the collagen fibrils are arranged perpendicular to the articular cartilage. The calcified layer plays an integral role in securing the cartilage to bone, by anchoring the collagen fibrils of the deep zone to subchondral bone ⁶.

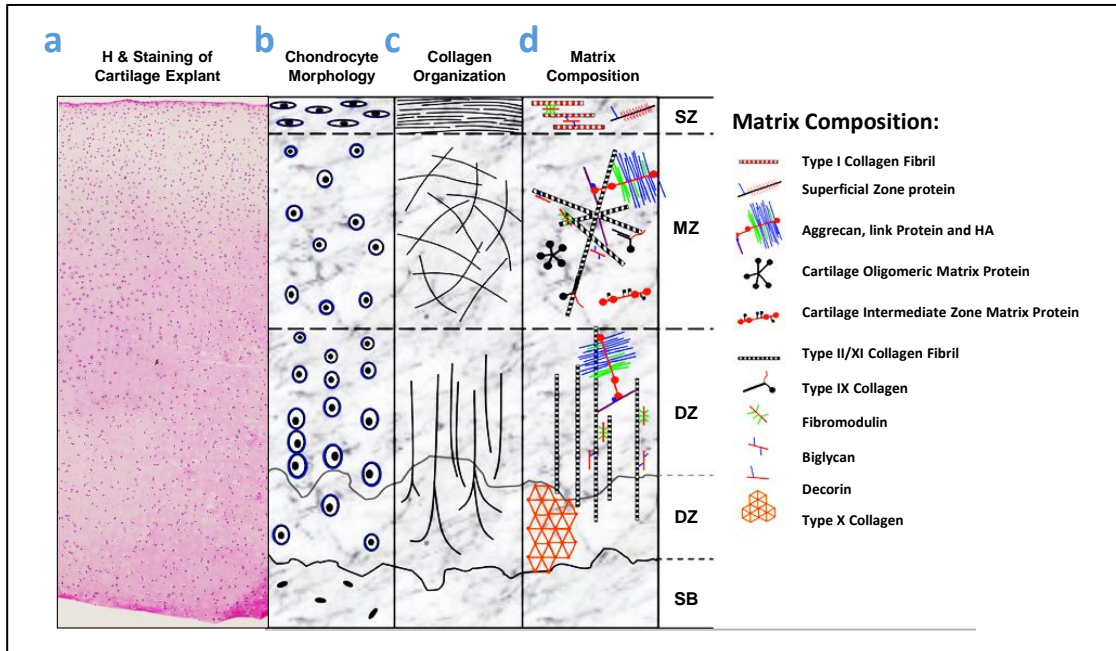


Figure 1.1 Articular cartilage structure. (a) H&E staining of bovine cartilage explant cultured in our Cartilage Bioengineering Lab, at University of Delaware. Schematic representation of (b) chondrocytes morphology, (c) Collagen organization, and (d) matrix composition of hyaline cartilage. SZ, superficial zone; MZ, middle zone; DZ, deep zone; CZ, calcified zone; SB, subchondral bone. Picture is used with permission from *J Cytochem Biochem* ⁷.

1.1.2 Chondrocytes

Chondrocyte is the sole cell population, sparsely residing in articular cartilage. They are highly specialized, metabolically active, terminally differentiated cells, which play an essential role in maintaining the homeostasis of the cartilage ECM turnover ⁸. It's of note that chondrocyte has a limited capacity for intrinsic healing and repair of cartilage tissue, and thus the preservation and health of articular cartilage are paramount to joint health ⁹.

Along with collagen fiber ultrastructure and ECM, chondrocytes also contribute to the various zones of articular cartilage ⁶. As shown in Fig. 1.1a-b, the

superficial layer contains a relatively high number of flattened chondrocytes; while the chondrocytes of middle zone are spherical and at low density. The main function of chondrocytes in the superficial and middle zone is to synthesize ECM proteins, including collagen type II, IX, and XI and proteoglycans ^{2,10}. These ECM proteins facilitate compressional and tensile forces across the diarthrodial joint. The deep-zone chondrocytes are typically arranged in columnar orientation, parallel to the collagen fibers and perpendicular to the joint line; and the calcified-zone cells are scarce and hypertrophic ². Chondrocytes of the deep zone are terminally differentiated and actively synthesize collagen type X. The upregulation of collagen type X is associated with endochondral ossification and proteolytic enzymes production ¹¹. Thus collagen type X is generally believed to a biomarker of OA development ^{9,11}.

Articular chondrocytes are mechanosensitive, which can sense and respond to mechanical loading stimuli, *e.g.* standing, walking, running, etc. ^{12,13} These stimuli have both anabolic and catabolic effects on chondrocytes ^{14,15}. Dynamic loading has been shown to promote these anabolic responses in chondrocytes by promoting the synthesis and production of ECM; whereas, static loading is known to inhibit the ECM synthesis and induce secretion of proteases, which results in the breakdown of ECM proteins ¹⁴. All these mechanotransduction of chondrocytes enables the transduction of mechanical stimuli to biochemical and biological outputs through activating the intracellular pathways ¹². The transduction from mechanical signal to the biological outputs is carried out through a wide range signaling cascades, including Rho GTPase signaling pathways, NF- κ B pathway, Mitogen-Activation Protein Kinase (MAPK) pathway, Insulin Growth Factor 1 (IGF-1) and Fibroblast Growth Factor 2 (FGF-2) pathways and etc. ¹⁶⁻²¹ These pathways are specifically responsible for different

aspects of cellular activities, while working in coordination to regulate the articular cartilage growth, maintenance and repair.

The intracellular calcium ($[Ca^{2+}]_i$) signaling is an essential universal secondary messenger engaged in the regulation of almost all cellular functions and metabolic activities²². In chondrocytes, ($[Ca^{2+}]_i$) signaling has been shown to be one of the earliest cellular responses under various physical stimuli including mechanical loading, fluid flow, electrical stimulation, and osmotic stress (Fig. 1.2)²³⁻³¹. Previous evidences reveal that chondrocytes also have spontaneous $[Ca^{2+}]_i$ oscillations, which is similar to those in neurons and myocytes³². Without the presence of any external stimulation, chondrocytes located in hydrogels or their own ECM can release robust and repetitive $[Ca^{2+}]_i$ peaks^{29,32}. Different cell types employ various strategies to generate $[Ca^{2+}]_i$ signaling with distinct spatiotemporal characteristics. For chondrocyte, during the formation of Ca^{2+} influx across plasma membrane, extracellular Ca^{2+} , gap junction, extracellular ATP, and purinergic receptors on membrane play critical roles. In chondrocytes, endoplasmic reticulum (ER) acts as the major cytosol Ca^{2+} reservoir to regulate the $[Ca^{2+}]_i$ signaling, the release of which is regulated by the phospholipase C (PLC) activities. On the membrane of chondrocytes, mechanical sensitive ion channels e.g., PIEZO1&2 channels, transient receptor potential vanilloid 4 (TRPV4), and voltage-gated ion channels (VGCC) are all regulating the fluctuation of $[Ca^{2+}]_i$ ^{32,35}. Most importantly, recent studies have demonstrated the crosstalk of calcium signaling and other important signaling transductions, such as Rho GTPase signaling, in the OA development. More results will be discussed in the next section 1.2 of Chapter 1.

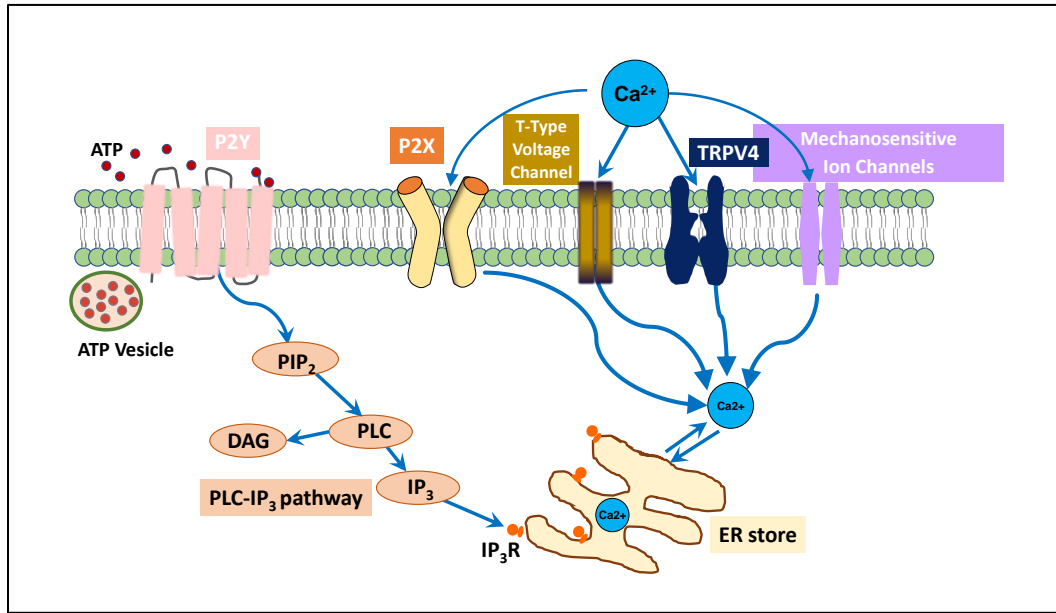


Figure 1.2 A schematic drawing of the calcium signaling pathways in chondrocytes. The cytoplasm calcium can exchange with extracellular calcium source in medium and intracellular calcium store in ER. Voltage-gated calcium channels, P2 receptor, TRPV4, mechanosensitive ion channels can transfer Ca^{2+} between intra- and extracellular environments. The calcium store in ER can be released by activation of IP3 receptors on ER membrane. Picture generated by M. Lv in Dr. X. Lucas Lu's lab.

1.1.3 Extracellular Matrix

From the mechanical point of view, articular cartilage is regarded as a triphasic tissue constituting a fluid phase, a solid phase, and an ion phase⁵. The fluid phase, taking up 80% by weight, consists of the interstitial fluid. The ion phase has many ionic species of dissolved electrolytes with positive and negative charges, into account³⁶. The solid phase, occupying 20% of the total tissue by weight, is composed of extracellular matrix (ECM). The ECM of cartilage is composed of the most abundant structural macromolecules, collagens and proteoglycans, as well as a small number of other classes of molecules, such as lipids, phospholipids, non-collagenous proteins,

and glycoproteins (Fig. 1.3). Together, these three phases and their interactions help to retain water within the ECM, which is critical to maintain its unique mechanical properties.

1.1.3.1 Water

Water is the most abundant component of articular cartilage, accounting for ~80% of the tissue wet weight. The relative concentration of water decreases from about 80% at the superficial zone to 65% at the deep zone. In healthy cartilage, approximately 30% of the water is associated with the intrafibrillar space within the collagen, a small percentage is in the intracellular space, and the remainder is in the pore space of the matrix. The intrafibrillar water appears to exist as a gel, and most of it may be moved through the ECM by applying a pressure gradient across the tissue or by compressing the solid matrix. Frictional resistance against this flow through the matrix is very high; thus, the permeability of the tissue is very low. It is the combination of the frictional resistance to water flow and the pressurization of water within the matrix that forms the basic mechanisms of articular cartilage. The flow of water through the cartilage and across the articular surface helps to transport and distribute nutrients to chondrocytes, in addition to providing lubrication.

1.1.3.2 Collagens

Collagens are the most abundant macromolecules of the ECM, making up 60% of the wet weight of the cartilage. Collagens are composed of triple helical peptide chains, and the amino acid composition of these polypeptide chains is primarily glycine and proline, with hydroxyproline providing stability via hydrogen bonds along the length of the molecule. The triple helix structure of the polypeptide chains

provides articular cartilage with important shear and tensile properties, which help to stabilize the matrix structure of cartilage.

Among collagens, type II collagen represents approximately 90% of the total collagens within ECM and forms fibrils and fibers interwoven with proteoglycans. Collagens type IX and XI, representing around 10% of the articular cartilage, offer support for the collagen fibrillar crosslinking. Other collagen types such as type I, IV, V, and VI collagen, are also present but contribute only a minor proportion. The minor collagens help to form and stabilize the type II collagen fibril network. Their roles are believed to facilitate to form and stabilize the type II collagen fibril network. Together, these components help to retain water within the ECM, which endows cartilage with its biomechanical properties for joint loading.

1.1.3.3 Proteoglycans

In articular cartilage, Proteoglycans are the second largest ECM macromolecules of ECM and account for ~ 15% of the wet weight. Proteoglycans are heavily glycosylated protein monomers, which is consisted of a protein core covalently attached with one or more glycosaminoglycan (GAG) chains. The GAG chains, negatively charged, extend out from the protein core while remained separated from one another because of charge repulsion

Aggrecan, the major proteoglycans, forms supramolecular aggregates with hyaluronan (HA) and is entrapped in the collagen II/IX/XI fibrillar network ⁵. The nonaggregating proteoglycans, *i.e.*, fibromodulin, biglycan, decorin, and lumican, can bind with various types of collagens and regulate the formation of fibril networks ³⁷.

1.1.3.4 Non-collagenous Proteins and Glycoproteins

Although a number of non-collagenous proteins and glycoproteins are found within articular cartilage, their specific function has not been fully characterized. Some of these molecules, *e.g.* such as fibronectin and CII, a chondrocyte surface protein, are likely to play a role in the organization and maintaining the macromolecular structure of the ECM in cartilage.

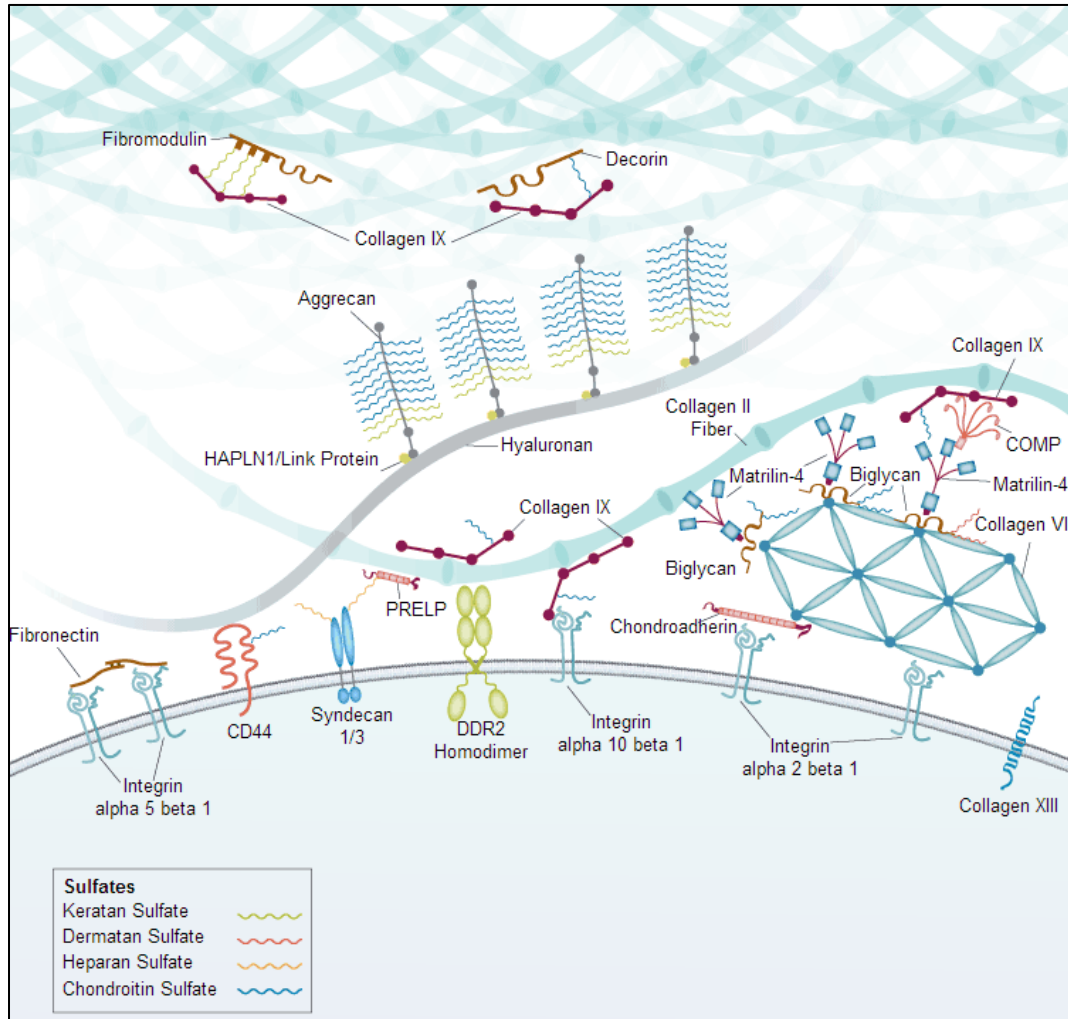


Figure 1.3 Extracellular matrix of cartilage. Three classes of proteins exist in articular cartilage: collagens, proteoglycans, other noncollagenous proteins, and the smaller proteoglycans. The interaction between highly negatively charged cartilage proteoglycans and typed II collagen fibrils is responsible for the compressive and tensile strength of the tissue, which resists load *in vivo*. This figure is used from *R&D Systems Inc* ³⁸ with permission.

1.2 Osteoarthritis

Osteoarthritis (OA), a degenerative joint disorder disease, is the most common cause of long-term disability, affecting nearly 27 million (12%) adult population of the

United States³⁹. This disease involves not only the articular cartilage, but also all surrounding tissues of the joint, including periarticular muscles, ligaments, subchondral bone, and synovial membranes⁴⁰. While the etiology of OA remains controversial, researchers commonly believe that it's multifactorial, including aging, female gender, sports participation, injury to the joint, obesity, and genetic susceptibility³⁹. In addition, lower educational levels, repetitive use of joints, bone density, muscle weakness, and joint laxity are also shown to play roles in the development of joint OA³⁹. Persist pain, limited morning stiffness, and reduced function are the three symptoms that are recommended for the diagnosis of OA⁴¹.

Posttraumatic OA (PTOA), arises from traumatic joint injuries, accounts for 12% of total OA cases. Joint trauma can lead to a spectrum of acute lesions, including osteochondral fractures, ligament or meniscus tears and damage to the articular cartilage^{42,43}. Such trauma injuries often occur among adolescent athletes and military service, predisposing patients to the development of premature OA⁴⁴. For example, previous knee trauma can increase the risk of knee OA development by 3.86 times⁴⁵. Even with the current care of joint injuries, such as anatomic reduction and rigid fixation of intra-articular fractures and reconstruction of ruptured ligaments with successful restoration of joint biomechanics, the risk of PTOA after joint injuries ranges from 20% to 60%^{44,46}.

1.2.1 Posttraumatic OA Development Stages

The time course of PTOA progression following joint injury is very variable, which may dependent on the mechanical injury impact and severity of tissue damage. To facilitate research, the pathogenetic processes of PTOA is widely separated into

three phases, acute post-traumatic phase, asymptomatic phase, and the chronic phase (Fig. 1.4).

In the acute phase, traumatic joint injuries are often followed by hemarthrosis, inflammation, and changes in the loading profiles. On cellular level, it has been observed regarding initial chondrocyte necrosis due to impact, elevated inflammatory cytokines in synovial fluid, and production of ECM-degrading enzymes⁴⁷. All these factors may cause the normally “quiescent” chondrocytes to undergo a phenotypic shift and become ‘activated’ cells², characterized by cell volume increase^{3,4}, cell proliferation, cluster formation, hypertrophy, and apoptosis⁵. This hypertrophic-like process of chondrocytes is associated with elevated synthesis and release of matrix-degrading enzymes, *i.e.* Matrix Metalloproteinase 13 (MMP13)⁴⁸⁻⁵⁰, directly destructing the ECM and compromising functions of cartilage tissues⁵¹⁻⁵³.

Following the acute phase, the injured joint enters a asymptomatic phase, which is recently caught great attention and recommended to defined as “pre-osteoarthritis (pre-OA)”^{54,55}. Pre-OA refers to a state that many cellular processes have been activated in response to OA-inducing factors while have not yet resulted in any pain or any detectable structure changes on the joint. Currently, some biomarkers, *e.g.* COMP, CTX-II and collagen II fragments have been shown to correlate with the radiographic markers and clinical grading of OA; whereas breakthroughs in the biochemical marker in pre-OA disease are still limited so far. Future studies are still of necessity to further understand the metabolic changes at the cellular and molecular levels in this asymptomatic period⁴⁷.

In the chronic phase, metabolic changes in articular cartilage slowly progress through a long, asymptomatic period to a clinically symptomatic OA phase with joint

pain and dysfunction as a result of joint destruction⁵³. The majority of patients with OA are not clinically diagnosed until the symptomatic phase. In general, once severe articular destruction has developed, the remaining surgical options are joint arthroplasties, osteotomies, and joint fusions⁵³.

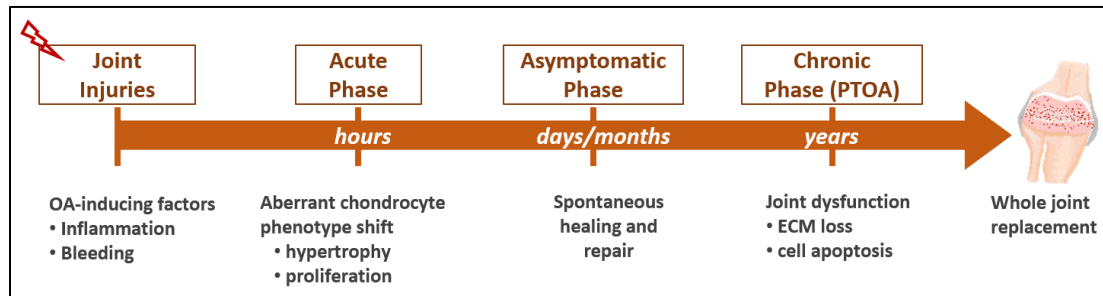


Figure 1.4 Timeline of the pathogenic processes following joint injury. After the immediate consequences of injury, mechanobiological, molecular and cellular changes in cartilage and other joint structures slowly progress into an acute post-traumatic phase. This acute phase can spontaneously resolve after a couple of months or persist through a long latency period without clinically symptom. The chronic phase last years and may eventually lead to chronic OA. Picture was regenerated by M Lv with permission from *BMJ*⁴⁷.

1.2.2 Phenotypic Shift of Chondrocytes in Posttraumatic Cartilage

The OA progression is accompanied with a change in chondrocyte behaviors, such as elevated production of proteolytic enzymes, expression of hypertrophy markers, and ECM calcification. These aberrant processes resemble the phenotypic shift of chondrocytes during OA progression. In this thesis, we will focus on the aberrant differentiation trend toward hypertrophy in chondrocytes, which leads to irreversible apoptosis and cartilage degradation, both initiating and perpetuating OA disease (Fig. 1.5). A better understanding of these serial events of phenotypic

instability in chondrocytes can help us to identify targets that can prevent disease onset.

One of the best-established biomarkers for chondrocyte hypertrophy-like changes in cartilage is type X collagen. The expression of type X collagen is low in healthy human cartilage; while its expression is significantly elevated in human OA cartilage samples⁵⁶. It's worthy to mention that the basal expression of type X collagen varies with sample species, populations, zones, and disease states. Some expression array studies, also including my RNA sequencing of bovine cartilage explants, have not detected expression of COL10A1 in OA samples⁵³⁵⁷. These observations suggest that there may existing an alternative mechanism by which chondrocyte hypertrophy is regulated in a type X collagen independent manner.

MMP13 is another marker of hypertrophy, which is usually observed during cartilage development⁵⁸. In addition to catabolic effects in cartilage degradation, collagenases also play an important role in cell enlargement and cartilage growth. During cartilage maturation, MMP13 is required to prepare cartilage matrix for subsequent calcification, before endochondral ossification. The mRNA expression level of MMP13 has been shown to be paralleled that of type X collagen, suggesting their cooperating roles during cartilage development. Both microarray and qRT-PCR have shown the upregulation of MMP13 by more than 40 folds in OA human cartilage on gene level⁵⁸.

The ultimate fate of hypertrophic chondrocytes is to undergo apoptosis; and thus, apoptosis markers is also considered as marker for chondrocyte hypertrophy⁵⁹. In OA cartilage, the Tunnel staining for apoptotic cells and expression of apoptosis markers such as annexin II/V, caspase-3/9, and FAS were increased⁶⁰. Such abundant

presence of apoptosis markers in OA chondrocytes suggests a phenotype that resembles that of terminally differentiated hypertrophic chondrocytes.

Autophagy is a process related to apoptosis and has attracted significant attention in OA studies. Autophagy is a cellular catabolic activity related to protein degradation, organelle turnover, and non-selective breakdown of cytoplasmic components. Constitutive level of autophagy plays a key role in cellular homeostasis and maintains the quality of essential cellular components. Autophagy is a protective mechanism in normal cartilage; however, compromised autophagy activity is associated with OA development^{61,62}. In normal cartilage, chondrocyte autophagy is constitutively active and apparently protective process for the maintenance of the homeostatic state. By contrast, human OA as well as aging-related and surgically-induced mice OA cartilage present a significant reduction and loss of expression of Atg genes (ULK1, Beclin1 and LC3), which are major regulators of the autophagy pathway⁶³. These results suggest that compromised autophagy represents an important mechanism in the development of OA.

Other genes or proteins, related to chondrocyte hypertrophy, that have been demonstrated to be more highly expressed in OA cartilage than normal cartilage include osteocalcin, osteopontin, osteonectin, Indian Hedgehog, VEGF, beta-catenin, alkaline phosphatase. Expression of Sox9 and Runx2, two crucial transcription factor for chondrocytes, is down regulated in human OA cartilage as is observed in terminal differentiating growth plate chondrocytes.

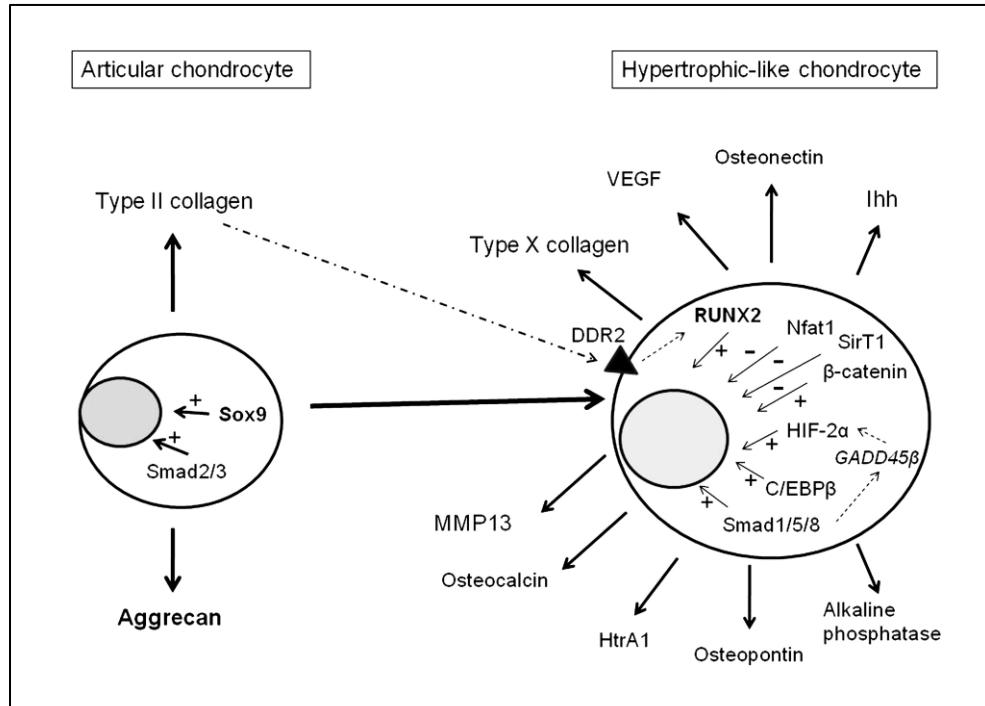


Figure 1.5 Molecular mediators involved in OA-related hypertrophic-like changes of chondrocytes. During hypertrophy-like shift, a number of transcription factors regulate the differentiation from a normal articular chondrocyte to a terminal differentiated chondrocyte. Meanwhile, chondrocytes produce many proteins that are regulating cartilage ECM remodeling and calcification. Picture is obtained with permission from *J Osteoarthritis and Cartilage*⁵³.

1.2.3 Signaling Molecules in the Pathogenesis of OA

Trauma injuries are often followed by joint inflammation, bleeding, and altered loading patterns, which are all OA-inducing stimulations leading to chondrocyte phenotypic modulation. During the phenotypic-shift process, many signaling transductions in chondrocytes are initiated to take action to stimulate the ECM-degrading enzymes production as well inhibit cartilage self-repair. With the use of *in vitro* and *in vivo* models, many signaling molecules involved in the PTOA

pathogenesis have been identified and their roles in dysregulated chondrocyte function in OA have been examined.

1.2.3.1 Inflammatory Cytokines

Based on metabolic effects of cytokines in the context of PTOA, cytokines can be divided into inflammatory and anti-inflammatory category. The pathophysiological processes occurring in the joint affected by OA are largely mediated by inflammatory cytokines; while the anti-inflammatory cytokines mainly modulate an inflammatory response acting protectively on joint tissue⁵¹. Herein I focus on the inflammatory cytokines, the mediators exerting destructive effects of cartilage integrity.

The cytokine interleukin -1 (IL-1 β) is a principal mediators of the acute posttraumatic inflammatory phase after mechanical joint injury⁶⁴. At the acute phase after joint trauma, the increased expression of IL-1 is correlated with the duration and severity of cartilage damage⁶⁵. The known effects of inflammatory cytokines include disturbing the catabolism and anabolism processes. As result, the disrupt metabolism is related to the progressive degeneration of articular cartilage performing a key role in the biomechanics of each joint and other components of the joint, which results in the development of a difficult-to-interrupt disease process that involves both inflammatory, degradation, and production processes, which together lead to a gradual loss of joint function and pain. In addition, IL-1 β has been shown to suppress the expression of a number of genes associated with the differentiated chondrocyte phenotype, including COL2A1 and CD-RAP. Early *in vitro* studies showed that IL1 and TNF- α can inhibit the synthesis of type II collagen by chondrocytes by suppressing gene transcription. IL1 and TNF α also stimulate the synthesis of prostaglandin E2, which feedback-regulates COL2A1 transcription in a positive

manner, depending upon receptor activities. Furthermore, synovial fluid levels of the IL-1 receptor antagonist (IL-1Ra) decrease after ACL injury. IL-1 induces mediators of joint pain, and it promotes cartilage matrix degradation by inducing expression of ECM-degrading enzymes and inhibiting extracellular matrix synthesis and the anabolic activity of growth factors ^{66,67}.

Tumor necrosis factor alpha (TNF- α), in combination with IL-1 β , can produce intense synergistic effects in inducing catabolic activities of cartilage. The receptors of IL-1 β and TNF- α co-localized in the superficial regions of OA cartilage, responding to their cytokines elevated in the synovium fluid. Both IL-1 β and TNF- α can directly act on chondrocytes and induce the production of destructive proteinases. The levels of TNF α in human synovial fluid also increase significantly after acute joint injury ⁶⁸. TNF α can directly induce cell apoptosis and stimulate inflammatory mediators of chondrocyte, such as IL-6 and IL-1, leukocyte inhibitory factor, proteases, nitric oxide production and prostaglandin E₂ ⁶⁹⁻⁷¹. Previous studies have shown that TNF- α and IL-1 β regulate apoptosis differently in this human chondrocyte model and that the differing effects of these cytokines are PGE₂-independent. The catabolic effects of TNF α can be potentiated by IL-6 and its soluble receptor, resulting in the degradation and loss of sGAG of cartilage. Furthermore, mechanical injury potentiates proteoglycan catabolism induced by this combination of TNF α and IL-6 with its soluble receptor. This provides a potential mechanism linking the immediate and acute events following trauma.

Other inflammatory cytokines exerting catabolic effects on cartilage include IL-6, IL-15, IL-17, and IL-18. Although several biological properties overlap for these

cytokines, more studies reported their different functions in regulating cartilage integrity. Future investigation is still of necessity to elucidate their specific roles.

1.2.3.2 ECM-degrading Enzymes

Degradation of collagen and aggrecan is a key feature of OA development. Studies with cartilage explants that are subjected to mechanical impact injury demonstrate that the remaining viable chondrocytes express increased levels of matrix metalloproteinases^{72,73}. Analyses of synovial fluid samples from patients with ACL or meniscal tear revealed increased MMP-3 levels that remained elevated for many years⁷⁴. Joint fluid also showed an initial and persistent elevation of the neoepitope Col2CTx in the C-telopeptide of type II collagen, indicating digestion of mature, cross-linked collagen by MMPs. Fragments of cartilage oligomeric protein and aggrecan were also elevated.

Aggrecan loss is an earlier event in the OA progression compared to that of collagen. A considerable amount of research has been done to establish the specific role of aggrecan-degrading enzymes, which are mainly from the A Disintegrin and Metalloproteinase with Thrombospondin motifs (ADAMTS) family. So far ADAMTS-5 is considered as the most important enzymes responsible for pathological cleavage of aggrecan. In a ADAMTS knockdown mice (*Adamts5^{-/-}*), less severe cartilage degradation was observed compared to the wild type. Similarly, transgenic mice with mutated aggrecan that is resistant to aggrecanases cleavage also develop less severe OA in the surgical OA and antigen-induced OA models. ADAMTS-4 also contributes to cartilage degradation in other species, including human and bovine. Other aggrecanases including ADAMTS-1, -8, -9, -15, -16 and -18, can also degrade aggrecan; while their specific roles are still under investigation. Some studies have

reported aggrecan cleavage at the MMP-sensitive bond which may occur during the later stage of OA.

Along with aggrecan breakdown, degradation of collagen is also a central feature of OA. Type II collagen is the primary collagen of cartilage ECM and forms a fibrillar network, providing the cartilage matrix with mechanical strength. Such fibrillar collagen are highly stable molecules, which can only be degraded by MMPs, such as MMP-13, MMP-1, and MMP-9⁷⁵. The primary collagenase in OA cartilage is MMP-13, which has been widely used as biomarkers in the studies of human, mice, and bovine OA models⁷⁶. The expression level of MMP-13 significantly increased in OA patient cartilage, and in rodent surgical OA models. In contrast, the knockdown mice (*Mmp13*^{-/-}) have less degraded cartilage in a surgical OA model. MMP-3 and MMP-9 are also strongly expressed in the early stage of OA progression, which gradually decreased over time. In few surgically induced OA animal models, mice with MMP-3/MMP-9 knockdown surprisingly developed more severe cartilage degradation and OA progression. These data suggested that MMP-3 and MMP-9 may also be involved in maintaining routine ECM turnover and cartilage hemostasis.

ECM cleavage fragments, such as collagen or fibronectin fragments that are degraded by protease enzymes, are biologically active signaling fragments. These function fragments can further reinforce the production of proteases and induce more catabolic activities^{42,77}. For example, the proteoglycan fragments generated by ADAMTS can induce cell death and promote regression of interdigital webbing during mouse limb development⁷⁸. Chondrocytes have receptors for ECM fragmented components, such as integrins and receptors for fibronectin and type II collagen fragments. These receptors can trigger a feedback amplification mechanism once

ECM degradation occurred and consequently induce a wide range of other cellular activities such as inducing apoptosis.

1.2.3.3 Rho GTPase Family Proteins

Rho family of GTPases in total includes 20 “Ras-like” proteins members, of which the best-characterized members are Cdc42, Rac1, and RhoA. Rho GTPases is referred to as “molecular switches” for signal transduction from environment stimuli to imitate intracellular signaling transduction ⁷⁹. Rho GTPase proteins have been shown to involve in regulating a wide range of cellular processes, including cell proliferation, hypertrophy, apoptosis, and gene expression ⁷⁹.

Rac1 and Cdc42 are important regulators of chondrocyte differentiation and chondrogenesis. Both of them serve as positive mediator during chondrogenesis by upregulating a chondrogenesis biomarker type X collagen promoter activity ⁸⁰. Using chondrocyte-specific target gene deletion mice model, Kamijo and colleagues reported that both Rac1 and Cdc42 are required for chondrogenesis during limb development, partially due to their regulatory effects on the expression of apoptosis marker genes Bmp, Msx1, and Msx2 ^{81,82}. In addition, another Rac1-deficient (Rac1^{-/-}) mice model displayed consistent results. Absence of Rac1 protein causes the delayed ossification, reduced chondrocyte proliferation, and increased apoptosis in the growth plate cartilage ⁸³. The positive role of Rac1 on chondrocytes has been suggested to be related to its ability to reduce levels of inducible nitric oxide synthase protein and nitric oxide production ⁸⁴. Another mechanism study reveals that the Rac1 activation is also required by canonical Wnt signaling transduction, an essential pathogenic pathway in both human and mice OA cartilage ^{85,86}.

A number of recent studies imply the antagonistic effects RhoA compared to Rac1/Cdc42 on chondrocyte differentiation and chondrogenesis. The effects of RhoA regulating chondrogenesis seem to be context-dependent, monolayer cultured or three-dimensional cultured cells ⁸⁷. For monolayer ATDC5 cells, over-expression of RhoA resulted in delayed hypertrophic differentiation with reduced COLX and MMP13 expression ⁸⁸. Similarly, inhibition of the RhoA/ROCK pathway in monolayer mesenchymal cells results in the enhancement of a number of markers of chondrogenesis such as Sox9 activity and collagen II and aggrecan transcripts levels. However, the inhibitory effects of RhoA on chondrocyte differentiation are not observed in a three-dimensional micromass culture system ⁸⁷. In response to ROCK inhibition, the gel-cultured cells display a decrease in the transcript levels of collagen II and aggrecan as well as reduced activity of a Sox9-responsive reporter gene. Similar results are also reported by Lassar and colleagues that RhoA regulates Sox9 transcriptional activity in limb bud micromass cultures ⁸⁹. In summary, RhoA, Rac1, and Cdc42 signaling pathways are all expressed during chondrogenesis. RhoA has adverse effects on chondrocyte terminal hypertrophy-like change by delaying differentiation; while the Rac1/Cdc42 signaling pathway, on the other hand, accelerates chondrocyte hypertrophy. All their regulatory effects are seem to be through regulation of Sox9 activity, but the underlying mechanisms are still poorly understood.

With significant attention on Rho GTPase activities involved in chondrocyte hypertrophy-like changes, the pathological roles of RhoA, Rac1, and Cdc42 during OA progression are under intensive investigation. Using an *in vitro* cartilage explant model. RhoA-ROCK signaling has been shown to be involved in actin cytoskeletal

reorganization at the early phase of mechanical insult, which is considered as a pathological factor to OA initiation and progression ⁹⁰. In addition, RhoA plays an important role in regulating chondrocyte phenotypic shift and cartilage matrix degradation under OA-inducing stimulations, such as inflammatory cytokine IL-1 β . In monolayer chondrocytes or *in vivo* animal study, RhoA can interact with growth factors that are associated with OA, including epidermal growth factor receptor signaling factors ⁹¹, insulin-like growth factor-1 (IGF-1) ⁹² and fibroblast growth factor ⁹³, suggesting a universal role of RhoA in OA progression. Furthermore, another Rho GTPase family member, RhoB, is also indicated to be an important mediator associated with OA development. In a human genetic association study, a significant association between RhoB and knee OA has been observed using Chinese population ⁹⁴. Meanwhile, inhibition of Rho activity by AS1892802 significantly inhibited the cartilage degradation and pain responses in both monoiodoacetate-induced OA rat models and *in vitro* synovial cell lines ⁹⁵.

With regards to the Rac1/Cdc42 signaling pathway in OA progression, Cdc42-GTP content decreases ⁹⁶ while Rac1-GTP increases with chondrocyte aging. This provides new insights into age-related primary OA development. Additionally, an *in vitro* cartilage explant study shows that Rac1 is required for fibronectin fragment-induced signaling that results in MMP-13 production and can further promote this effect ⁹⁷. The active role of Rac1 in OA cartilage and its promotion of MMP-13 production suggest its metabolically disturbing role in cartilage matrix destruction seen in OA. Furthermore, a most recent animal study proves that Cdc42 is apparently required for ECM degeneration, chondrocyte hypertrophy, and high expression of

MMP-13 and collagen X in articular cartilage of mouse OA model with surgical destabilization of the medial meniscus ⁹⁸.

Overall, OA articular chondrocytes undergo hypertrophy-like changes, which intensively relies on Rho GTPases. RhoA, Rac1, and Cdc42 are well recognized as crucial mediators of chondrocyte maturation during cartilage development as well as chondrocyte hypertrophy associated with OA pathology. Their regulatory effects on chondrocyte hypertrophy-like change warrants the use of Rho GTPase activators or inhibitors for OA prevention and cartilage tissue engineering. Therefore, Rho GTPases inhibitors may be promising drugs for preventing early-stage OA where chondrocytes are undergoing hypertrophic-like phenotype shift and initiating cartilage matrix destruction.

1.2.4 Existing and Potential Preventions and Treatments of PTOA

Although the initial diagnosis of PTOA is considerably earlier than that of primary OA, the treatment options available for patients with PTOA are limited. Especially for young population, doctors often seek a compromise between clinically effective in pain relief with functional improvement and treatment safety and durability.

1.2.4.1 Current Treatments for PTOA Patients

The traditional first-line non-pharmacological approaches to the PTOA patients of any age consist of low impact exercise, bracing, lifestyle changes (losing weight if necessary), and physical therapy. The. Pharmacological treatments contain analgesics, anti-inflammatory drugs (non-steroidal anti-inflammatory drugs, NSAIDs), and other disease-modifying OA drugs. Some combinations of these non-

pharmacological and pharmacological modalities seems to exert better effects on OA symptom relief. Unfortunately, none of these therapies can successfully alter the course of OA progression.

For late-stage OA patients, the last choice available is a costly intervention, whole joint replacement surgery. This procedure can be considered for patients of all ages except of children due to the fact that their bones are still growing. As the replacement parts can eventually break down over time, the healthcare providers generally recommend delaying knee replacement until it is absolutely necessary, *e.g.* significant pain or disability. So far approximately 700,000 total knee arthroplasty (TKA) procedures are performed annually in the U.S.; and this number is projected to increase to 3.48 million procedures per year by 2030. Although the rapid increase in utilization, the success of TKA procedure is partially dependent upon the surgeon experience and the hospital condition. The potential complications following TKAs should be considered, *e.g.* blood clot, infection, stiffness, and early failure.

For younger population, the clinical outcomes of early preventions and final TKA surgery are often sub-optimal and sustainable compared to adults. For example, the decision-making process for TKA surgery is further complicated in the younger patient as to their higher physical demand on the prosthesis components. Unlike older patients who place lower mechanical demands, younger patients expect to remain physically active after surgery, with the resulting high likelihood of outliving the implant. Consequently, approximately 40% of patients who are aged 40 years or less and with TKA can recover their joint function; and 10% of patients need to undergo implant revision over the next 10 years.

1.2.4.2 Emerging Pharmacological Treatment Options

As the trauma joint injuries is often followed by a well-recognized acute inflammation phase, there is an urgent need to development a treatment strategy that to prevent the onset of PTOA. It is appealing to envision a biologic therapy that could prevent, delay, or effectively manage OA, especially for young patient with post-traumatic knee injury. Here I focus on pharmacological interventions, while people should understand that combination with surgical interventions and physical therapy often achieve optimal outcomes.

A number of preclinical studies have shed light on several molecules as potential targets for PTOA treatment. Several major pathways of chondrocytes involved in the pathogenetic mechanism of OA have been identified, including posttraumatic inflammatory responses, cell death, ECM-degrading enzyme production, and regeneration of new cartilage ECM proteins. Consequently, the inhibitors for these pathogenesis pathways are considered as potential OA-modifying drugs *e.g.* IL-1/TNF inhibitor, MMPs inhibitors, caspase inhibitors, growth factors, and antioxidants. For example, few animal studies have shown that inhibition of IL-1 production through knockout of IL-1 β gene or overexpression of IL-1Ra to be therapeutically effective in preventing PTOA progression. Similarly, TNF α inhibition by subcutaneous injection of a soluble TNF receptor fusion protein showed disease-modifying activity in a PTOA rats model (with anterior cruciate ligament transection). Another promising candidate is antioxidants. Traumatic cartilage and joint injury is associated with increased production of reactive oxidant species and reduced antioxidant defenses, and this imbalance contributes to apoptosis and ECM degradation. According to our recent findings, chondrocyte death induced by mechanical injury was reduced by resveratrol, an antioxidant extract from grape skin

(unpublished). Resveratrol has been extensively studied due to its health benefits. In our lab, we elaborated the protective effects of resveratrol at both cellular and tissue levels. As results, this antioxidant shows great potential for the treatment of OA, especially the middle-to-late stage OA when a limited number of functional chondrocytes are left in the cartilage.

Despite these promising results from *in vitro* and *in vivo* animal models, the translation of these results into effective, FDA-approved therapies remain challenging and long way to achieve. One of the major challenges is the long time span from joint trauma occurrence to the radiographic/MRI diagnosis, and that's the reason why a well-designed, large randomized clinical trial is still lacking. To my best knowledge, currently the only existing clinical study is a small randomized pilot clinical trial has been conducted for IL-1Ra. However, the ability of IL-1 inhibition to prevent the long-term onset of chronic PTOA is unclear and a larger size of randomized clinical study is still of necessity to generate valid conclusion.

Taken all, OA is a common diagnosis in the patient with previous traumatic knee injury. Following joint injury, OA develops and progresses rapidly, with no known therapies that can prevent or alter the course of disease. In an effort to prevent or delay invasive joint arthroplasty in the post-traumatic knee OA patient, biologics and disease-modifying drugs are emerging technologies intended to address the biochemical environment at the joint, whereas minimally invasive unloading implants address abnormal joint biomechanics. Thus, a significant unmet clinical need exists for early clinical interventions that can be applied immediately after joint injury to slow or stop PTOA progression.

1.3 Bisphosphonate and Statins

Bisphosphonates (BPs) are a class of drugs that have revolutionized the treatment of bone resorption related disorders over the past 40 years (Fig. 1.6, left). They are the first line of treatment for osteoporosis and metastatic bone cancer ⁹⁹. Because BPs contain two phosphonate groups BP's bind strongly to calcium in bone (Fig. 1.4). When osteoclasts dissolve the bone, the BP's are taken up by the cells, and can exert their anti-resorptive effects. The remarkable anti-resorptive effects of the current crop of nitrogen-containing BPs result from their inhibition of the enzyme farnesyl pyrophosphate synthase (FPPS), a key enzyme in the mevalonate pathway ¹⁰⁰, which regulates osteoclast cell morphology, membrane ruffling, and apoptosis ¹⁰¹.

Previous results have successfully demonstrated the protective effect of BPs using animal PTOA models more than a decade ago; however, the clinical studies of BPs on OA prevention remain controversial. Podworny et al. found that subcutaneous injections of zoledronic acid (ZA) partially protected articular cartilage from inflammatory arthritis induced by carrageenan, without affecting the induced synovitis. Later the chondro-protective effects of alendronate, another bisphosphonate family drug, were revealed in a rat ACL transection model ¹⁰². Two more recent studies confirmed these earlier findings using different PTOA animal models (rabbit osteochondral defect and rat monosodium iodoacetate injection) ^{103,104}. Inspired by such promising animal results, a large randomized trial in humans was conducted in both North America and the European Union ¹⁰⁵. Enrolled patients include the subjects who are diagnosed with preexisting knee OA and suffering from knee pain, knee stiffness, or knee crepitus. However, little positive effect of risedronate treatment on idiopathic OA was demonstrated in this large study.

Such conflict between animal studies and clinical studies suggested that the timing of bisphosphonate treatment may be critical to OA benefit ¹⁰⁶. This idea has been reinforced by multiple clinical late-stage OA trials with BPs that have shown equivocal effectiveness ^{105,107}, whereas results from animal model studies continue to prove the capacity of BPs to inhibit the initiation of OA. Thus, the initiation and progression of OA may involve different pathogenesis and could require distinct treatment strategies [3-5, 8, 19]. Therefore, the insight into the cellular or biochemical mechanisms by which BP mediated chondro-protection in PTOA pathogenesis can improve our understanding of OA pathology as well as discovery of novel therapy.

As another potent inhibitor of the mevalonate pathway, statins are a class of drugs used by ~ 40 million (13%) people in the U.S.A to control the cholesterol levels, with well-understood side effects ¹⁰⁸. In cell, statin-mediated reduction of cholesterol synthesis is through inhibiting HMG-CoA, a rate-limiting enzyme of mevalonate pathway. By lowering the cholesterol levels, statins help prevent heart attacks and stroke by up to 35% (Fig. 1.6 right).

Recently, statins have received significant attention as potential disease-modifying therapeutics for OA. Two clinical studies from the Netherlands and the United Kingdom suggest that statins have a significant, modifying role in OA disease. However, another large clinical study from the U.S. didn't find any positive association between statin use and improvements in knee pain, function or structural progression over a 4-year period observation. The conflict between published studies arouse heated debates on the methodological factors and remains unsolved due to lacking knowledge of statin's protective mechanism on cartilage. As results, the clinical application of statins for OA treatment is hindered.

As potent mevalonate pathway inhibitors, both BPs and statins show “pleiotropic” effects on various cell types. For example, BPs have been demonstrated to regulate the metabolism, mechano-sensitivity, and gene expression of mesenchymal stem cells, osteoblasts^{109–111}, chondrocytes^{112–114}, adipocytes¹¹⁵, and breast cancer cells¹⁰⁹. Statins appear to involve improving endothelial function, enhancing the stability of atherosclerotic plaques, decreasing oxidative stress and inflammation, and inhibiting the thrombogenic response. In fact, inhibition of mevalonate pathway results in a decrease in not only the biosynthesis of cholesterol but also other intermediate metabolites that regulate the prenylation of intracellular signaling proteins Rho GTPases. The family of Rho GTPase protein is “molecular switch” playing an essential role in the regulation of multiple aspects of cellular biological processes^{116,117}. In chondrocytes, RhoA, Rac1 and Cdc42 are the best characterized Rho GTPases, which play essential roles in regulating cell hypertrophic change^{118,119}, apoptosis^{81,82}, and MMP13 synthesis^{97,120} during the OA progression of joint. Inhibition of their activates has been proven to significantly delay the cartilage degeneration in animal studies^{82,121}. Therefore, it is tempting to speculate that statin-induced inhibition of the mevalonate pathway can lead to inactivation of downstream Rho GTPase proteins, which consequently prevents the chondrocyte from abnormal phenotypic shift and responding to OA-inducing factors stimulation.

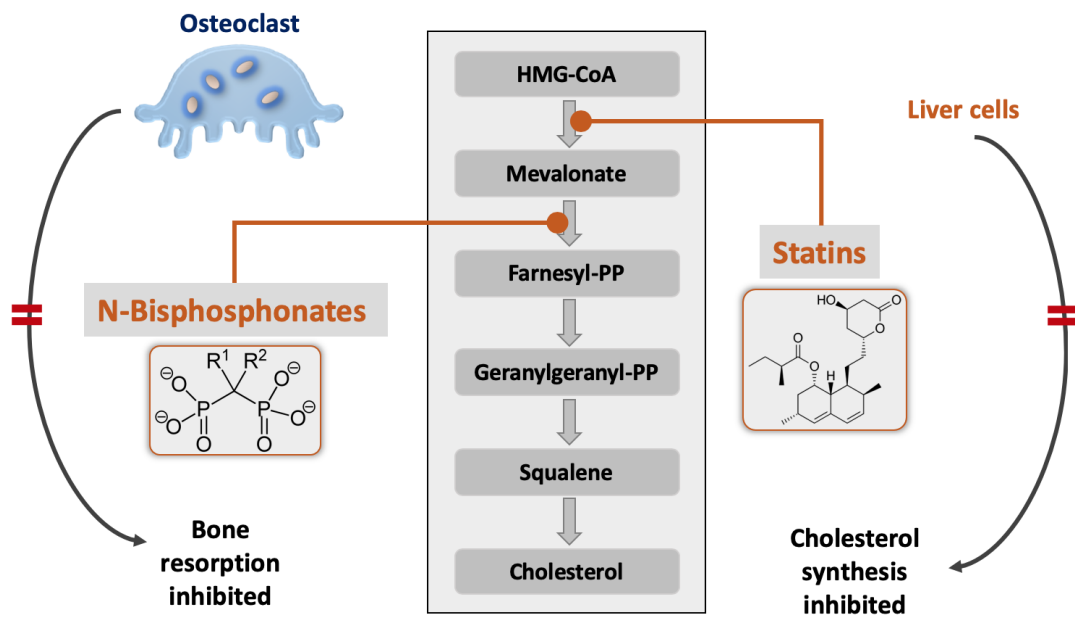


Figure 1.6 Schematic representation of the Mevalonate pathway. The inhibitory effects of statins and Nitrogen-containing Bisphosphonates (N-BPs) are indicated.

Chapter 2

THE ROLE OF CALCIUM SIGNALING IN MECHANOTRANSDUCTION OF IN SITU CHONDROCYTES UNDER COMPRESSEION¹

Calcium Signaling of in situ Chondrocytes in Articular Cartilage under Compressive Loading

Mengxi Lv¹, Yilu Zhou¹, Xingyu Chen¹, Lin Han², Liyun Wang¹, X. Lucas Lu¹

¹Department of Mechanical Engineering, University of Delaware, Newark, DE 19716

²School of Biomedical Engineering, Science, and Health Systems, Drexel University,
Philadelphia, PA 19104

¹ This chapter was published in *Journal of Orthopaedic Research* 36.2 (2017): 730-738. The permission for full-article use was attached in Appendix.

2.1 Abstract

Mechanical loading on articular cartilage can induce many physical and chemical stimuli on chondrocytes residing in the extracellular matrix (ECM). Intracellular calcium ($[Ca^{2+}]_i$) signaling is among the earliest responses of chondrocytes to physical stimuli, but the $[Ca^{2+}]_i$ signaling of *in situ* chondrocytes in loaded cartilage is not fully understood due to the technical challenges in $[Ca^{2+}]_i$ imaging of chondrocytes in a deforming ECM. This study developed a novel bi-directional microscopy loading device that enables the record of transient $[Ca^{2+}]_i$ responses of *in situ* chondrocytes in loaded cartilage. It was found that compressive loading significantly promoted $[Ca^{2+}]_i$ signaling in chondrocytes with faster $[Ca^{2+}]_i$ oscillations in comparison to the non-loaded cartilage. Seven $[Ca^{2+}]_i$ signaling pathways were further investigated by treating the cartilage with antagonists prior to and/or during the loading. Removal of extracellular Ca^{2+} ions completely abolished the $[Ca^{2+}]_i$ responses of *in situ* chondrocytes, suggesting the indispensable role of extracellular Ca^{2+} sources in initiating the $[Ca^{2+}]_i$ signaling in chondrocytes. Depletion of intracellular Ca^{2+} stores, inhibition of PLC-IP₃ pathway, and block of purinergic receptors on plasma membrane led to significant reduction in the responsive rate of cells. Three types of ion channels that are regulated by different physical signals, TRPV4 (osmotic and mechanical stress), T-type VGCCs (electrical potential), and mechanical sensitive ion channels (mechanical loading) all demonstrated critical roles in controlling the $[Ca^{2+}]_i$ responses of *in situ* chondrocyte in the loaded cartilage. This study provided new knowledge about the $[Ca^{2+}]_i$ signaling and mechanobiology of chondrocytes in its natural residing environment.

2.2 Introduction

Chondrocytes are the sole cell type in articular cartilage and responsible for the biosynthesis and catabolism of extracellular matrix (ECM). Metabolic activities of chondrocytes can be regulated by the physical stimuli induced by the daily mechanical loading on cartilage¹²². Due to the multi-phasic nature of cartilage, compressive loading on cartilage can generate changes in mechanical, hydrostatic, chemical, and electrical signals across the tissue^{123,124}. Oscillation of intracellular calcium ($[Ca^{2+}]_i$) concentration is among the earliest and most fundamental molecular responses of chondrocytes to most physical stimuli, including compression^{23–25}, fluid flow²⁶, hydrostatic pressure²⁷, osmotic stress^{28–30} and electric current³¹, as shown by previous studies using monolayer chondrocytes or chondrocytes seeded in hydrogels. Calcium signaling plays significant roles in numerous biological functions including cell adhesion, metabolism, secretion, proliferation and apoptosis¹²⁵. Recent studies found that chondrocytes have spontaneous $[Ca^{2+}]_i$ signaling without the presence of any exotic stimuli^{30,33,34}, suggesting the fundamental roles of $[Ca^{2+}]_i$ in modulating the biological processes and metabolic activities within chondrocytes.

At rest status, cells maintain a 20,000-fold gradient of Ca^{2+} concentration between the intracellular (~ 100 nM) and extracellular space (\sim mM)²². The rapid $[Ca^{2+}]_i$ ascent in cytosol mainly relies on two mechanisms, Ca^{2+} influx from the extracellular environment and the release from intracellular Ca^{2+} stores such as endoplasmic reticulum (ER). In chondrocytes, both mechanisms play essential roles in regulating the physical stimuli-induced $[Ca^{2+}]_i$ responses²³. Several types of channels on chondrocytes membrane, such as transient receptor potential vanilloid channels (e.g., TRPV4 channel)²⁹, mechanosensitive ion channels (e.g., PIEZO channels)¹²⁶, and voltage gated calcium channels (e.g., T-type VGCC)¹²⁷, can be activated by

various physical stimuli and lead to extracellular Ca^{2+} influx in milliseconds. Physical stimuli and Ca^{2+} influx can also trigger the release of adenosine triphosphate (ATP) from membrane vesicles into the extracellular space and activate the purinergic receptors (*e.g.*, P2Y family) and ligand gated ion channels (*e.g.*, P2X family) on plasma membrane¹²⁸. Activation of P2Y receptors can subsequently stimulate the activation of intracellular phospholipase C (PLC) and the generation of inositol 1,4,5-trisphosphate (IP_3), which can bind to the IP_3 receptor on ER and induces rapid Ca^{2+} release into cytosol. The PLC- IP_3 pathway can also be activated by many other G protein-couple receptors or even mechanical stress on the cell membrane¹²⁹.

Most studies on chondrocyte $[\text{Ca}^{2+}]_i$ signaling were performed on short-term monolayer cultured cells, freshly-isolated cells, and cells seeded in hydrogel constructs^{23,130-133}. The unnatural residing environment can significantly affect chondrocyte phenotype, metabolic activities, and mechanotransduction behaviors¹³⁴. However, imaging of *in situ* chondrocytes in their native ECM, when cartilage is under mechanical loading, remains technically challenging. Loading on cartilage often incurs large, long lasting, and inconstant speed displacement of cells exceeding the imaging field of microscope. In light of a novel microscopy indentation system, Madden et al. first investigated the calcium signaling of *in situ* chondrocytes residing in the superficial zone using intact cartilage-bone explants. The calcium signaling of *in situ* chondrocytes during and immediately after indenting showed a unique correlation pattern with the loading magnitude and also differed in cartilage from femoral condyle and patellar regions²⁴. These findings proved that the calcium signaling of chondrocytes can significantly depend on their surrounding environment and the loading profiles, which intrigued further questions such as how *in situ* chondrocytes

respond during the loading phase and how the calcium responses depend on the aforementioned essential calcium sources and ion channels. As the phenotype of chondrocytes changes along depth, mature chondrocytes may also have different mechanotransduction characters with the pre-mature chondrocytes in the superficial zone. In this study, a custom-designed microscopy loading device was built to apply controlled mechanical loading on cartilage explant, so that the $[Ca^{2+}]_i$ transient of *in situ* mature chondrocytes can be recorded during the loading phase. $[Ca^{2+}]_i$ responses were compared with the spontaneous $[Ca^{2+}]_i$ signaling of chondrocytes in terms of spatiotemporal characteristics. Moreover, roles of seven essential pathways related to $[Ca^{2+}]_i$ signaling were investigated in the loading induced $[Ca^{2+}]_i$ responses of *in situ* chondrocytes.

2.3 Materials and Methods

2.3.1 Cartilage Explant

Cartilage samples were harvested from the central region of femoral condyle heads of fresh calf knee joints (3-6 months old) with mixed gender and side (six joints from Green Village, NJ). The full thickness of cartilage is approximately 5-6 mm. Cylindrical explants (diameter = 3 mm, thickness = 2 mm) from the middle-to-deep zone cartilage were isolated using a biopsy punch and a custom-designed cutting tool³⁴. After harvest, samples were balanced and cultured in DMEM supplemented with 1% ITS+Premix, 50 $\mu\text{g}/\text{ml}$ L-proline, 0.1 μM dexamethasone, 0.9 mM sodium pyruvate and 50 $\mu\text{g}/\text{ml}$ ascorbate 2-phosphate at 37 °C and 100% humidity for 3 days before use³⁴. Dexamethasone was added in the culture medium to preserve the mechanical integrity of calf cartilage explant¹³⁵. On the day of calcium imaging, each

cartilage explant was halved axially by a cutting tool (ASI-Instruments, MI) and stained in the fluorescent calcium dye solution, DMEM with 5 μ M Fluo-8 AM (AAT Bioquest, CA) at 37°C for 40 minutes. Afterwards samples were gently washed in pure DMEM three times with 10 minutes each time. The half-cylindrical cartilage sample, with the cross-section area facing down, was then placed in a glass-slide imaging chamber, which itself was secured on a microscopy-loading device as described below.

2.3.2 Mechanical Loading and Calcium Imaging

A unique loading device was designed and built to apply mechanical loading on cartilage samples during the microscopy imaging (Fig. 2.1A-B). Each of the two opposing loading platens, locating in the imaging chamber, was driven by a high-resolution (0.016 μ m) linear actuator (M-235.5DG, Physik Instrumente, Germany). The two identical actuators, aligned along the same axis, are controlled by two independent servo controllers (C863, Physik Instrumente, Germany). Cartilage samples placed between the two loading platens were compressed from both sides at identical speed (Fig. 2.1C). Displacement of the central region in the explant was offset by the opposing movement of two actuators, which allowed a relatively steady imaging area during the time course of imaging. A miniature load cell (Model 31, Sensotec Inc., Columbus, OH, USA; range 0–10 lbs) was mounted between a loading platen and the corresponding actuator to record the transient resisting forces from the cartilage (Fig. 2.1D). The entire loading device can be secured on the XY stage of a confocal microscope (Zeiss LSM510) to record the fluorescent images of *in situ* chondrocytes.

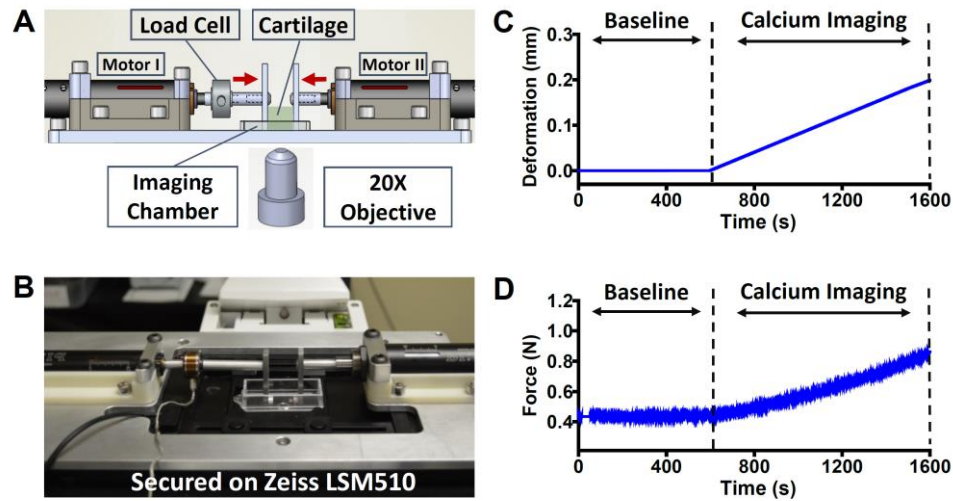


Figure 2.1 A bidirectional microscopy loading device for cartilage explant. (A) A schematic illustration of the device. Cartilage sample is placed in an imaging chamber and submerged in medium. Two parallel loading platens on both sides of the sample are driven by two coaxial motors, respectively. Load cell can record the responding force from cartilage. All components are fixed on a based plate, which itself can be mounted on the X-Y stage of a microscope. (B) A picture of the loading device mounted on a confocal microscope (Zeiss LSM510). (C) Loading profile during the calcium imaging of the cartilage sample. Tissue was compressed at $0.2 \mu\text{m/s}$ for 1,000 seconds ($\sim 10\%$ compression of the cartilage explant). (D) A typical force response curve of the cartilage sample under the compressive loading. Due to the slow loading rate, increase of responding force is close to a linear curve.

During the test, a 0.5 N (0.14 MPa) tare load was first applied to the sample to ensure the full contact between loading platens and cartilage, followed by a 10-minute resting period for cells to recover from previous agitation^{136,137}. The center region of the explant was imaged at a focal plane $\sim 30 \mu\text{m}$ deeper below the cross-section surface, which avoided the cells damaged by previous cutting. During calcium imaging, each loading platen was driven at the speed of $0.1 \mu\text{m/s}$ for 1000 seconds to

reach ~10% final strain, and the real time fluorescent images of the chondrocytes were captured every 1.5 s by confocal microscope during the loading. To compare the mechanically induced $[Ca^{2+}]_i$ responses to the spontaneous $[Ca^{2+}]_i$ signaling in chondrocytes, a half explant was imaged following protocols described above, while the other half was imaged without loading and served as the non-loaded control.

2.3.3 Calcium Signaling Pathways

To understand the molecular mechanisms of the loading-induced $[Ca^{2+}]_i$ responses in chondrocytes, extra cartilage samples were harvested and separated into seven groups. Each sample was cut into two halves and stained in calcium dye solution. A half explant was treated with a specific pathway antagonist 30 min prior to and/or during the calcium imaging, while the other half was incubated in DMEM and served as the untreated control ¹²². Extracellular Ca^{2+} source: After Fluo-8 AM dye, cartilage sample was transferred into calcium-free DMEM for imaging. EGTA, a Ca^{2+} chelator, was also supplemented into the medium to further remove the extracellular Ca^{2+} trapped in the cartilage by the negative charges on glycosaminoglycan (GAG) chains ¹²³. ER calcium store: Cartilage explants were incubated in 1 μ M thapsigargin to deplete the calcium stored in the ER, which is the major intracellular calcium store in chondrocytes ¹³⁸. As the vehicle control for thapsigargin treated samples, cartilage samples were incubated in DMEM supplemented with 0.25% v/v DMSO ¹²⁴. PLC-IP₃ pathway: Cartilage sample was incubated in 11 mM neomycin to inhibit the phospholipase C (PLC) from hydrolyzing phospholipids into inositol triphosphate (IP₃) and diacylglycerol (DAG). IP₃ can induce the calcium release from ER ²³. P2 purinoceptors: PPADS (pyridoxalphosphate-6-azophenyl-2',4'-disulfonic acid) was employed to inhibit the P2

receptors on the cell membrane ($167 \mu\text{M}$)¹²⁸. Although PPADS is known as a P2X inhibitor, it does not completely discriminate between P2X and P2Y receptors. Here, PPADS is utilized as a non-selective antagonist for all P2 receptors

^{24,139}. Mechanosensitive ion channels: Gadolinium chloride (GdCl_3 , $10 \mu\text{M}$) was applied to the cartilage explants to inhibit the mechanosensitive ion channels on the plasma membrane^{25,131}. T-type voltage gated calcium channel (VGCC): NNC55-0396 ($17.7 \mu\text{M}$) was supplied in the medium to block the T-type VGCCs on chondrocytes^{26,137}. TRPV4 channel: GSK205 ($10 \mu\text{M}$) was introduced to cartilage explants to deactivate the TRPV4 channel²⁹. According to the calcium imaging setup and molecular weights of seven chemicals, it was estimated that all chemicals can reach the imaged chondrocytes in < 5 seconds. During the calcium imaging of the treated and control samples, compressive loading was applied to the sample following the loading profile described above.

2.3.4 Data Analysis and Statistics

For each cartilage explant, 50-100 cells located in the center of the imaging area along the thickness direction were analyzed. The total number of explants and cells analyzed for the seven $[\text{Ca}^{2+}]_i$ signaling pathways was listed in Table 1. For each cell, $[\text{Ca}^{2+}]_i$ concentration oscillation was represented by the fluorescent signal intensity of its transients. A cell was defined as responsive if a calcium peak was released with a magnitude four times higher than the maximum fluctuation along the baseline³⁴. The fraction of responsive cells over total cells was calculated as the responsive rate of a sample. For all responsive cells, the number of $[\text{Ca}^{2+}]_i$ peaks during the 16 min loading period was counted. Three extra temporal features of the $[\text{Ca}^{2+}]_i$ peaks, including the time to reach a peak (t_1), relaxation time from a peak (t_2),

and time interval between two neighboring peaks (t_3), were extracted and compared between the control and treated samples as described in our previous studies^{30,136} (Fig. 2.2B). Chi-squared test was utilized to detect the significant difference in the responsive rate between groups. To characterize the intrinsic variation among individual explant, the linear mixed effects model was used to compare the temporal parameters of $[Ca^{2+}]_i$ signaling. The effects of antagonist-treatment on cartilage explant was set as a fixed, constant factor; while the basal $[Ca^{2+}]_i$ signaling parameters of each explant was a random factor. All data were shown as mean \pm SEM. Statistical significance was indicated when $P < 0.05$.

Table 2.1 Number of the Total Cartilage Explants and Chondrocytes Analyzed in $[Ca^{2+}]_i$ Signaling for Seven Pathways

	Extracell. Ca ²⁺	ER store	PLC- IP ₃	P2 receptor	Mechanosensitive ion channel	T-type VGCC	TRPV4
Explant #	3	5	6	3	5	5	5
Cell # of control group	256	408	495	183	294	281	438
Cell # of drug- treated group	216	480	430	186	335	284	546

2.4 Results

2.4.1 Mechanical Loading Enhanced $[Ca^{2+}]_i$ Signaling

The time-lapse images of a sample are shown in Fig. 2.2A. Four cells showing $[Ca^{2+}]_i$ oscillations were marked by white arrows (Fig. 2.2A). $[Ca^{2+}]_i$ oscillation of a cell can be obtained by measuring the average image intensity of each cell in all time-

lapse images (Fig. 2.2B). Typical transient curves of $[Ca^{2+}]_i$ intensity in chondrocytes, loaded or unloaded, were presented in Fig. 2.3A. Cells under both conditions demonstrated prominent $[Ca^{2+}]_i$ oscillations with repetitive and spike-like $[Ca^{2+}]_i$ peaks. The responsive rate of loaded cells was $23.7 \pm 1.4\%$, significantly higher than the spontaneous responsive rate of the non-loaded cells ($16.8 \pm 1.2\%$, $P < 0.01$). The average numbers of multiple $[Ca^{2+}]_i$ peaks per responsive cell were similar between two groups, 2.5 ± 0.17 for the loaded group and 2.5 ± 0.18 for the unloaded group ($P > 0.05$). Consistently, there was no significant difference in the time interval of two neighboring peaks (t_3) between the two groups ($P > 0.05$, Fig. 2.3B). However, it took the loaded chondrocytes significantly shorter time to relax from $[Ca^{2+}]_i$ peaks than the control group (t_2 : 14.6 ± 0.9 s vs. 19.9 ± 1.6 s, $P < 0.01$); and there was a trend toward cells taking shorter time to rise from $[Ca^{2+}]_i$ peaks than the control group (t_1 : 11.9 ± 1.3 s vs. 19 ± 2.3 s, $P = 0.07$).

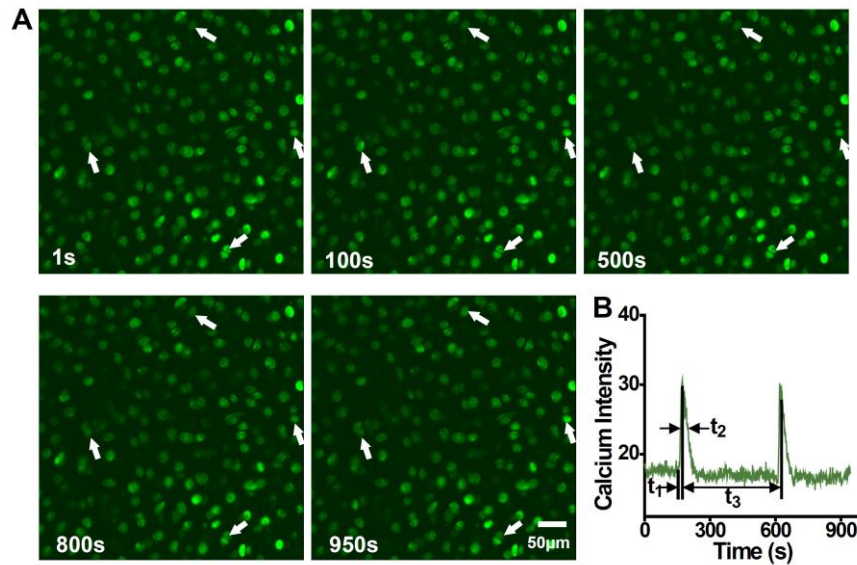


Figure 2.2 $[Ca^{2+}]_i$ responses of *in situ* chondrocytes in a loaded cartilage explant. (A) Calcium images of the chondrocytes stained with Fluo 8 AM at five different time points taken by confocal microscope. White arrows highlight cells with oscillating $[Ca^{2+}]_i$ concentration. Some cells showed multiple calcium peaks. Scales bars = 50 μ m. (B) A typical $[Ca^{2+}]_i$ transient of chondrocyte in cartilage. The characteristic temporal parameters are defined. t_1 denotes the time from baseline to the maximum value of the peak. t_2 is the time from peak value to the 50% relaxation. t_3 is the time interval between two neighboring peaks.

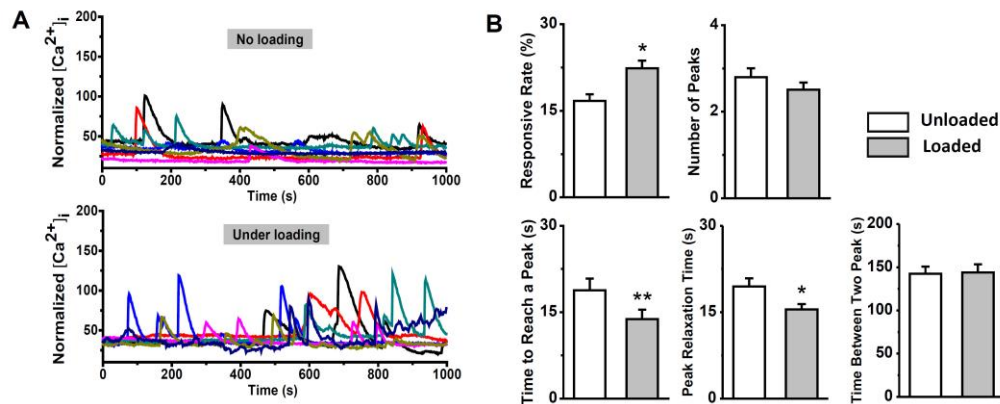


Figure 2.3 Comparison of $[Ca^{2+}]_i$ signaling of *in situ* chondrocytes in the loaded and unloaded cartilage explants. (A) Typical $[Ca^{2+}]_i$ intensity curves of chondrocytes in 1,000 seconds from the loaded and unloaded groups. Each curve represents the calcium transient of a single cell. A large number of chondrocytes can release multiple $[Ca^{2+}]_i$ peaks in 1,000 seconds. (B) Percentage of chondrocytes showed $[Ca^{2+}]_i$ peaks in loaded cartilage is significantly higher than the unloaded sample, while the average number of peaks in each responsive cell had no difference. Temporal parameters of $[Ca^{2+}]_i$ peaks, including time to reach a peak, peak relaxation time, and time between two peaks are compared between two groups. *: P value < 0.05; and **: P value < 0.01.

2.4.2 Extracellular Calcium Influx

Treatment of EGTA that chelated the extracellular Ca^{2+} in medium almost abolished the $[Ca^{2+}]_i$ signaling of *in situ* chondrocytes under compressive loading. Only 2 out of 216 cells exhibited $[Ca^{2+}]_i$ oscillation with a single peak, which was significantly lower than that of the control group ($29.5 \pm 2.1\%$ for responsive rate, $P < 0.001$; 3.0 ± 0.25 for number of peaks, $P < 0.01$) (Fig. 2.4). The limited number of responsive cells ($n = 2$) in the EGTA treated group hindered further comparison of the temporal parameters between two groups.

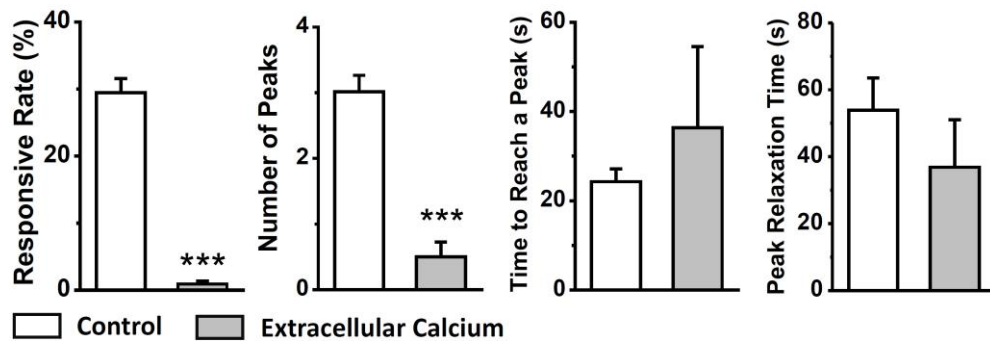


Figure 2.4 Role of extracellular Ca^{2+} source in the $[\text{Ca}^{2+}]_i$ responses of *in situ* chondrocytes in loaded cartilage explants. Few chondrocytes can have $[\text{Ca}^{2+}]_i$ transients after the depletion of extracellular Ca^{2+} in the medium. No responsive cells can have multiple $[\text{Ca}^{2+}]_i$ peaks (time between peaks not showing). Time to reach a peak and peak relaxation time of responsive cells have no difference between the two groups. ***: P value < 0.001.

2.4.3 Roles of ER Calcium Store

Depletion of the ER store by thapsigargin significantly reduced the $[\text{Ca}^{2+}]_i$ responsive rate of *in situ* chondrocytes under loading ($5.2 \pm 0.75\%$ vs. $23.5 \pm 1.4\%$ in the control, $P < 0.001$; Fig. 2.5A). DMSO-treated samples showed similar calcium responsive rate as the non-treated samples, which were randomly selected from the other groups without DMSO supplement ($23.5 \pm 1.42\%$ vs $23.7 \pm 1.43\%$, $n = 5$). A consistent phenomenon was observed when the PLC- IP_3 pathway was blocked by neomycin ($7 \pm 0.84\%$ vs. $34.3 \pm 1.6\%$ in the control, $P < 0.001$) (Fig. 2.5B). The responsive cells treated by neomycin also presented a lower number of peaks compared to the control (1.8 ± 0.26 vs. 2.9 ± 0.22 ; $P < 0.01$) and an increased time interval between peaks (152.70 ± 2.26 vs. 211.02 ± 4.22 ; $P < 0.05$). Compared to thapsigargin and neomycin treatment, PPADS exerted weaker inhibitory effects on the

intracellular Ca^{2+} release. $24.2 \pm 2.2\%$ of cells presented $[\text{Ca}^{2+}]_i$ responses in the PPADS treated group compared to $38.8 \pm 2.5\%$ responsive cells in the untreated control ($P < 0.01$, Fig. 2.5C). Under compressive loading, none of the three drugs exerted substantial effects on the $[\text{Ca}^{2+}]_i$ temporal parameters compared to those of the untreated control samples.

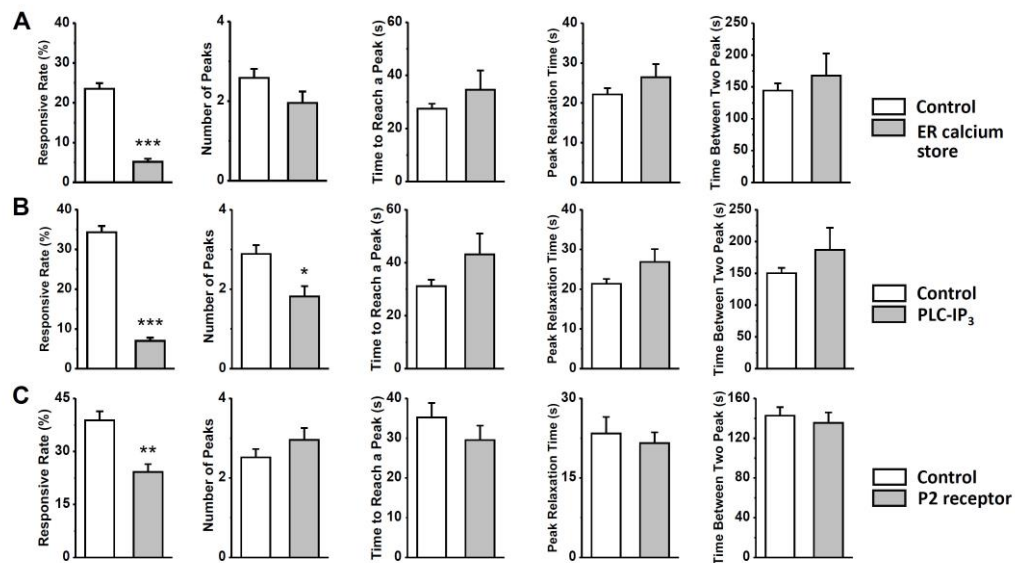


Figure 2.5 Role of P2 receptors and intracellular ER calcium release in the $[\text{Ca}^{2+}]_i$ responses of *in situ* chondrocytes. Cartilage explants are loaded in both control and chemical treated groups. (A) $[\text{Ca}^{2+}]_i$ responses after the ER calcium store was depleted by thapsigargin. (B) $[\text{Ca}^{2+}]_i$ responses with inhibited PLC-IP₃ activities by neomycin. (C) $[\text{Ca}^{2+}]_i$ responses with the presence of PPADS, a P2 receptor inhibitor. *: P value < 0.05; and **: P value < 0.01; and ***: P value < 0.001.

2.4.4 Ion Channels on Plasma Membrane

Blocking the mechanosensitive ion channels by GdCl_3 significantly reduced the responsive rate in loaded chondrocytes ($17.0 \pm 1.5\%$ vs. $28.9 \pm 1.8\%$ in the untreated

group, $P < 0.001$, Fig. 2.6A), but didn't affect the number of $[Ca^{2+}]_i$ peaks or other temporal parameters ($P > 0.05$). Treatment with NNC-55-0936, a selective blocker of T-type VGCCs, also inhibited the *in situ* chondrocytes from releasing $[Ca^{2+}]_i$ peaks under compression ($14.4 \pm 1.5\%$ vs. $30.2 \pm 1.9\%$ for responsive rate, $P < 0.001$, Fig. 2.6B). The blockage of TRPV4 channels by GSK205 prominently reduced the proportion of chondrocytes with $[Ca^{2+}]_i$ responses under compressive loading, as only $6\% \pm 0.76\%$ of cells responded ($18.3 \pm 1.9\%$ in control, $P < 0.001$) (Fig. 2.6C). Interestingly, the relaxation duration of $[Ca^{2+}]_i$ peaks was significantly shortened when the TRPV4 channel was blocked ($P < 0.05$). These results indicated the important roles of T-type VGCCs and TRPV4 channel in regulating the temporal rhythm of $[Ca^{2+}]_i$ signaling.

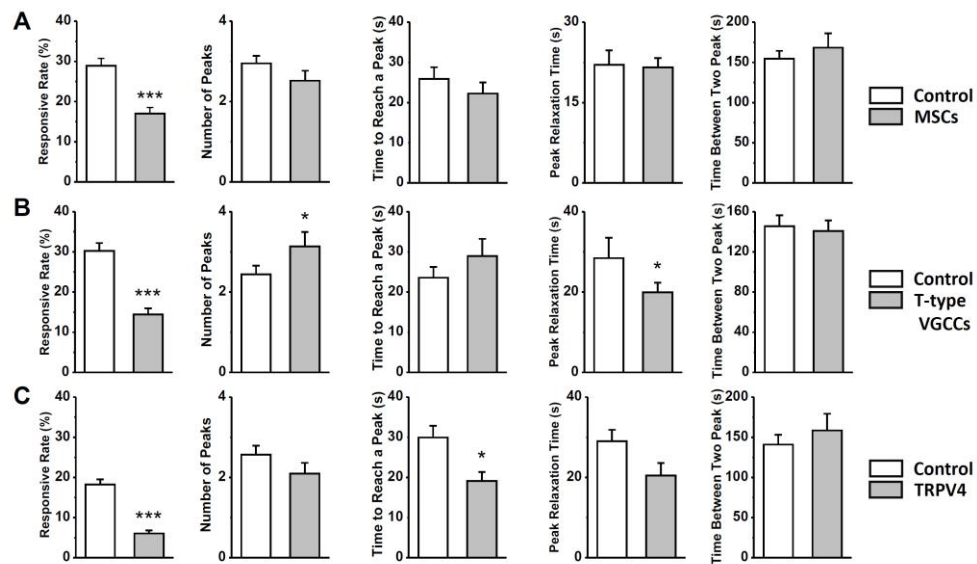


Figure 2.6 Role of three nonselective ion channels in the $[Ca^{2+}]_i$ responses of *in situ* chondrocytes. Cartilage explants are loaded in both control and chemical treated groups. (A) $[Ca^{2+}]_i$ responses with the mechanosensitive channels blocked by gadolinium. (B) $[Ca^{2+}]_i$ responses with the T-type VGCCs blocked by NNC55-0396. (C) $[Ca^{2+}]_i$ responses with the TRPV4 channel blocked by GSK205. *: P value ≤ 0.05 ; and **: P value ≤ 0.01 ; and ***: P value < 0.001 .

2.5 Discussion

Metabolic activities of chondrocytes are extensively regulated by the mechanical and other physical stimuli from the ECM and surrounding fluid. The profiles and magnitudes of these stimuli are dependent on the unique composition, nanostructure, organization, and mechanical behaviors of the peri- and extra-cellular matrix. In addition, phenotype and mechanobiology behaviors of chondrocytes change with the surrounding environment. Therefore, primary chondrocytes cultured in monolayer, 3-dimensional hydrogel, and residing in their native environment could have distinct responses to identical physical stimuli. As a soft connective tissue,

cartilage deforms easily over 10% strain in its daily activities, which makes the microscopy recording of the cell activities in its natural environment challenging. In this study, a bi-directional loading device was built to minimize the movement of tissue in the center of loaded cartilage sample, so that the calcium imaging of *in situ* chondrocytes can be recorded. Compressive loading was chosen here as it is the dominant physiological loading pattern on articular cartilage.

Under compression, a number of physical stimuli are generated and applied on the chondrocytes. Although mechanical loading on cell body can induce vigorous $[Ca^{2+}]_i$ responses, actual stress or strain on the cell body could be much lower than those of the ECM due to the presence of a pericellular matrix, which functions as a soft cushion surrounding the chondrocyte and dampens the actual loading on the cell body in a largely deformed cartilage^{140,141}. Deformation of *in situ* chondrocytes was found to be lower than the ECM strain in an experimental study¹⁴². A 15% compressive strain in ECM may result in merely 9% compression of cell height. Therefore, the actual decrease of chondrocyte height could be lower than 10% in the present study. In contrast to the dampened stress and strain on chondrocytes, ascent of hydrostatic pressure in the loaded cartilage can be fully sensed by the cells, which can also induce calcium responses. Compression of ECM can squeeze the interstitial fluid out of the cartilage, which in theory should generate fluid flow or shear stress on cell membrane. Due to the low permeability of ECM, fluid flow speed in the loaded cartilage is extremely slow and at tens of nanometers per second^{143,144}, and the resulting fluid shear stress on cell membrane is negligible in comparison to those in most fluid flow induced calcium signaling studies (~5-40 dynes/cm²). Thus fluid flow

might be a minor stimulation responsible for the $[Ca^{2+}]_i$ responses of *in situ* chondrocytes.

The extracellular matrix of cartilage is negatively charged due to the presence of GAG chains. The fixed charges in ECM attract extra cations into the tissue and further generate the so-called Donnan's osmotic pressure in cartilage¹²³. Compression of the ECM increases the density of fixed charges (~12% increase at 10% volume change of ECM), which causes a cascade of mechano-electrochemical stimuli on the chondrocytes. First, higher fixed charge density will result in higher osmotic pressure, which represents a major source of osmotic stress on chondrocytes. Osmotic stress can induce vigorous $[Ca^{2+}]_i$ responses in chondrocytes due to the presence of TRPV4 channels²⁹. As the PCM of chondrocytes is much softer than the ECM, volume of chondrocytes can easily expand or shrink under different osmolarity, which can further activate the mechanosensitive channels on plasma membrane. Second, denser fixed charges will attract more cations to maintain electric neutrality. Fluctuation of cation concentration can activate calcium or ion channels on the plasma membrane and cause Ca^{2+} influx¹³¹. Third, increased fixed charge density changes the electrical potential across the ECM at millivolt level¹⁴⁵, which represents another strong stimulation for $[Ca^{2+}]_i$ responses³¹. Lastly, due to the unbalanced free cations and anions in the fluid phase, compression of ECM results in both streaming potential and diffusion potential across the tissue¹⁴⁶. All of these mechano-electrochemical stimuli, especially the stress/strain^{27,147}, osmotic stress^{28,29}, and electric potential³¹, could be responsible for the promoted $[Ca^{2+}]_i$ signaling in the loaded cartilage as observed in this study.

Temporal features of the $[Ca^{2+}]_i$ peaks in the loaded cartilage are different to those in the unloaded tissue. The rising time, defined as the time for $[Ca^{2+}]_i$ rising from the baseline to the highest value, is significantly shortened in the loaded sample, while the relaxation or recover time of $[Ca^{2+}]_i$ is also reduced. This finding is consistent with a previous study using chondrocyte-agarose model subjected to cyclic compression²³. Mechanical loading induced stimuli, as aforementioned, could activate or open extra ion channels on the plasma membrane, which accelerate the influx and efflux of Ca^{2+} . Moreover, as mechanical loading promotes the convection and diffusion of free Ca^{2+} in ECM, abundant extracellular Ca^{2+} may also attribute to the short duration of $[Ca^{2+}]_i$ peaks. In this study, mechanical loading had no significant effect on the frequency of $[Ca^{2+}]_i$ peaks or the time interval between two neighboring peaks. Therefore, the refractory time after a $[Ca^{2+}]_i$ peak is not changed in chondrocytes by the mechanical loading, which was also observed in literature²³.

Although the increase of $[Ca^{2+}]_i$ has two sources, the extracellular Ca^{2+} influx and the release of intracellular store, removal of extracellular Ca^{2+} with EGTA almost completely abolished the $[Ca^{2+}]_i$ signaling of *in situ* chondrocytes. According to the results in this study, $[Ca^{2+}]_i$ signaling of chondrocytes, either spontaneous or load induced, has to be initiated by the extracellular Ca^{2+} influx. Previous studies also found that deformation of chondrocyte surface cannot induce any $[Ca^{2+}]_i$ responses after removing the extracellular Ca^{2+} , even with the presence of full intracellular calcium stores^{23,131}. We also noticed that osteocytes and osteoblasts have no $[Ca^{2+}]_i$ responses under fluid flow or AFM indenting in Ca^{2+} free medium^{136,148}. In this study, when cartilage was balanced in abundant Ca^{2+} free medium, $[Ca^{2+}]_i$ responses can still be observed in the chondrocytes unless extra EGTA was supplemented into the

medium (results not shown). Due to the negatively charged nature of ECM, Ca^{2+} can be tightly trapped inside cartilage. It is difficult to fully deplete the interstitial Ca^{2+} by putting the tissue in Ca^{2+} free medium. In contrast, EGTA can actively chelate and deplete the trapped Ca^{2+} . $[\text{Ca}^{2+}]_i$ signaling of *in situ* chondrocytes observed in the Ca^{2+} free medium also implies that even a low density of extracellular Ca^{2+} is sufficient to initiate the $[\text{Ca}^{2+}]_i$ responses in chondrocytes. This may explain the significantly reduced, but not completely abolished, $[\text{Ca}^{2+}]_i$ responses found in the Ca^{2+} depleted environment using chondrocyte-agarose construct models ^{23,147}.

Significant inhibitory effects on $[\text{Ca}^{2+}]_i$ responses were observed by blocking purinergic receptors, depletion of ER store, or inhibition of PLC-IP₃ pathway of *in situ* chondrocytes, which are consistent with previous studies ^{23,138}. Influx of Ca^{2+} can stimulate vesicular ATP release, which in turn activates the purinergic (P2) receptors on cell membrane ¹²⁸. P2X, one of the five subclasses of P2 family, are ligand-gated nonselective ion channels, which can directly facilitate extracellular Ca^{2+} influx. In contrast, activation of P2Y receptors results in the Ca^{2+} release from ER via PLC-IP₃ pathway. Therefore, extracellular ATP has the capability to induce full $[\text{Ca}^{2+}]_i$ responses in cells ²³. Moreover, as a small molecule, ATP can easily diffuse or transport in fluid to neighboring cells. We have reported that extracellular ATP diffusion is a major mechanism facilitating the calcium wave propagation across the cell networks ^{148,149}. In this study, responsive rate of chondrocytes was significantly reduced when ATP-related pathway was interrupted. Therefore, the calcium signaling observed in the loaded cartilage are not all induced by the mechanical loading or related stimuli. $[\text{Ca}^{2+}]_i$ responses of many chondrocytes are actually initiated by the release of ATP from neighboring cells, while the mechanical loading could promote

the diffusion and convection of ATP in the ECM. This study demonstrated that extracellular ATP serves as an essential second messenger for cell-cell communication among the isolated chondrocytes.

TRPV4 ion channel can be activated by various stimuli, including osmotic stress, mechanical loading, and heat. TRPV4 plays a key role in regulating calcium homeostasis and matrix metabolism in cartilage^{29,150}, while TRPV4-dysfunction is associated with the development of osteoarthritis^{151–153}. In the compressed cartilage, both mechanical loading and osmotic stress can activate the TRPV4 channel and initiate the $[Ca^{2+}]_i$ transients. In this study, inhibition of TRPV4 significantly reduced the $[Ca^{2+}]_i$ responses in loaded cartilage. In addition, TRPV4 is believed to be a slow non-selective ion channel, as a delay in response to osmotic stimulation was observed in TRPV4-expressing cells¹⁵⁴. This feature may attribute to the shortened rising time of $[Ca^{2+}]_i$ peak in the TRPV4-blocked chondrocytes. Mechanosensitive ion channels on the cell membrane are believed to be responsible for the mechanotransduction of most musculoskeletal cells. The treatment of cartilage explants with gadolinium led to a significantly decreased percentage of cells responding to the compressive loading. This is consistent with most of the previous studies^{23,147}. Recently, PIEZO1 and PIEZO2 are identified as two mechanosensitive channels on chondrocytes, which have to work synergistically to initiate the $[Ca^{2+}]_i$ responses in the loaded cells¹²⁶. Future study is of necessity to understand the roles of different mechanosensitive channels in the $[Ca^{2+}]_i$ signaling of *in situ* chondrocytes¹³¹. Another important finding is that T-type VGCCs play a critical role in chondrocyte $[Ca^{2+}]_i$ signaling. T-type VGCC is activated by low voltage stimulation followed by depolarization of the plasma membrane and elevation of $[Ca^{2+}]_i$ concentration¹⁵⁵. The physiological roles of T-type

channels are often accomplished by the distinctive low activation threshold of these channels, which boosts up membrane depolarization in excitable cells. In this study, inhibition of T-type VGCC on chondrocytes reduced the $[Ca^{2+}]_i$ responsive percentage by ~50%, implying that a large number of chondrocytes are relying on the activation of T-type VGCCs to initiate the $[Ca^{2+}]_i$ responses under loading, although chondrocyte is often regarded as non-excitable cells. Our recent study also found that inhibition of T-type VGCCs suppressed the OA progression in meniscus dislocated mouse model¹²⁷.

There are several limitations we would like to point out regarding this study. First, to study the mature chondrocytes in the middle layer of cartilage, a cross section area had to be created to image the cells underneath the cutting surface. This sample preparation process may change the mechanical behaviors of cartilage and further the stimuli on chondrocytes when the tissue was loaded. Calcium signaling of superficial zone chondrocytes has been studied *in situ* previously²⁴. The middle zone cartilage, with randomly oriented collagen fibrils, serves as the first line of resistance to compressive forces. Therefore, it is also important to understand the mechanobiology behaviors of mature chondrocytes in the middle layer. Second, although the 10% compressive strain on cartilage is physiological relevant, the loading rate in this study was much slower than that in daily activities. The slow loading rate assisted the imaging of the same cell population during the entire loading phase. The displacement of chondrocytes in the middle area was largely cancelled out by the bi-directional loading, but the residual displacement at fast speed could still affect the track and imaging of chondrocytes.

we successfully recorded the $[Ca^{2+}]_i$ response during compressive loading phase, the loading profile employed herein is at low speed, non-dynamic. This loading protocol was designed to overcome the dramatic shifts of $[Ca^{2+}]_i$ imaging under confocal microscope due to directly mechanical loading. We optimized the loading protocol to be able to apply ~10% strain during the imaging period, reasonably mimicking the strain of hyaline cartilage of knee during moderate daily activities. The interpretation of results still need to be in caution.

In conclusion, a new microscopy loading device was built to record the $[Ca^{2+}]_i$ responses of *in situ* chondrocytes in the loaded cartilage. Compressive loading induced $[Ca^{2+}]_i$ responses in more chondrocytes and also shortened the duration of $[Ca^{2+}]_i$ peaks in comparison to the non-loaded tissues. Roles of seven pathways in chondrocyte $[Ca^{2+}]_i$ signaling were identified. Extracellular Ca^{2+} influx is required for the initiation of $[Ca^{2+}]_i$ transients. Diffusion of extracellular ATP represents an essential mechanism for the intercellular communication between chondrocytes. TRPV4, mechanosensitive, and T-type VGCC ion channels on plasma membrane all play critical roles in the initiation of $[Ca^{2+}]_i$ signaling in the chondrocytes.

Chapter 3

IDENTIFICATION OF CHONDROCYTE GENES AND SIGNALING PATHWAYS IN RESPONSE TO ACUTE JOINT INFLAMMATION²

Identification of Chondrocyte Genes and Signaling Pathways in Response to Acute Joint Inflammation

Mengxi Lv^{1,2}, Yilu Zhou², Shawn W. Polson¹, Leo Q. Wan³, Meiqing Wang⁴, Lin Han⁵,
Liyun Wang², X. Lucas Lu^{1,2}

¹*Center for Bioinformatics and Computational Biology, University of Delaware, Newark, DE, United States*

²*Department of Mechanical Engineering, University of Delaware, Newark, DE, United States*

³*Department of Biomedical Engineering, Rensselaer Polytechnic Institute, Troy, NY, United States*

⁴*Department of Oral Anatomy and Physiology and TMD, the Fourth Military Medical University, Xi'an, Shanxi, China*

⁵*School of Biomedical Engineering, Science, and Health Systems, Drexel University, Philadelphia, PA, United States*

² This chapter was published in *Scientific Report* 9, Article number: 93 (2019). The permission for full-article use was attached in Appendix.

3.1 Abstract

Traumatic joint injuries often result in elevated proinflammatory cytokine (such as IL-1 β) levels in the joint cavity, which can increase the catabolic activities of chondrocytes and damage cartilage. This study investigated the early genetic responses of healthy *in situ* chondrocytes under IL-1 β attack with a focus on cell cycle and calcium signaling pathways. RNA sequencing analysis identified 2,232 significantly changed genes by IL-1 β , with 1,259 upregulated and 973 downregulated genes. Catabolic genes related to ECM degeneration were promoted by IL-1 β , consistent with our observations of matrix protein loss and mechanical property decrease during 24-day *in vitro* culture of cartilage explants. IL-1 β altered the cell cycle (108 genes) and Rho GTPases signaling (72 genes) in chondrocytes, while chondrocyte phenotypic shift was observed with histology, cell volume measurement, and MTT assay. IL-1 β inhibited the spontaneous calcium signaling in chondrocytes, a fundamental signaling event in chondrocyte metabolic activities. The expression of 24 genes from 6 calcium-signaling related pathways were changed by IL-1 β exposure. This study provided a comprehensive list of differentially expressed genes of healthy *in situ* chondrocytes in response to IL-1 β attack, which represents a useful reference to verify and guide future cartilage studies related to the acute inflammation after joint trauma.

3.2 Introduction

Interleukin 1 β (IL-1 β) is an essential mediator of acute joint inflammation after traumatic injuries, one of the potential causes of post-traumatic osteoarthritis (PTOA). Within 24 hours after trauma injuries, the concentration of IL-1 β in synovial fluid can increase up to 70 times to 140 pg/mL in human^{156,157} and 7 times to 6 ng/mL in mice¹⁵⁸. Overexpression of IL-1 β protein is also observed in chondrocytes of early osteoarthritic cartilage^{159,160}. High level of IL-1 β aggravates the catabolic activities of synovial cells and chondrocytes^{161,51} and stimulates chondrocytes to enter an abnormal phenotypic shift, such as proliferation of pre-chondrocytes, swelling of mature chondrocytes, and hypertrophic differentiation of cells in deep zone^{48,49}. Associated with these changes are the increased release of enzymes from chondrocytes, such as the MMP (matrix metalloproteinases) and ADAMTS (a disintegrin and metalloproteinase with thrombospondin motifs) families. Thus acute inflammatory attack often results in the degeneration of healthy cartilage^{51,52}.

Due to its important role in OA pathology, IL-1 β -treated articular cells or tissues have been widely adopted as *in vitro* models to study OA initiation or PTOA^{161,162}. For both isolated and *in situ* chondrocytes, IL-1 β has been observed to induce transient concentration changes of intracellular calcium [Ca²⁺]_i and small GTPases. The coordination of Rho GTPases signaling and [Ca²⁺]_i signaling plays a fundamental role in cytoskeleton organization, regulating the chondrocyte phenotypic shift and cartilage ECM homeostasis^{48,49}. Many of these studies focused on specific genes/pathways in chondrocytes. A systematic study to clarify the effects of IL-1 β on the entire gene expression profile and signaling transduction coordination remains lacking. In this study, we put special focus on the healthy chondrocytes under intensive inflammatory cytokine attack, which is a common scenario during acute

inflammation phase after traumatic injuries, such as ACL rupture or meniscus tear in the knee joint.

The objective of this study is to obtain a complete list of gene expression changes in the healthy chondrocytes that are subjected to acute inflammatory attack. To maintain the natural environment of chondrocytes and perform longitudinal evaluation of cells and ECM, fresh cartilage explants were cultured *in vitro* and treated with IL-1 β . We performed RNA sequencing analysis on the treated chondrocytes, as well as the enrichment analysis in KEGG curated pathways. To verify and understand the changes in genetic profiles, we also tracked the loss and synthesis of ECM components longitudinally, the poroelastic properties of ECM, the proliferation of cells, the change of cell volume and calcium signaling of *in situ* chondrocytes.

3.3 Materials and Methods

3.3.1 Effects of IL-1 β on Cartilage Matrix and Chondrocytes

Cartilage explant harvest: Overall experimental design was outlined in Fig. 3.1a. Fresh young bovine knee joints (3-6 months old) were obtained from a local slaughter house (Green Village, NJ). Cylindrical cartilage explants (diameter = 3 mm, thickness = 2 mm) were harvested from the central, load-bearing region of femoral condyle head using a biopsy punch (Fig. 3.1a). After harvesting, samples were cultured in the chondrogenic medium (DMEM, 1% ITS + Premix, 50 μ g/mL L-proline, 0.9 mM sodium pyruvate, 50 μ g/mL ascorbate 2-phosphate) at 37 °C for 72 hours before further experiments^{135,34}. After the balance to *in vitro* environment, cartilage explants were cultured in the medium supplemented with 1, 10, or 25 ng/mL bovine IL-1 β recombinant protein (RBOIL1BI, Thermo Fisher) for 8 days. Matching

samples from the same region on the condyle head were cultured in regular medium and served as the non-IL-1 β treated control.

Loss of sGAG and collagen contents over time: During the *in vitro* culture of cartilage explants (n = 10 explants from 5 animals per group), the culture medium (500 μ L/sample) was changed and collected every other day. The sGAG and collagen assay were performed as described previously^{163,20}. The accumulative sGAG or collagen loss was calculated as the sGAG or collagen released into the medium divided by the sum of sGAG or collagen contents in both explant and culture medium²⁰. According to the temporal features of IL-1 β -induced ECM degradation from cartilage explant²⁰, the sGAG loss was measured during the first 8-day culture, while the collagen loss was tracked for 24 days. Different cartilage explants were used to track the losses of sGAG and collagen, respectively.

Histology: After 2- and 8-day culture, histological analysis was performed on cartilage explants from the IL-1 β treated and control groups (n = 2 explants from 2 animals per group). Explants were cut into 5- μ m thick sections along depth direction and stained with Safranin O (Sigma) and Hematoxylin and Eosin Y (H&E, Sigma).

Cell swelling and proliferation: To evaluate the effect of IL-1 β on chondrocyte volume, cartilage explants cultured in the regular medium and IL-1 β -supplemented medium (n = 4 explants from 2 animals per group) were dyed with red fluorescent cell tracker (Red CMTPX Dye, Thermo Fisher) and imaged on a confocal microscope (Zeiss 510) after 4-day culture. The fluorescent image stacks were reconstructed into a 3D image in Image J¹⁶⁴. The volume of *in situ* chondrocytes was registered and quantified (n \approx 30 cells from each explant). To estimate the cell proliferation rate, primary chondrocytes were extracted from cartilage explants (n = 4 explants from 2

animals per group). MTT assay was then performed following the previous instructions¹⁶⁵.

Mechanical properties: Unconfined compression test was used to longitudinally measure the mechanical properties of the cartilage explants at days 2 and 8 (n = 10 explants from 5 animals per group; samples cultured for mechanical testing only)¹⁶⁶. During the test, a 10% strain was applied on the cartilage sample at a constant speed followed by a 20-min relaxation period. After the reaction force reached an equilibrium state, sinusoidal dynamic loading was applied on the sample for 15 minutes at 0.5 Hz with a magnitude of $\pm 1\%$ ³². Equilibrium Young's modulus and dynamic modulus of the samples were determined using the recorded force. Hydraulic permeability of the tissue was obtained by curve-fitting the stress relaxation curve using a nonlinear poroelastic model for cartilage^{124,167}.

3.3.2 RNA Sequencing Analysis and qRT-PCR of IL-1 β Treated Cartilage

Cartilage explants were assigned into two groups and cultured in: 1) regular medium, and 2) 1 ng/mL IL-1 β supplemented medium for 48 hours (n= 4 explants from 4 animals per group). The cellular RNA was extracted¹⁶⁸. RNA samples with mass > 2 μ g and RIN score > 6.5 were qualified for the following RNA sequencing and qRT-PCR tests. The sample size and quality test threshold were determined according to literature guidelines^{169,170}.

RNAseq library of each sample was constructed from 1 μ g of RNA using the TruSeq® Stranded mRNA Sample Preparation Kit (Illumina). Samples were pooled and sequenced on the Illumina HiSeq 2500, and at least 13 million reads (51 bp single-end read) were generated for each sample. Data processing was performed using CLC Genomics Workbench v7.5 (QIAGEN). The low-quality sequence ends (> Q15),

sequencing adapters, read with ambiguous nucleotides (> 1 nucleotide), and short sequences (< 40 bp after trimming) were removed before mapping to the bovine genome (version 4.6.1). Gene expression value was calculated as the total number of unique reads mapped to the exon sequence and normalized to reads per kilo base of transcript per million mapped reads (RPKM), and RPKM should correlate positively to the expression level of each gene. The differential expression of each gene was determined by the generalized linear model with animal as a random variable ¹⁷¹. A stringent cutoff of False Discovery Rate (FDR) < 0.05 and absolute fold change > 2 was adopted to identify the differentially expressed genes (DEGs) between the IL-1 β treated and the control samples.

Enrichment analysis of protein families and Gene Ontology annotations on DEGs data set was performed by Panther Classification System ¹⁷². Enrichment analysis of pathways was performed using Reactome software ¹⁷³. To remove redundancy, only the enriched pathways from levels two to three defined by Reactome were reported and grouped by the level one parent pathway. The KEGG pathways generated by Pathview (version 3.6) were used to visualize the changes in a specific signaling pathway ^{174,175}.

To verify the RNA sequencing data, qRT-PCR was performed on the same RNA used for sequencing. Expression levels of seven major metabolic genes in chondrocytes were quantified, including aggrecan (ACAN), type II collagen (COL2A1), MMP-1, -9, -13 and ADAMTS-4, -5. Gene expression fold change was calculated using the $2^{-\Delta\Delta C(T)}$ method after data normalized to the average of reference gene (β -actin, ACTB).

3.3.3 Calcium Signaling of Chondrocytes

Spontaneous $[Ca^{2+}]_i$ signaling of *in situ* chondrocytes in cartilage explant was analyzed after 48-hour IL-1 β treatment and compared to that of control. After the IL-1 β treatment, cartilage explants (n = 5) were halved axially and dyed with 5 μ M Fluo-8AM for 40 minutes^{34,32}. Dyed sample was placed in an imaging chamber and mounted on a confocal microscope (Zeiss LSM510) (Fig. 3.4b). Calcium images of the *in situ* chondrocytes located in the center of cross section area were recorded every 1.5 seconds for 15 minutes. $[Ca^{2+}]_i$ signaling of chondrocytes was analyzed as we described previously^{32,35}. The responsive percentage of cells was calculated as the fraction of cells with one or more $[Ca^{2+}]_i$ peaks over the total number of cells. The spatiotemporal parameters of the $[Ca^{2+}]_i$ peaks, including the number of multiple peaks, the magnitude of peaks, the time to reach a peak and the time interval between neighboring peaks, were also measured and compared.

3.3.4 Statistical Analysis

Tukey's Honestly Significant Difference test was performed following the one-way ANOVA to compare the sGAG loss induced by multiple IL-1 β dosage. The Chi-square test was utilized to compare the responsive rate of $[Ca^{2+}]_i$ signaling. Student's *t*-test was performed to compare all the other data between the IL-1 β (1ng/mL) and control groups. All data were shown as mean \pm 95% confidence intervals. Statistical significance was indicated when P value < 0.05.

3.4 Results

3.4.1 Cartilage Degradation Induced by IL-1 β

To assess the direct effects of IL-1 β on cartilage structure integrity, we tracked the ECM contents loss using an *in vitro* culture cartilage explant model (Fig. 3.1a). Cylindrical cartilage explants were harvested from femoral condyle head of calf knee joints and cultured in chemically defined medium up to 24 days. IL-1 β was supplemented into the culture medium, inducing the loss of sGAG content from cartilage explant in a dosage- and time-dependent manner (Fig. 3.1b). After 8-day treatment, IL-1 β at concentration of 10 ng/mL and 25 ng/mL resulted in greater than 90% sGAG loss from the cartilage respectively (Fig. 3.1b). In contrast, 1 ng/mL IL-1 β induced a stable, almost linear sGAG loss accumulating up to 50% on day 8 ($46.0 \pm 6.4\%$ vs. $13 \pm 1.2\%$ in the control group) (Fig. 3.1b). According to this data, we adopted 1 ng/mL IL-1 β treatment in the following tests. In mouse knee joint, the concentration of IL-1 β can reach 6 ng/mL after traumatic damage¹⁵⁸. IL-1 β concentration of 1 ng/mL has been adopted widely in previous studies using animal cartilage samples^{20,176}. Loss of collagen content induced by 1 ng/mL IL-1 β remained at a low rate on the first 8 days and significantly accelerated afterwards (Fig. 3.1c). After 24 days, collagen loss accumulated to $32.7 \pm 4.3\%$ (control: $4.9 \pm 0.5\%$). IL-1 β at 1 ng/mL showed no significant effects on the sGAG or collagen synthesis rate of the *in situ* chondrocytes (Fig. 3.1d-e).

Safranin O staining revealed the spatial pattern of sGAG loss across the cartilage explant (Fig. 3.1f). After mere 2-day IL-1 β treatment, sGAG loss can be noticed in the surrounding areas of the treated explant. The difference between the control and treated samples became even more evident on day 8. Loss of sGAG

content showed a sharply increasing gradient along the center to edge direction. Such inhomogeneous sGAG loss pattern can significantly compromise the tissue stiffness at small strain, as the outer layer with low sGAG content has little resistance to compression and will be easily compressed under small loading. Mechanical properties of cartilage explants reflected the degradation and loss of ECM components. After 8-day IL-1 β treatment, both Young's modulus (treated vs. control: 0.09 ± 0.02 vs. 0.21 ± 0.03 MPa) and dynamic modulus (4.14 ± 0.38 vs. 5.89 ± 0.7 MPa) decreased significantly, while the hydraulic permeability of the tissue increased by over 150% (treated vs. control: $3.71 \pm 0.81 \times 10^{-15}$ vs. $1.43 \pm 0.32 \times 10^{-15}$ m⁴/N·s) (Fig. 3.1g). No significant differences in mechanical properties were detected after 2-day IL-1 β treatment.

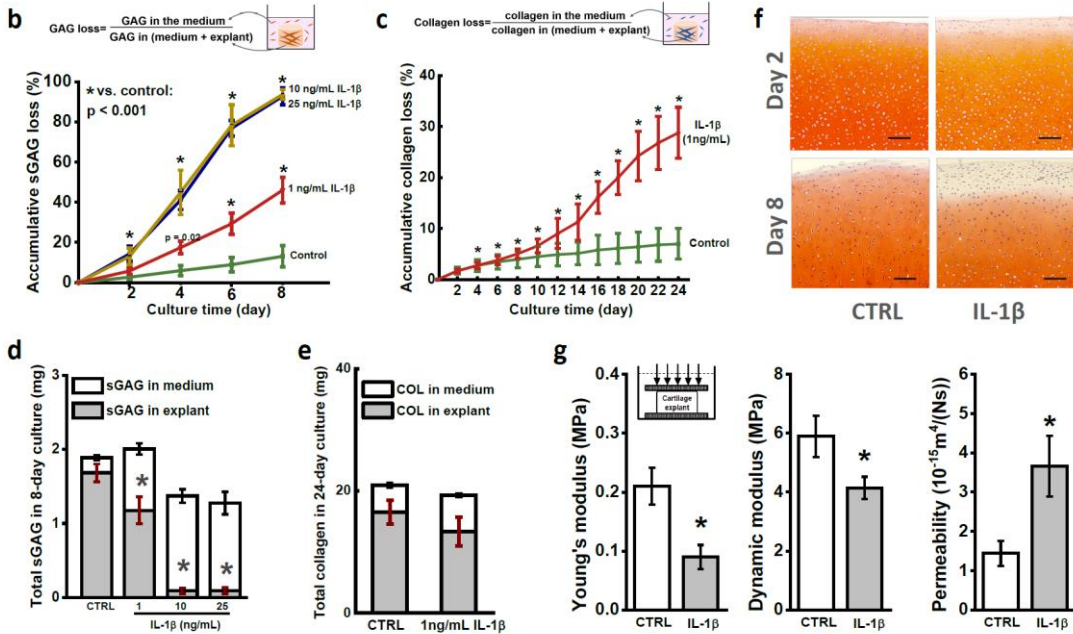
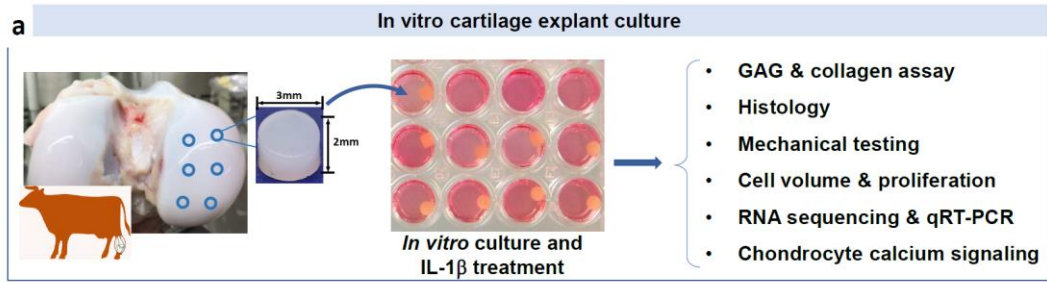


Figure 3.1 Effects of IL-1 β during the long-term *in vitro* culture of cartilage explants. (a) Schematic diagram of experimental design. Cylindrical cartilage explants (diameter = 3 mm, thickness = 2 mm) were harvested from the central region of femoral condyle head of bovine knee joint using a biopsy punch. (b) Accumulative loss of sGAG content from cartilage explants during 8-day treatment of different doses of IL-1 β . The accumulative sGAG loss was defined as the total sGAG released into the culture medium divided by total sGAG content in explant and culture medium. (c) Accumulative collagen loss from cartilage explant in 24-day treatment of 1 ng/mL IL-1 β . (d) The total sGAG content of cartilage explants, which includes the sGAG released into medium (white bar) and sGAG left in explants (grey bar) at the end of 8-day culture. (e) The total collagen content and distribution of collagen in medium and explant after 24-day culture. (f) Safranin O staining of the superficial zone of cartilage explant after 2- and 8-day culture. Scale bar = 200 μ m. (g) Mechanical properties of cartilage explants after 8-day IL-1 β treatment, including equilibrium Young's modulus, dynamic modulus, and permeability. All data were shown as mean \pm 95% confidence intervals. *: vs control, $p < 0.001$ if otherwise marked.

3.4.2 Differentially Expressed Genes (DEGs)

RNA sequencing was used to assess the early gene expression profile of *in situ* chondrocytes under the stimulation of IL-1 β . Compared to the healthy control, IL-1 β treatment induced 2,232 DEGs (absolute value of fold change > 2 and FDR < 0.05) in the chondrocytes, among which 1,259 genes were upregulated (fold change = $\frac{\text{expression level in IL-1 } \beta}{\text{expression level in control}}$) and 973 genes downregulated (fold change = $\frac{\text{expression level in control}}{\text{expression level in IL-1 } \beta}$). The heat map of DEGs is composed of four sharply isolated blocks that indicated the prominent effects of IL-1 β on chondrocyte transcriptional profiles (Fig. 3.2a). Fold changes of all the genes were analyzed in Fig. 3.2b. In total, 12,655 genes were mapped, with 17.6% DEGs. The fold changes of MMP-1, MMP-9, MMP-13, ADAMTS-4, ADAMTS-5, ACAN, and COL2A1, determined by the qRT-PCR and RNA sequencing were highly consistent, with a

Pearson's R value of 0.99 and an adjusted R^2 of 0.97 (Fig. 3.2c). IL-1 β -induced expression changes in catabolic genes (MMPs and ADAMs) were hundreds of folds and much higher than the changes (a few folds) of anabolic genes (COL2 and ACAN) 20,177.

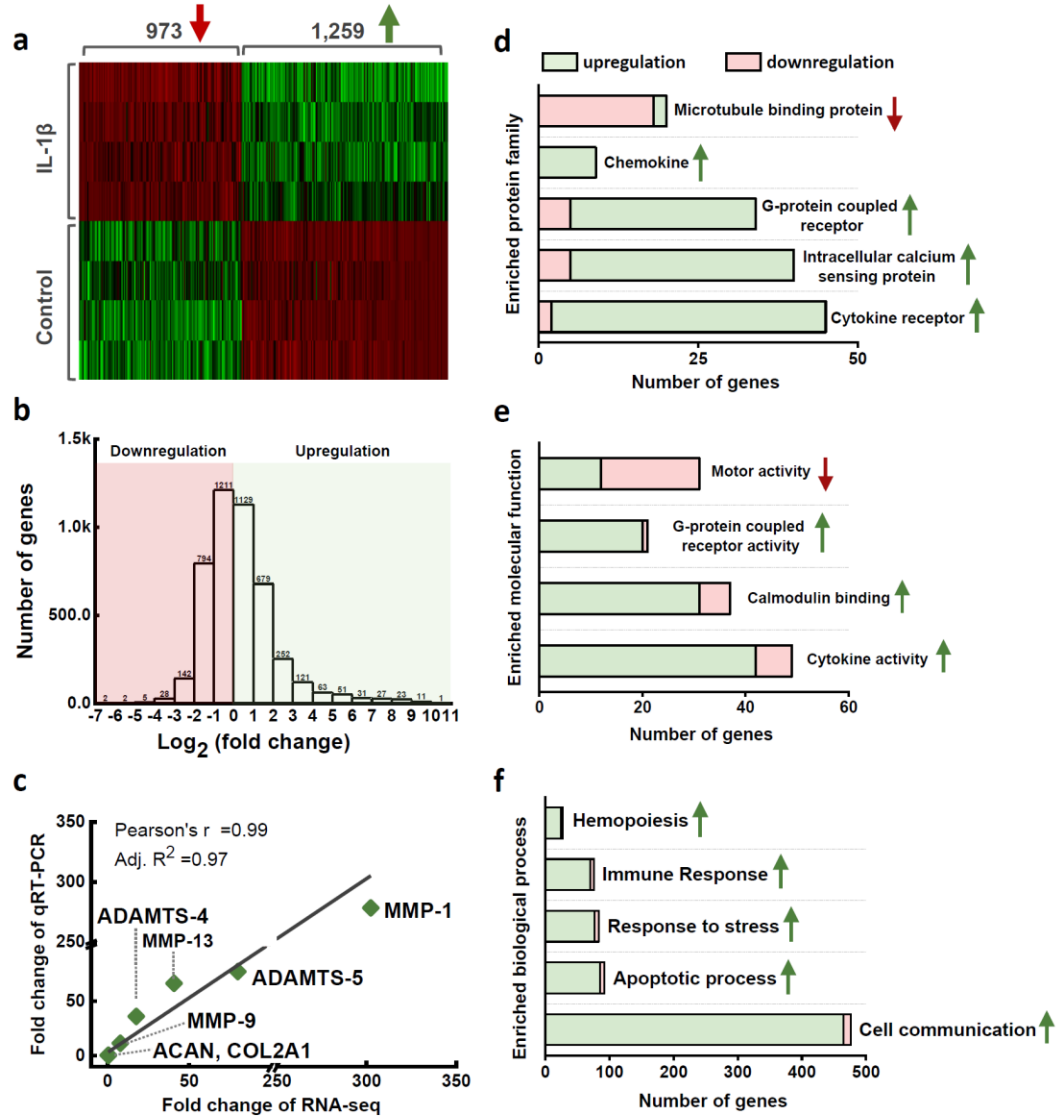


Figure 3.2 Summary statistics of RNA sequencing data. (a) Unsupervised hierarchical clustering was performed for differentially expressed genes (absolute value of fold change > 2 and FDR < 0.05) in the IL-1 β treated cartilage explants. (b) Distribution of gene expression fold changes according to \log_2 transformation. (c) Validation of RNAseq results with qRT-PCR. Seven selected genes were tested and correlated with the Pearson's correlation analysis. (d) Enrichment analysis of the protein family classification and Gene Ontology annotations in terms of (e) molecular functions and (f) biological processes.

3.4.3 Matrix Protein Related DEGs

According to previous studies, we summarized the cartilage-specific biological function of each gene from collagen, aggrecan, MMP and ADAMTS family in Table 3.3. The expression levels of collagen of type II (COL2A1), type IX (COL9A1, 2, 3), and type XI (COL11A1, 2) were significant in the healthy cells with RPKM over 10,000 (for reference, RPKM of actin: 1137.52). Expression changes of COL9 and COL11 were decreased by more than 2 folds by IL-1 β , and COL2 was decreased by 1.82 folds (FDR < 0.05, RPKM of control: 224154.47). The pericellular matrix (PCM) genes, COL6A1 (3.89 folds) and COL6A2 (4.03 folds) were promoted; while the perlecan (HSPG2) and COL6A3 (the most abundant COL6 gene) were not significantly altered by IL-1 β . Only three proteoglycan related genes were significantly changed: aggrecan (ACAN: -2.33 folds, RPKM of control: 55400.32), hyaluronan (HAS2: -2.49 folds, RPKM of control: 81.56) and decorin (DCN: 2.68 folds, RPKM of control: 336.41). No significant changes were detected in other proteoglycans, *e.g.*, biglycan (BGN, RPKM: 6514.63), fibromodulin (FMOD, RPKM: 7487.12), lumican (LUM, RPKM: 254.16) or perlecan (HSPG2, RPKM: 2399.10).

Expression levels of MMPs could vary between species¹⁷⁸. Our data suggested that IL-1 β promoted the expression of MMP-3 (188.78 folds), MMP-9 (6.77 folds), and MMP-13 (41.48 folds) in bovine chondrocytes. MMP-1, which is essential for the pre-processing of pro-collagens, was also changed by 317.73 folds, but its RPKM value in the control was as low as 0.19. MMP-28, which maintains cell adhesion to ECM network, was downregulated by 2.5 folds. MMP-2, 14 and 16, which maintain the routine cartilage ECM remodeling, were highly expressed in bovine chondrocytes but not changed by IL-1 β (absolute value of folds change < 2 or FDR > 0.05). The most upregulated ADAMTSs included ADAMTS-4 (16.37 folds),

ADAMTS-5 (82.62 folds), and ADAMTS-7 (12.29 folds). IL-1 β decreased the expression of ADAMTS-3 and ADAMTS-14, which play essential roles in processing the precursor of type II collagen for fibril formation¹⁷⁹. ADAMTSL-4, a barely studied gene in chondrocytes, was downregulated by 12.71 folds by IL-1 β and showed the highest mRNA level (RPKM: 106.97) among the ADAMTS family.

Table 3.1 Pathway enrichment analysis identified 20 child pathways (sub level 2 to 3) that are significantly changed by IL-1 β . The child pathways of FDR < 0.1 were selected and grouped together if belonging to one parent (top-level, left column) pathway.

Group	Reactome pathway	Gene number	FDR
Cell cycle	Cell cycle, mitotic	108	0.00
	Chromosome maintenance	23	0.00
	G2/m checkpoints	21	0.02
Cell-cell communication	Cell-cell communication	26	0.06
Cellular responses to stress	Senescence-associated secretory phenotype	14	0.10
DNA replication	DNA replication	26	0.03
ECM organization	Degradation of the extracellular matrix	33	0.00
	Collagen formation	28	0.00
	Integrin cell surface interactions	19	0.02
	Elastic fiber formation	13	0.02
	ECM proteoglycans	15	0.03
	Laminin interactions	9	0.05
	Non-integrin membrane-ECM interactions	12	0.06
Immune system	Toll-like receptors cascades	37	0.00

	Cytokine signaling in immune system	95	0.00
Metabolism	Glycosaminoglycan metabolism	26	0.03
Metabolism of proteins	Regulation of IGF transport and uptake by IGF binding proteins	8	0.03
Programmed cell death	Caspase activation via extrinsic apoptotic signaling	10	0.03
Signal transduction	Rho GTPases signaling	72	0.00
	PDGF signaling	55	0.08

3.4.4 Enrichment Analysis of Gene Ontology and Pathway

To understand the functions and interconnections of the 2,232 DEGs, enrichment analysis in terms of protein family classification and Gene Ontology (GO) annotation was performed. Gene family definition and a gene's function are described using GO annotation based on the experimental findings in literature. The enriched protein families included microtubule binding protein, chemokine, G-protein coupled receptor, intracellular calcium sensing protein, and cytokine receptor (Fig. 2d). The enriched molecular functions, including G-protein coupled receptor activity, calmodulin binding, and cytokine activity, were promoted; while the motor activity was mainly inhibited (Fig. 3.2e). In the enriched biological process families, hemopoiesis, immune response, stress response, apoptotic process, and cell communication were all significantly upregulated (Fig. 3.2f).

The pathway enrichment analysis identified 20 IL-1 β -changed pathways. For each pathway, the number of related DEGs and the associated P value were reported (Table 1). The cell cycle pathway was interrupted by IL-1 β , which was confirmed by our experimental observations. In the H&E staining images, proliferation of pre-chondrocytes was obvious in the superficial zone, where many cells aggregated into

cell clusters. In the center of explant, IL-1 β induced a significant cell volume increase (Fig. 3.3a). Confocal imaging showed 68% cell volume increase in the IL-1 β treated group (control vs. IL-1 β , $2.27 \pm 0.59 \times 10^3$ vs. $3.83 \pm 0.84 \times 10^3 \mu\text{m}^3$) (Fig. 3.3b). MTT assay showed that the proliferation rate of the primary chondrocytes doubled in the IL-1 β -supplemented medium (Fig. 3.3c). RNAseq revealed that IL-1 β suppressed the negative regulators of chondrocyte hypertrophy, including insulin-like growth factor (IGF2: -3.36 folds), pappalysin (PAPPA: -2.49 folds; PAPPA2: -4.52 folds), and IGF-binding protein (IGFBP2: -5.41 folds). Plate derived growth factor (PDGF) pathway can promote the chondrocyte proliferation¹⁸⁰, among which 55 related genes were significantly changed, such as PDGFC (16.76 folds) and PDGFD (3.67 folds) (Table 1).

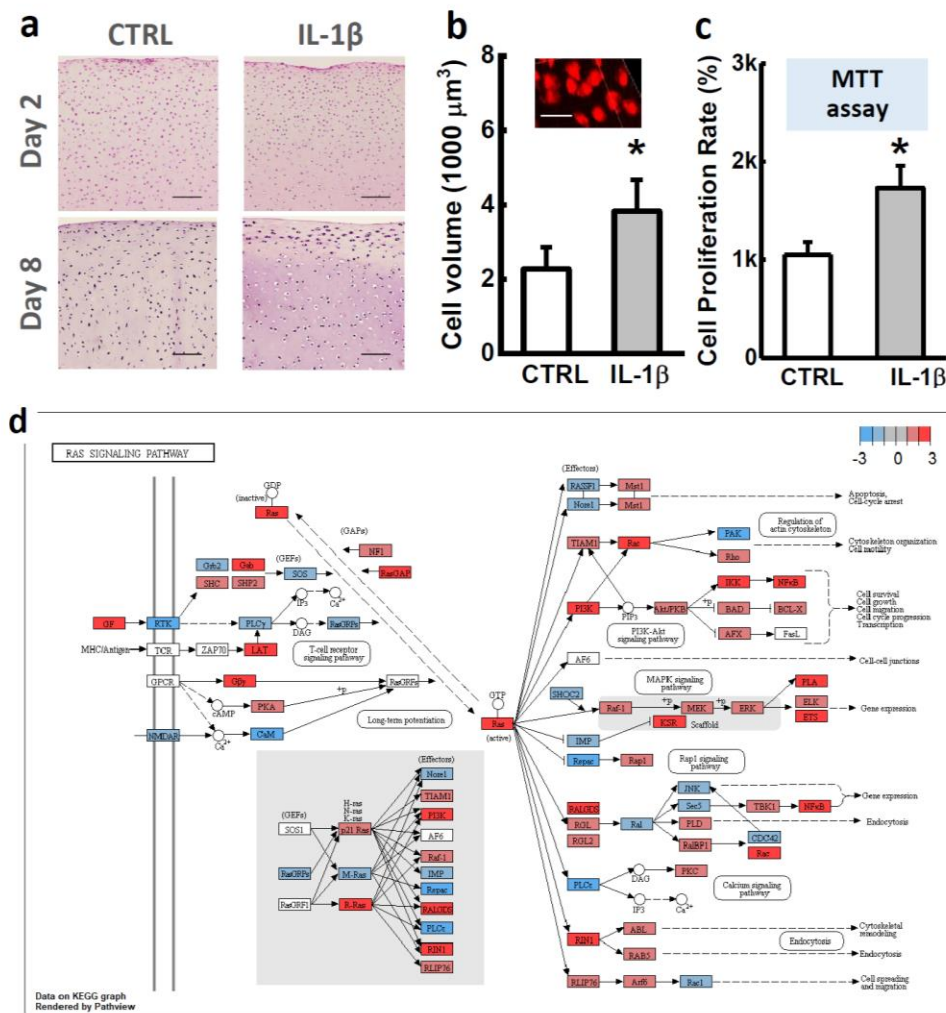


Figure 3.3 Chondrocyte swelling and proliferation. (a) H&E staining of cartilage explants after 2- and 8-day IL-1 β treatment. Cell swelling, also termed as fattening, and proliferation can be observed after 8-day IL-1 β culture. Scale bar = 200 μ m. (b) Cell volume of chondrocytes in cartilage explants measured by 3D confocal imaging. Scale bar = 30 μ m. (c) Cell proliferation rate determined by MTT assay. (d) Visualization of Ras superfamily signaling pathway regulated by IL-1 β -treatment. Flowchart was plotted using RNAseq data in Pathview (version 3.6). Each node represented a gene, and the associated node color represented the expression changes in log2 ratios. For better readability, multiple genes with similar or redundant functional roles were pooled together as a single node. Absolute value of the maximum of expression changes of these genes was reflected by the node color. All data were shown as mean \pm 95% CI.

The course of cell cycle is highly correlated with cytoskeleton metabolism¹⁸¹. Rho/Ras GTPases are essential “molecular switches” for the cytoskeleton organization of chondrocytes^{48,92}. Expression change of Rho/Ras signaling related genes was summarized in the flow chart of Fig. 3.3d, where each node represents a gene, and node color indicates the expression changes revealed by our RNAseq. If multiple genes with similar or redundant functional roles were pooled together as a single node, the node color was indicated by the absolute value of the maximum expression changes of these genes. In Rho/Ras signaling, 72 genes were changed significantly, such as Ras-related GTPase effector (RALGDS: 9.37 folds), Ras homolog family gene (RHOQ: 2.92 folds), Ras-Rab interactor (RIN1: 5.28 folds), R-Ras gene (RRAS: 2.31 folds), and Rho GTPase activating protein (ARHGAP10: 2.91 folds). These data revealed the important role of Rho/Ras GTPases in the mediation of the catabolic signaling pathways in chondrocytes.

IL-1 β changed the expression of 95 (19.4%, 489 in total genes) genes in cytokine signaling pathway and 37 (28.0%, 132 in total) genes in toll-like receptors (TLRs) cascades pathway. The basal expression levels of cytokine genes in healthy chondrocytes were low (RPKM: 0.03-5.24), while IL-1 β significantly increased the expressions of IL1B, IL6, IL34 by > 30 folds. A central pro-inflammatory regulator, NF- κ B, was significantly promoted (NFKB2: 7.11 folds; and NFKB1: 4.46 folds). TLR2, 3, 4, 6, 7, and 10 showed similar basal expression levels in healthy chondrocytes. TLR2 (160.66 folds, RPKM: 1.49) and TLR4 (6.14 folds, RPKM: 1.72) were upregulated by IL-1 β , similarly as reported in literature^{182,183}.

3.4.5 Intracellular Calcium Signaling

Using our RNAseq data, we specifically looked into a fundamental pathway, $[Ca^{2+}]_i$ signaling pathway, which regulates a wide range of biological processes, such as cell metabolism and morphology (Fig. 3.4a). The expression changes of 24 genes related to 5 calcium-signaling pathways were listed in Table 2. Transient receptor potential vanilloid 4 (TRPV4) was substantially expressed in healthy chondrocytes and promoted by 1.31 folds by IL-1 β (RPKM: 159.77, FDR<0.05), while TRPV1, 2, and 3 were barely expressed in bovine chondrocytes (RPKM < 1). Piezo-type mechanosensitive ion channel, PIEZO1 and PIEZO2, had similar mRNA levels in chondrocytes (RPKM: 107.22 and 152.53). PIEZO1 was upregulated by 4.11 folds by IL-1 β , with PIEZO2 unchanged (-1.13 folds). Voltage-Gated Calcium Channels (VGCCs) were significantly regulated by IL-1 β , including N-type channel (CACNA1B: -15.34 folds, RPKM: 2.44), R-type channel (CACNA1E: -3.13 folds, RPKM: 11.72), and L-type channel (CACNA1C: 5.2 folds, RPKM: 4.13). T-type VGCC (CACNA1H) had no significant change despite its abundant mRNA level in chondrocytes (1.04 folds, 121.86 RPKM). A VGCC auxiliary subunit, CACNA2D1, was the most expressed VGCC gene in chondrocytes and suppressed by IL-1 β (-1.72 folds, RPKM: 232.39).

Table 3.2 Summary of key genes involved in six calcium-related pathways. The “-” represents downregulation, and “+” represents upregulation. The RPKM was calculated to assess the abundance of transcript of each gene, which is correlated positively to the gene expression level.

Calcium-related pathway	Gene symbol	RNAseq gene expression			
		Fold change (IL-1 β /CTRL)	RPKM (CTRL)	RPKM (IL-1 β)	FDR
	TRPV4	+ 1.31	159.77	209.80	0.09

Mechano-sensitive channel	PIEZO1	+	4.11	107.22	440.92	0.00
Ligand-gated ion channel	GRIN2C	+	2.19	0.67	1.47	0.06
	GRIN2D	+	2.29	10.32	23.61	0.00
	GRINA	+	2.59	21.95	56.82	0.00
Voltage-sensitive calcium channels	CACNA1B	-	15.34	2.44	0.16	0.00
	CACNA1E	-	3.13	11.72	3.75	0.03
	CACNA2D1	-	1.72	232.39	135.42	0.00
	CACNA1C	+	5.20	4.13	21.44	0.00
Purinergic receptor	P2RX6	-	3.69	1.88	0.51	0.00
	P2RX4	-	1.43	20.30	14.21	0.03
	P2RY2	-	1.36	12.66	9.28	0.06
	P2RX5	+	1.97	4.95	9.73	0.00
PLC-IP3	PLCH1	-	14.64	3.08	0.21	0.00
	PLCD1	-	2.29	297.00	129.71	0.00
	PLCE1	-	2.26	179.13	79.20	0.00
	PLCD3	+	2.27	4.75	10.76	0.00
	PLCH2	+	2.29	1.08	2.48	0.02
	PLCH2	+	2.29	1.08	2.48	0.02
	ITPRIP	+	3.37	8.19	27.62	0.00
	ITPR3	+	6.35	0.79	4.99	0.00
ER store	STIM2	-	1.64	41.68	25.43	0.00
	STIM1	+	1.31	14.45	18.89	0.10
	ORAI2	+	1.95	2.96	5.76	0.01

To evaluate the ultimate effects of IL-1 β on chondrocyte $[Ca^{2+}]_i$ signaling, we recorded the spontaneous $[Ca^{2+}]_i$ signaling of *in situ* chondrocytes after 2-day IL-1 β treatment (Fig. 3.4b). Typical $[Ca^{2+}]_i$ oscillations of *in situ* chondrocytes were shown in Fig. 3.4c-d and videos in Supplemental Movie. 203 out of 661 (30.7 \pm 0.14 %)

cells showed spontaneous $[Ca^{2+}]_i$ oscillation in the control explants, a significantly higher responsive rate than that in the IL-1 β treated samples (87 out of 621 cells, $14.0 \pm 0.11\%$) (Fig. 3.4e). For each responsive cell, the spatiotemporal parameters of $[Ca^{2+}]_i$ peaks were also significantly altered by IL-1 β . The magnitude of $[Ca^{2+}]_i$ peaks was reduced (control vs. IL-1 β : 5.78 ± 1.01 vs. 2.98 ± 0.87), and the number of multiple peaks was decreased (control vs. IL-1 β : 3.55 ± 0.3 vs. 2.19 ± 0.27). The time between two neighboring peaks (control vs. IL-1 β : 111.26 ± 5.12 vs. 175.70 ± 13.24) and the time to reach a peak from baseline (control vs. IL-1 β : 17.58 ± 2.78 vs. 33.2 ± 6.62) were both significantly prolonged by IL-1 β , indicating slow Ca^{2+} transport (Fig. 3.4e).

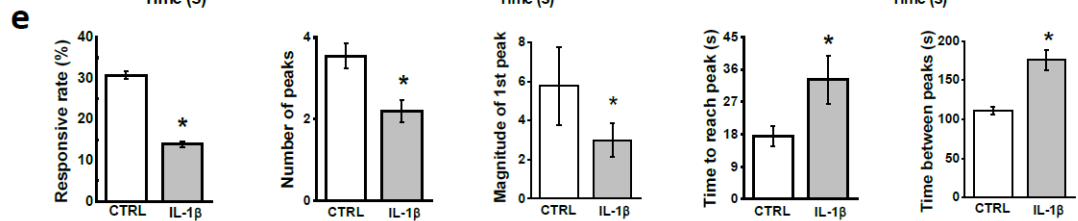
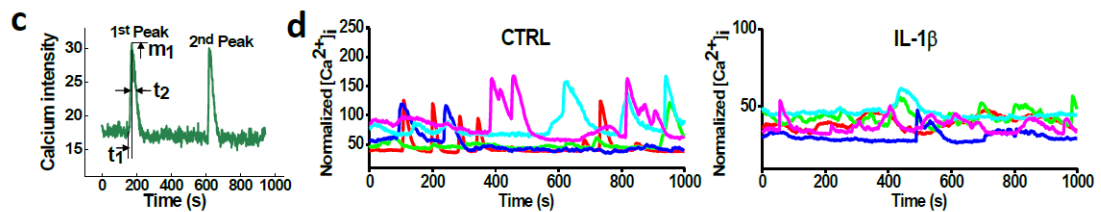
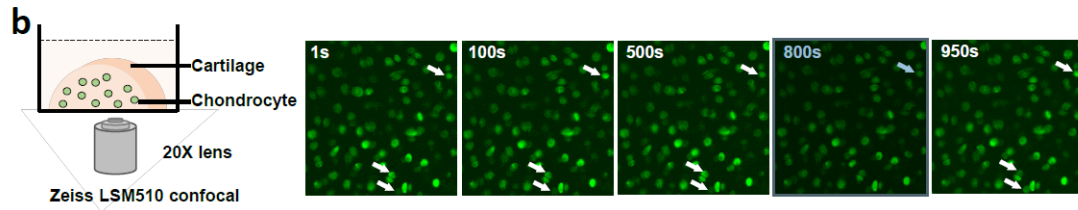
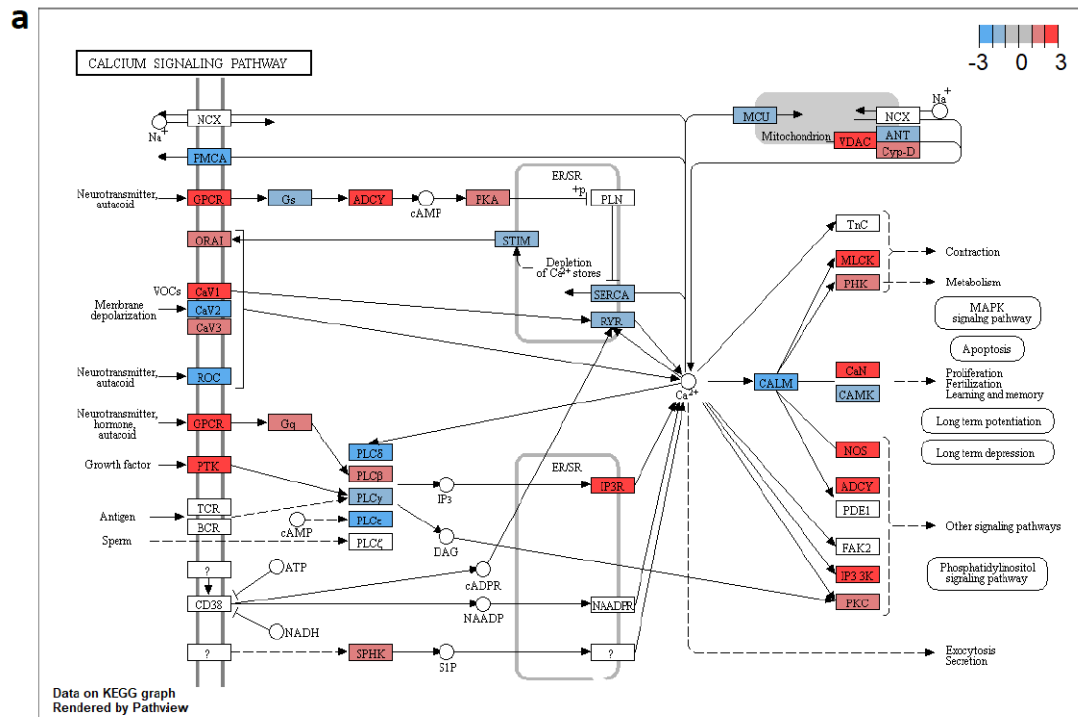


Figure 3.4 Calcium signaling of chondrocytes in cartilage explants. (a) Visualization of calcium signaling pathway regulated by IL-1 β . (b) Illustration of calcium signaling. Half cartilage explant was dyed with fluorescent indicator and imaged on a confocal microscope for 15 minutes. Due to the fluctuation of [Ca²⁺]_i concentration, image intensity of chondrocyte oscillates in recorded video. (c) Definition of spatiotemporal parameters of [Ca²⁺]_i peaks. (d) Representative [Ca²⁺]_i curves of *in situ* chondrocytes from the control group and IL-1 β treated group. (e) Parameters of [Ca²⁺]_i peaks, including the average number of [Ca²⁺]_i peaks, magnitude of peaks, time to reach a peak, and time between neighboring peaks. All data were shown as mean \pm 95% CI. *: vs control, p < 0.05 if otherwise marked.

Table 3.3 Major catabolic and anabolic genes in DEGs, including MMP- and ADAMTS-, collagen-, proteoglycan-family genes. The “-” in front of the fold change value represents downregulation of expression, and “+” represents upregulation of expression after IL-1 β treatment.

Family	Gene symbol	RNaseq Gene Expression				Identified Biological functions
		Fold change	RPKM (CTRL)	RPKM (IL-1 β)	FDR	
MMP	MMP28	- 2.50	21.81	8.71	0.00	regulate cell morphology ¹
	MMP23B	- 2.31	28.43	12.31	0.00	unknown
	MMP25	+ 4.46	0.25	1.11	0.00	unknown
	MMP9	+ 6.77	10.16	68.78	0.00	induce apoptosis of hypertrophic chondrocytes ²
	MMP12	+ 9.15	2.50	22.92	0.00	fetal development and malignant transformation ³
	MMP13	+ 41.48	4.80	199.14	0.00	degrade collagen ²
	MMP3	+ 188.78	15.32	2892.29	0.00	degrade a wide array of extracellular molecules ²
	MMP1	+ 317.73	0.19	60.54	0.00	degrade collagen types I, II, III ²
ADAMTS	ADAMTS14	- 35.12	13.14	0.37	0.00	process procollagen for collagen fibril formation ⁴
	ADAMTS6	- 6.59	88.10	13.37	0.00	unknown
	ADAMTS3	- 3.15	99.03	31.43	0.00	process procollagen for collagen fibril formation ⁴
	ADAMTS20	- 2.80	2.56	0.92	0.01	unknown
	ADAMTS12	- 2.38	15.35	6.46	0.00	degrade cartilage oligomeric protein (COMP) ⁴
	ADAMTS7	+ 12.29	2.75	33.77	0.00	degrade cartilage oligomeric protein (COMP) ⁴
	ADAMTSL4	+ 12.71	106.97	1359.54	0.00	bind to fibrillin for microfibril formation ⁵
	ADAMTS4	+ 16.37	5.86	95.94	0.00	degrade major cartilage proteoglycan ⁴
ADAMTS5	+ 82.62	0.20	16.40	0.00	degrade major cartilage proteoglycan ⁴	
Collagen	COL8A1	- 8.04	300.94	37.44	0.00	Unknown
	COL6A5	- 3.54	2.15	0.61	0.01	form Pericellular Matrix ⁶
	COL9A1	- 3.47	14440.75	4164.15	0.00	decorate fibril surfaces of PCM ⁶
	COL9A3	- 3.28	12160.36	3704.14	0.00	decorate fibril surfaces of PCM ⁶
	COL11A1	- 3.16	31786.93	10070.64	0.00	synthesize as a heterotrimeric molecule in developing cartilage ⁶
	COL9A2	- 2.94	10553.26	3587.21	0.00	decorate fibril surfaces of PCM ⁶
	COL12A1	- 2.60	2015.97	775.16	0.00	bind to fibril surfaces but not covalently attached (FACIT collagen subfamily) ⁶
	COL8A2	- 2.27	87.51	38.57	0.00	Unknown
	COL11A2	- 2.41	16250.45	6732.92	0.00	synthesize as a heterotrimeric molecule in developing cartilage ⁶
	COL13A1	+ 3.77	0.28	1.04	0.00	Unknown
	COL4A5	+ 4.01	1.44	5.75	0.01	form Pericellular Matrix ⁷
	COL6A1	+ 3.89	2110.85	8217.24	0.00	form Pericellular Matrix ⁶
	COL6A2	+ 4.03	669.30	2696.74	0.00	form Pericellular Matrix ⁶
COL25A1	+ 4.62	25.29	116.93	0.00	unknown	
Proteoglycan	ACAN	- 2.33	55400.32	23774.02	0.00	form the cartilage-specific proteoglycan core protein ⁸
	DCN	+ 2.68	336.41	900.56	0.00	control collagen fibrillogenesis ⁸

3.5 Discussion

Previous studies have attempted to evaluate the large-scale gene expression profile of chondrocytes using various OA models, including monolayer chondrocytes^{176,184}, cartilage of human knee joints^{185,186}, and cartilage from OA animal models^{177,57}. An important finding of these studies is that chondrocytes present declined transcriptomic changes along with OA progression. Chondrocytes demonstrate drastic genetic changes before cartilage shows visible degradation, whilst they adapt to the degenerated extracellular environment with little chondrogenic features at the late stage of OA^{160,186}. For instance, cartilage cells at late OA stage barely express catabolic genes, such as MMPs and ADAMTSs¹⁸⁶. A detailed comparison between our RNAseq data and that of late-stage OA cartilage found only 214 (9.26%) genes are sharing the same trend (upregulation/downregulation)¹⁸⁶. In contrast, high consistency was observed between our RNAseq data and those from chondrocytes at early-stage OA. Our study has 74% consistency with a microarray study of healthy human chondrocytes subjected to 96-hour IL-1 β treatment¹⁷⁶ and 67% consistency with a study of early degenerative human cartilage¹⁸⁷. There was 48% consistency with another gene expression profile of a middle-stage OA model (rats at 4 weeks post ACL rupture, 722 DEGs)⁵⁷. To the best of our knowledge, our RNAseq outcome is also highly consistent with a number of specific chondrocyte pathway studies, *e.g.*, NFAT¹⁸⁸, EGFR¹⁸⁹, IGF^{20,92,190}, and TRPV²⁹ pathways. Therefore, a major contribution of our RNAseq study is to generate a complete list of genes of chondrocyte in response to acute joint inflammation. This study identified 2,232 DEGs and 10,423 non-DEGs, with information about each gene's basal expression level at healthy status and the relative expression fold change in response to the IL-1 β stimulation. The expression changes identified by the RNAseq are highly consistent with those reported in specific

pathway or cartilage inflammation mechanism studies. Thus the present RNAseq data set can serve as a unique source to verify individual gene or pathway studies and provide guidance for future PTOA research.

In cartilage ECM, aggrecan, the major proteoglycan, forms supramolecular aggregates with hyaluronan and is entrapped in the collagen II/IX/XI fibrillar network⁵. The nonaggregating proteoglycans, *i.e.*, fibromodulin, biglycan, decorin and lumican, can bind with various types of collagens and regulate the formation of fibril networks³⁷. This specialized structure endows cartilage with its biomechanical properties for joint loading. In our RNAseq data, IL-1 β significantly reduced the gene expression of aggrecan (ACAN) and hyaluronan (HAS2); however, the expression of type II collagen (COL2A1), fibromodulin (FMOD), biglycan (BGN), and lumican (LUM) showed no significant changes. These results corroborate previous observation that the degradation of proteoglycan aggregates is prior to that of collagen network at the early stage of OA initiation^{20,37}. Decorin, another important nonaggregating proteoglycan, is known as an important regulator of collagen fibril and proteoglycan assembly³². Upregulation of decorin was observed in our RNAseq data as well as previous early-OA studies¹⁹¹. This response has been regarded as an attempt by chondrocytes to increase the adhesion between fragmented aggrecans, thereby delaying its loss from cartilage. During OA progression, the PCM of chondrocytes, which is mainly composed of type VI collagen and perlecan, also presents aberrant remodeling process¹⁹². The drastic PCM degradation is associated with and may be responsible for the phenotypic shift of chondrocytes. In the early OA stage, type VI collagen is increasingly expressed although its fibrils is disorganized with compromised density¹⁹³. Our RNAseq data also showed the upregulation of all three

collagen VI isoforms (COL6A1, 2, and 3) in the IL-1 β -treated cartilage samples. Perlecan, co-localized with type VI collagen in the PCM, plays an important role in regulating chondrocyte anabolic activities. The retention of growth factors by perlecan, such as fibroblast growth factor (FGF2) and bone morphogenetic proteins (BMP2/7), has been shown to promote chondrogenic differentiation and matrix production¹⁹³. WARP (von Willebrand factor A domain-related protein), a newly identified component of chondrocyte PCM, can also interact with perlecan to contribute to the assembly and maintenance of cartilage structures during cartilage development¹⁹⁴. In our RNAseq result, neither perlecan (HSPG2) or WARP (VWA1) genes was significantly changed by the IL-1 β treatment, indicating no drastic changes of their synthesis at the acute inflammation stage. Taken together, these ECM and PCM proteins may play synergetic but unique roles in regulating cartilage homeostasis, thus presenting distinct responses to acute inflammation stimulation.

An important finding from the present study was that IL-1 β can induce significant changes in the [Ca²⁺]_i signaling of chondrocytes. As illustrated in Fig. 3.4a, [Ca²⁺]_i signaling can be activated partially through G-protein coupled receptors (GPCRs), an important mediator regulating chondrocyte morphology. In both proliferating and hypertrophic chondrocytes, the expression of GPCRs and regulators of G-protein signaling (RGS) increases markedly^{184,195}. According to RNAseq data (Fig. 3.4a), the GPCR- and RGS-family genes were differentially regulated by IL-1 β , such as GPR84 (133.07 folds), GPR68 (-4.81 folds), RGS8 (80.49 folds), and RGS22 (-5.31 folds), with parallel changes of downstream calcium-related genes including PLC- and adenylyl cyclase-(ADCY) family genes. Another initiation mechanism of [Ca²⁺]_i signaling is through the ion channels on plasma membrane. In chondrocytes,

TRPV4 and PIEZO1 were recently identified as two key mechanosensitive ion channels. TRPV4 and PIEZO1 can be disturbed by inflammatory mediators, further inducing ECM degeneration^{29,152, 126}. According to our RNAseq data, TRPV4 and PIEZO1 were two highly expressed genes in healthy bovine chondrocytes, and both were changed by IL-1 β with consistent trends as reported previously^{29,126}. T-type VGCC, which exists mainly in excitable cells (*e.g.*, neurons and muscle cells) to facilitate environmental calcium influx, plays an important role in regulating [Ca²⁺]_i signaling of chondrocytes under mechanical stimulation³⁵. Our previous study showed that inhibition of T-type VGCCs can attenuate the OA-like phenotype of chondrocytes by reducing the expression of mechanical-stress responsive genes Prostaglandin G/H synthase 2 (PTGS2) and osteopontin (SPP1)¹²⁷. In this study, RNAseq detected minor expression change in T-type VGCC gene (CACNA1H), while both PTGS2 and SPP1 were promoted by 13.34 folds and 21.71 folds in the IL-1 β -treated chondrocytes, respectively.

High level of IL-1 β can shift chondrocytes towards an aberrant phenotype, including cell swelling, proliferation or hypertrophy. Rho GTPases, such as RhoA, Rac1, and Cdc42, are well recognized as crucial regulators of chondrocyte cytoskeleton and cell cycle⁹¹. IL-1 β can affect the Rho family via [Ca²⁺]_i signaling, leading to the rearrangement of F-actin networks in chondrocytes^{48,49}. Previous studies proved that overexpression of RhoA can suppress the ECM synthesis and chondrogenic differentiation of the chondrogenic cell line ATDC5^{91,18}. Insulin-like growth factors (IGFs), an important anabolic factor in chondrocytes, can inhibit the abnormal Rho GTPases activities and therefore protect the cytoskeleton structure^{20,92,190}. In our RNAseq data, IL-1 β inhibited the IGF-modulated signaling pathway via

suppressing IGF2 and IGF2R, with parallel decreases of PLCs genes (PLCH1, PLCD1, and PLCE1). Another growth factor that can activate Rho signaling is called platelet-derived growth factors (PDGFs), which is also involved in the chondrocytes proliferative process^{180,196}. IL-1 β promoted the PDGFC by 17 folds and PDGFD by 3.67 folds. Taken together, IL-1 β -induced chondrocyte phenotypic shift is related to the Rho GTPases signaling, whose regulatory effects are related to IGF and PDGF.

A few limitations of this study should be noted. First, due to the limited access to healthy young human cartilage, bovine cartilage samples were used in this study. Nevertheless, this substitution can at least be partially justified by the greatest evolutionary conservation present between human and cattle¹⁹⁷. Second, to avoid synergistic and interactive effects between cytokines, IL-1 β was employed as the cytokine to simulate the inflammatory attack on cartilage during acute joint inflammation. Despite playing a central role in cartilage degeneration, IL-1 β alone cannot recapitulate the complexity of multiple pro-inflammatory cytokines. A large number of cytokines are active in the joints, such as TNF- α , IL-1 and IL-6 families^{161,51}. The genetic responses of chondrocytes revealed in the present study could vary from the actual situations in inflammatory joints. Third, chondrocytes' reaction to cytokines is a highly time dependent behavior. This study focused on the effects of IL-1 β on cartilage gene expression after 2-day treatment, whereas acute joint inflammation could last 2-4 weeks after traumatic injuries (*e.g.*, meniscus tear). Fourth, investigation of either cell cycle or calcium signaling of chondrocytes could be complicated and have attracted tremendous efforts. Experiments in this study were designed as a verification of the ultimate effects of transcriptional changes induced by IL-1 β . The experiments also functioned as case studies to illustrate the potential

application of the RNAseq data in the verification and guidance of future OA studies related to the acute inflammation after joint trauma. For example, RNAseq data revealed that ACTB and GAPDH are proper reference genes for the genetic analysis of bovine chondrocytes.

This study performed a detailed transcriptional analysis of IL-1 β -treated healthy cartilage, which provides genetic evidence for the (1) short-term transcriptional responses and signaling transductions in chondrocytes during acute inflammation; and (2) the dysregulation of cell cycle and [Ca²⁺]_i signaling transductions of chondrocytes, both of which may play critical roles in modulating cell phenotypic shift under inflammatory attack. The comprehensive transcriptional profile identified here is highly consistent with other high-throughput studies and specific pathway studies in literature and may serve as useful guidance and verification for future chondrocyte research.

Chapter 4

STATIN PROTECTS THE CARTILAGE FROM INFLAMMATORY ATTACK BY INHIBITING THE RHO-GTPASES SIGNALING PATHWAY IN CHONDROCYTES

4.1 Introduction

Osteoarthritis (OA) is characterized by joint pain and stiffness, which is the first cause of disability in U.S. Posttraumatic OA (PTOA) arises from joint trauma and accounts for 12% of overall OA cases¹⁹⁸. Trauma injuries often cause inflammation, bleeding, and alteration of loading patterns of joints, which all exert OA-inducing stimulations on cartilage⁴³. Under these OA stimulations, one of the earliest cellular response in cartilage is chondrocyte phenotypic shift from a metabolic quiescence state toward a hypertrophy-like, degradative state⁵⁴. The chondrocyte phenotypic shift is characterized by elevated cellular proliferation, cluster formation, hypertrophy, and apoptosis⁴³, which is associated with elevation of matrix-degrading enzymes production, *i.e.* Matrix Metalloproteinase (MMP) family proteins⁴⁸⁻⁵⁰, and disrupts the balance of metabolism of cartilage extracellular matrix (ECM)⁵¹⁻⁵³. Fragments of ECM cleavage can be further sensed by chondrocytes through receptors localized on cell surface and induce a cascade of events, *e.g.* gene expression changes and overexpression of ECM-degrading enzymes and inflammatory mediators, ultimately leading to cartilage degradation and dysfunction of cartilage. Articular cartilage has limited potential of self-repair; and current treatments have shown minimal capability in preventing PTOA from development. Once severe PTOA has developed, the only

treatment available is costly whole joint arthroplasty, which is not a recommended procedure for younger patients ⁴⁴. Although recent animal studies have shown some progress in pharmacologic therapies, no medical therapies have been shown to prevent the onset of OA ⁴³. Therefore, inhibition of chondrocyte responses to the OA-inducing factors immediately after joint injuries constitutes a tempting approach for OA prevention.

In the U.S.A, statins are the most commonly prescribed drugs for reducing cholesterol level, which are used by up to 40 million people with well-understood side effects ¹⁹⁹. Recently, a number of studies using *in vitro* model, *in vivo* animal models, or patients' data have been conducted to explore the effects of statins on musculoskeletal conditions. However, the results generated from these studies are conflicting. Longitudinal studies from the Netherlands and United Kingdom report the favorable effects of statin on reducing OA outcome for population aged 40 years and over ^{200,201}. However, another studies using U.S.A population data found that statin use may even worsen the knee pain, function or structural progression over the long-term follow-up ²⁰²⁻²⁰⁴ (Table 1). Such conflicting results has aroused heat debate regarding their methodological factors ²⁰⁵ and remain unsolved due to lack of mechanism knowledge. Previous mechanism studies using *in vitro* models and *in vivo* animal models have elaborated the anti-inflammatory properties of statin, e.g. downregulation of inflammatory cytokines and NF-κB pathway in synovium, subchondral-bone, and cartilage (Table 2). However, this mechanism alone cannot justify the clinical usage of statins for OA prevention, as many anti-inflammatory drugs are dedicated to easing joint inflammation but unable to exert protective functions as effective as statins. Therefore, further investigation of the mechanisms by

which statins exert protective effects on cartilage is still of necessity to facilitate its clinical application for OA treatment.

In cell, the cholesterol-lowering function of statins is mainly through the inhibition of a fundamental metabolic pathway called mevalonate pathway²⁰⁶. Another important intermediate of this pathway is geranylgeranyl pyrophosphate (GGPP), which serve as important lipid attachment for the prenylation of variety proteins²⁰⁷, *i.e.* Rho GTPase proteins. The family of Rho GTPase proteins is “molecular switch” playing an essential role in the regulation of multiple aspects of cellular biological processes^{116,117}. In chondrocytes, RhoA, Rac1 and Cdc42 are the best characterized Rho GTPases, which play essential roles in regulating cell hypertrophic change^{118,119}, apoptosis^{81,82}, and MMP13 synthesis^{97,120} during OA pathogenic process. Using various *in vitro* model and animal OA models, inhibiting RhoA^{91,95}, Rac1¹²¹, and Cdc42¹²⁰ respectively has been proven to significantly preserve the chondrocyte phenotypic stability and delay the cartilage degeneration. Therefore, it is tempting to speculate that statin-induced inhibition of the mevalonate pathway can lead to inactivation of downstream Rho GTPase proteins, which suppresses the abnormal phenotypic shift of chondrocytes and eventually prevents the cartilage degeneration under OA-inducing stimulations.

In present study, we investigated the direct effects of statins on chondrocytes using an *in vitro* cartilage explant model. Using the explant model, the cell morphology and ECM contents were longitudinally measured during long-term culture under statins treatment. To assess the role of mevalonate pathway, we checked whether adding a mevalonate derivative (GGOH) can override the protection effects of statin. In addition, the protection effects of another mevalonate inhibitor

bisphosphonate and the specific inhibitors for RhoA, Rac1, and Cdc42 were assessed and compared with those of statin. Our findings in this study can provide: 1) a new target pathway in chondrocytes, *i.e.*, Rho GTPases, for the inhibition of OA initiation after joint injuries; 2) critical justifications regarding the application of statins for PTOA prevention; and 3) guidance for future clinical trials of the mevalonate inhibitors in OA prevention, including the targeted population, design of delivery methods, and timing of drug administration.

4.2 Materials and Methods

4.2.1 Cartilage Explant Culture

Overall experimental design was outlined in Fig. 4.2a. Fresh knee joints were obtained from 3-6 months old calf at a local slaughter house (Green Village, NJ). Cylindrical cartilage explants (diameter = 3 mm, thickness = 2 mm) were harvested from the central, load-bearing region of femoral condyle heads. After harvesting, samples were balanced in base medium overnight and then transferred to conditional medium for 4 weeks *in vitro* culture.

The conditional mediums used in this study was prepared as base culture medium supplemented with chemicals as listed below. IL-1 β (Interleukin-1 β human; Sigma-Aldrich) or fetal bovine serum (FBS; Sigma-Aldrich) was supplemented into the base medium for mimicking OA-inducing stimulation. Three forms of statins (simvastatin, lovastatin, and atorvastatin; Sigma-Aldrich) and a drug of bisphosphonate family called Zoledronic acid (an upstream inhibitor of mevalonate pathway, Sigma-Aldrich) were tested. Other chemicals included Geranylgeraniol (GGOH, a mevalonate derivative which can recover the activities of Rho family of

proteins; Sigma-Aldrich), Geranylgeranyl transferase 1 inhibitor (GGTI278, downstream of mevalonate inhibiting the geranylgeranylation of Rho family of proteins; Cayman), RhoA inhibitor (Y-27632, a selective p160ROCK inhibitor; Tocris), Rac1 inhibitor (NSC-23766, a selective inhibitor of Rac1; Tocris), and Cdc42 inhibitor (ZCL-278, a selective inhibitor of Cdc42).

4.2.2 Biochemical Assay and Mechanical Test of Cartilage Explant

Loss of sGAG and collagen contents over time: During the *in vitro* culture of cartilage explants (n = 10 explants from 5 animals per group), the culture medium (500 μ L/sample) was changed and collected every other day. The sGAG and collagen assay were performed as described previously^{163,20}. The accumulative sGAG or collagen loss was calculated as the sGAG or collagen released into the medium divided by the sum of sGAG or collagen contents in both explant and culture medium²⁰. The sGAG loss was measured during the first 8-day culture, and the collagen loss was tracked for 24 days. Different cartilage explants were used to track the losses of sGAG and collagen, respectively.

Histology and Immunohistochemistry: After 2- and 8-day culture, cartilage explants were fixed in formaldehyde solution for 48 hours and then embedded in paraffin blocks (n = 2 explants from 2 animals per group). Explants were sectioned into 5- μ m thick sections along depth direction for staining by Safranin O (Sigma-Aldrich), Hematoxylin and Eosin Y (H&E, Sigma-Aldrich) or Type II collagen antibody (Abcam).

Mechanical properties: Unconfined compression test was used to measure the mechanical properties of the cartilage explants (n = 10 explants from 5 animals per group; samples cultured for mechanical testing only)¹⁶⁶. During the test, a 10% strain

was applied on the cartilage sample at a constant speed followed by a 20-min relaxation period. After the reaction force reached an equilibrium state, sinusoidal dynamic loading was applied on the sample for 15 minutes at 0.5 Hz with a magnitude of $\pm 1\%$ ³². Equilibrium Young's modulus and dynamic modulus of the samples were determined using the recorded force.

4.2.3 RNA sequencing

The detailed RNA sequencing protocols were reported in Chapter 3, Materials and Methods section. To be brief, cartilage explants were assigned into two groups and cultured in: 1) 1 ng/mL IL-1 β supplemented medium and 2) IL-1 β plus 10 μ m simvastatin (n= 4 explants from 4 animals per group). After 48 hours culture, the cellular RNA was extracted from explant samples for RNA sequencing ¹⁶⁸. RNAseq library of each sample was constructed, pooled and sequenced on the Illumina HiSeq 2500. Data processing was performed using CLC Genomics Workbench v7.5 (QIAGEN). Gene expression value was calculated as the total number of unique reads mapped to the exon sequence and normalized to reads per kilo base of transcript per million mapped reads (RPKM). The differential expression of each gene was determined by the generalized linear model with animal as a random variable ¹⁷¹. A stringent cutoff of False Discovery Rate (FDR) < 0.05 and absolute fold change > 1.5 was adopted to identify the differentially expressed genes (DEGs) between the IL-1 β treated and the statin co-treated samples. The KEGG pathways generated by Pathview (version 3.6) were used to visualize the changes in a specific signaling pathway ^{174,175}.

4.2.4 Morphology Evaluation of in-situ Chondrocyte

To measure the chondrocyte volume, cartilage explants were dyed with red fluorescent cell tracker (Red CMTPX Dye, Thermo Fisher) and imaged on a confocal microscope (Zeiss 510) after 4-day culture (n = 4 explants from 2 animals per group). The fluorescent image stacks were reconstructed into a 3D image in Image J¹⁶⁴. The volume of *in situ* chondrocytes was registered and quantified (n ≈ 30 cells from each explant). To estimate the cell proliferation rate, primary chondrocytes were extracted from cartilage explants and MTT assay was then performed following the previous instructions¹⁶⁵ (n = 4 explants from 2 animals per group).

4.3 Results

4.3.1 Statins Protect Cartilage Explant from Inflammatory Attack

To assess the direct effects of statin on cartilage, we tracked the ECM proteins loss using an *in vitro* culture cartilage explant model. Cylindrical cartilage explants were harvested from calf knee joints and cultured in chemically defined medium up to 24 days (Fig. 4.1a). At day 0, IL-1 β (1 ng/mL) as a predominant catabolic cytokine of joint to simulate moderate inflammation attack and/or three forms of statin, simvastatin, atorvastatin, and lovastatin, were supplemented into the culture medium of cartilage explants (Fig. 4.1b). The sGAG and collagen loss from cartilage explant into medium were measured every other day for 24 days in vitro culture, respectively.

After 8-day culture, IL-1 β -induced sGAG loss from cartilage explant was accumulated to $46.27 \pm 7.62\%$ (Fig. 4.2b). All three forms of statins significantly inhibited the sGAG loss to as low as 20% at day 8 (Fig. 4.2b). At day 24, IL-1 β induced $32.66 \pm 3.48\%$ collagen loss from cartilage explants ($4.9 \pm 0.43\%$ for undamaged control). This collagen loss was almost fully abolished by statins treatment

($p < 0.001$ for three statins) (Fig. 4.2c). Without the presence of IL-1 β , adding statins alone didn't induce significant sGAG loss or collagen loss compared to the untreated control, indicating the negligible toxicity of statin to healthy chondrocytes (Fig. 4.2b-c). The concentration of statins used in this study was chosen based on a rigorous dosage study ranging from 1 μm to 60 μm (Fig. 4.2). All three forms of statins showed a clear dosage-dependent protective effect on cartilage ECM integrity with the presence of IL-1 β stimulation.

The favorable effects of statins on cartilage was also reflected on preserving its mechanical function. The indentation test showed that IL-1 β -treated cartilage had a significantly lower modulus than the untreated control (0.06 ± 0.04 vs. 0.13 ± 0.03 MPa for control) and statin treatment preserved the modulus (0.11 ± 0.03 MPa for IL-1 β + 10 μm simvastatin) similar to the healthy control (Fig. 4.2e). The histological images of Safranin O staining revealed the patterns of ECM content loss in cartilage explants. The surface of cartilage explant showed pronounced sGAG loss compared to internal ECM contents; while this loss was substantially reduced by 10 μm simvastatin treatment (Fig. 4.1f left).

We then examined the protective function of statin on chondrocyte phenotype by measuring the cell volume and proliferation rate. At the gross level, IL-1 β -treated cartilage explant presented substantial cell proliferation and cell swelling at day 24, especially at the surface area of cartilage explant; these hypertrophic-like phenotype shifts were alleviated by simvastatin treatment (Fig. 4.1f right). We also assessed these cell phenotypic changes in a quantitative manner via using MTT assay and fluorescent cell volume measurement. Compared to the untreated control, IL-1 β treatment induced 1.44 times higher cell proliferation rate, which was significantly inhibited by

simvastatin treatment during 3-day culture (Fig. 4.2g). Fluorescent measurement suggested 1.68 times increase in cell volume in IL-1 β -treated cartilage compared to the untreated control, while the cells in statin-treated cartilage had similar size with the control ($2176.52 \pm 203.03 \mu\text{m}^3$ vs. $2273.96 \pm 588.35 \mu\text{m}^3$ for the control) (Fig. 4.2h). Taken together, IL-1 β -induced deleterious effects on cartilage explants were significantly alleviated by statins treatment during long-term *in vitro* culture. This protective actions of statin on cartilage integrity were related to its direct regulation of chondrocyte phenotype stability.

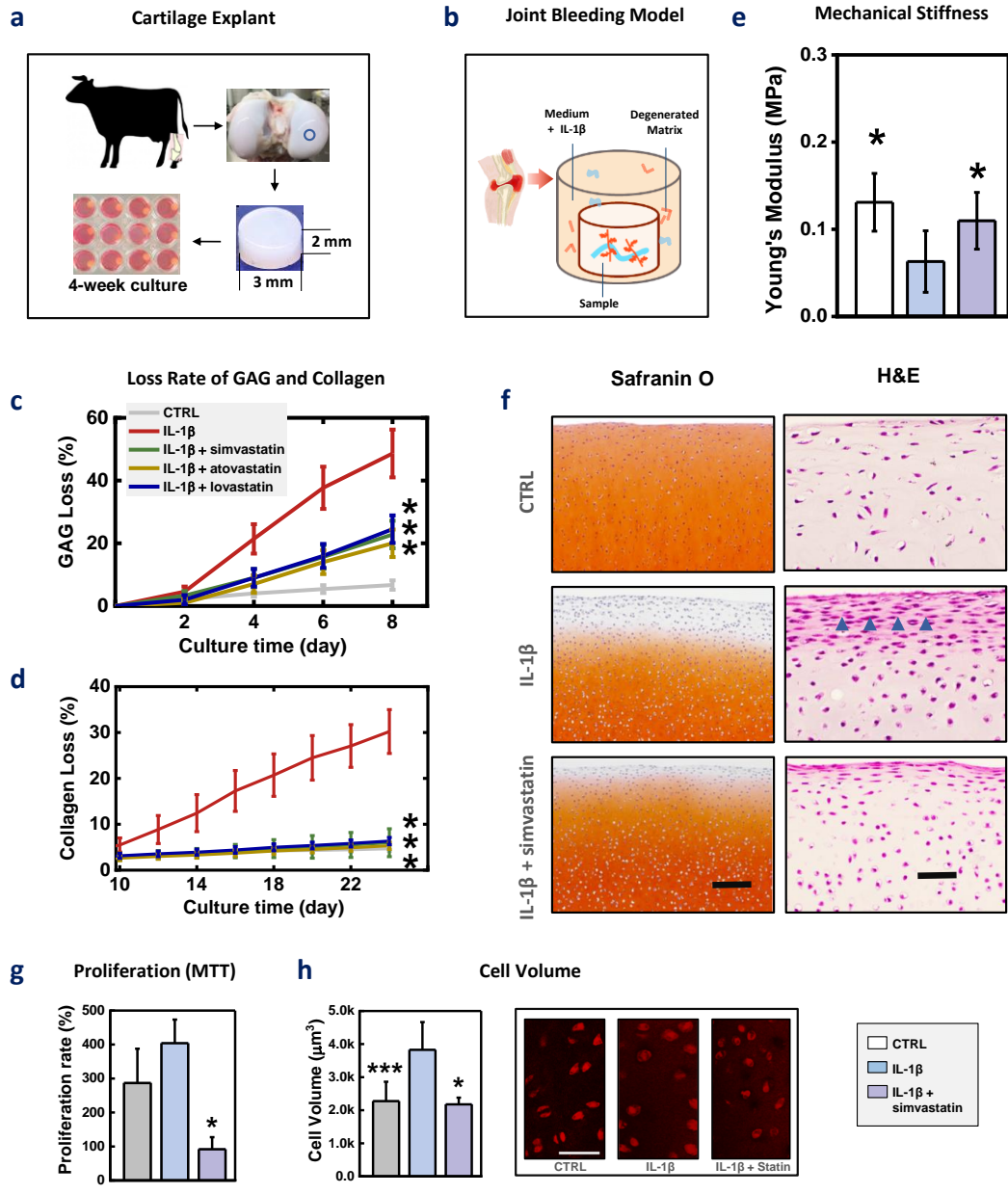


Figure 4.1 Protective effects of statins on IL-1 β treated cartilage explant. (a) cartilage explant harvest and *in vitro* culture. (b) 1 ng/mL IL-1 β was supplemented into the culture medium to mimic a moderate inflammatory attack to cartilage explant. (c) Simvastatin treatment preserved the mechanical function of cartilage explant with the presence of IL-1 β . All three types of statins prevented the (e) loss of GAG and (f) loss of collagen contents from cartilage explants during *in vitro* culture. IL-1 β -induced collagen loss was completely abolished by statins treatment. (g) Simvastatin treatment mainly suppressed the GAG loss from the surface of cartilage explant (Safranin O staining) and the phenotypic shift of chondrocytes (H&E staining). Scale bar = 200 μ m. Statin prevents chondrocyte phenotypic shift in terms of (g) cell volume and (h) cell proliferation rate by MTT. All data were shown as mean \pm 95% CI. * vs IL-1 β : p value < 0.01, and ** vs IL-1 β : p value < 0.001.

4.3.2 Protective Effects of Statin is Dependent on Rho Activities

We hypothesized that the protective effects of statins on cartilage is related to its inhibition of mevalonate pathway and the downstream Rho GTPase signaling in chondrocytes. Deactivation of Rho GTPase signaling can prevent the chondrocytes from entering a hypertrophic, degradative state under OA-inducing stimulations, and thus preserve the cartilage integrity (Fig. 4.2a). To verify this hypothesis, we tested an intermediate production of mevalonate pathway called GGOH, which is required for the geranylgeranylation of Rho GTPases. During cartilage explants long-term culture, GGOH was added together with simvastatin and IL-1 β . As expected, IL-1 β alone groups induced substantial amount of sGAG and collagen release from cartilage explant, which were significantly attenuated in the statin-treated group (IL-1 β + simvastatin in the culture medium). It's of note that compared to the IL-1 β + simvastatin group, IL-1 β + simvastatin + GGOH presented significantly higher sGAG loss ($39.92 \pm 6.44\%$ vs. $27.24 \pm 5.56\%$ for IL-1 β + statin group) and collagen loss ($33.23 \pm 5.36\%$ vs. $7.66 \pm 1.44\%$ for IL-1 β + statin group) (Fig. 4.2b). These data

suggested that addition of GGOH almost completely eliminated the favoring effects of statins on cartilage ECM integrity. The modifying-role of statins on cartilage act, at least partially, through inhibiting geranylgeranylation of downstream signaling molecules.

To further investigate the statin-mediated protein geranylgeranylation, experiments were performed with the geranylgeranylation inhibitors (GGTI298). GGTI298 can strongly inhibits the processing of geranylgeranylated Rho GTPase proteins by regulating the geranylgeranyl transferase. In this study, we wanted to check whether GGTI298 can show similar protection effects on cartilage ECM integrity as statin. During long-term *in vitro* culture of cartilage explants, GGTI298 significantly alleviated the IL-1 β -induced loss of sGAG by 38% ($25.96 \pm 6.98\%$ vs. $42.02 \pm 4.01\%$ for IL-1 β at day 8) and also complete abolished the collagen loss ($6.16 \pm 1.24\%$ vs. $26.79 \pm 5.26\%$ for IL-1 β at day 22), which showed a consistent trend with statins (Fig. 4.2 c). These results further confirmed that the modifying role of statins on cartilage were related to the geranylgeranylation of Rho GTPase proteins in chondrocytes.

To investigate the specific role of Rho GTPase proteins, we tested three well-established Rho GTPase proteins, RhoA, Rac1, and Cdc42 in cartilage explants. We used their specific, selective inhibitors including Y27632, NSC237, and ZCL278 to deactivate the RhoA, Rac1, and Cdc42 in cartilage respectively. For *in vitro* cartilage explants, the RhoA inhibitor, Y27632, didn't present significantly protective effects on either sGAG or collagen loss during long-term culture; while both Rac1 inhibitor and Cdc42 inhibitor (NSC237, ZCL278) significantly inhibited the cartilage ECM contents loss (Fig. 4.3d). To be specific, Rac1 inhibitor and Cdc42 inhibitor almost completely

blocked the collagen loss from cartilage explant during 24-day *in vitro* culture; in addition, Cdc42 inhibitor also significantly reduced the sGAG loss ($40.13 \pm 13.46\%$ vs. $66.56 \pm 10.51\%$ for IL-1 β at day 8). It's of note that the combination of these three inhibitors showed synergetic effects compared to each single inhibitor. The combination of these three inhibitors significantly reduced both the sGAG release ($44.12 \pm 10.1\%$ vs. $66.56 \pm 10.51\%$ for IL-1 β at day 8) and collagen release (5.08 ± 1.05 vs. $46.90 \pm 11.78\%$ for IL-1 β at day 22) during *in vitro* culture. The concentration of each inhibitor used in this study was chosen based on a rigorous dosage study ranging from 40 μm to 100 μm . Taken together, these data confirmed that statin protection effects on cartilage integrity were dependent on the inhibition of mevalonate pathway and its downstream Rho GTPases in chondrocytes.

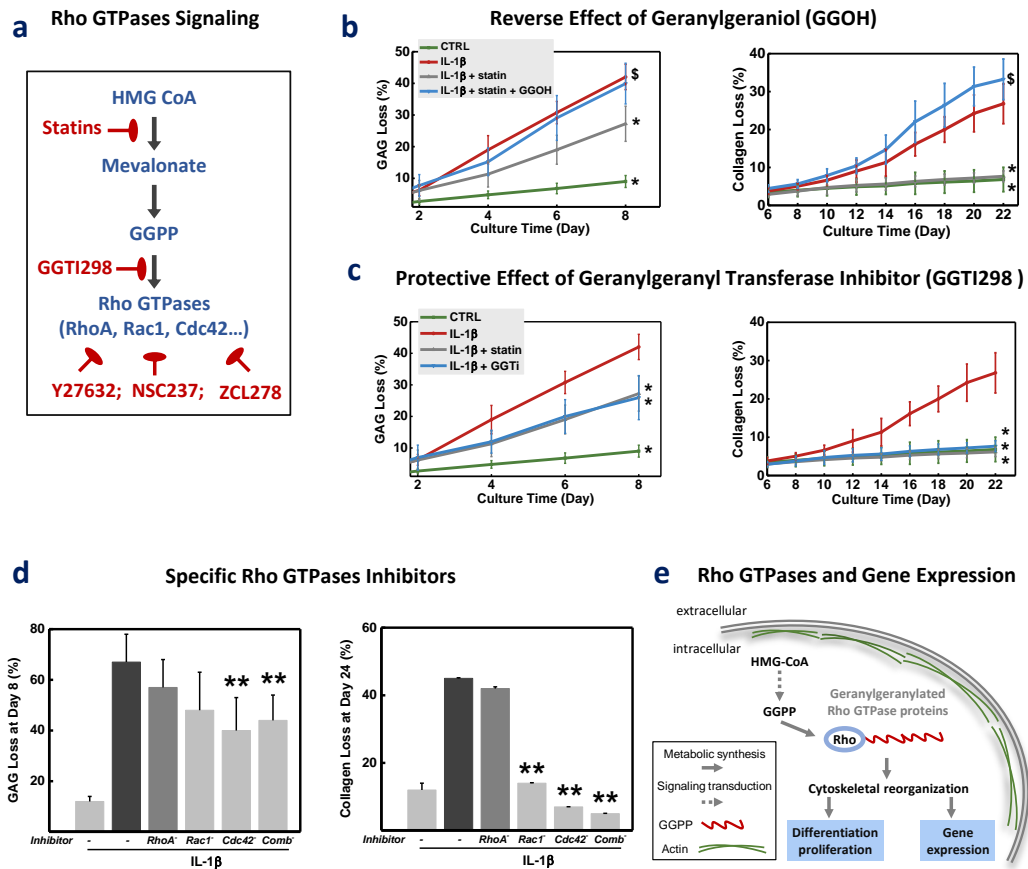


Figure 4.2. Chondro-protective effects of statins are related to the inhibition of Rho activities. (a) Illustration of mevalonate pathway and its related inhibitors. (b) A mevalonate pathway derivative GGOH which is required for Rho GTPase proteins geranylgeranylation abolished the chondro-protective effects of statin. (c) A downstream mevalonate inhibitor GGTI298 which can inhibit the geranylgeranylated Rho GTPase proteins showed similar protective effects as statin. (d) Specific inhibitors of Rho GTPases also prevented the IL-1 β -induced collagen loss. (e) Illustration of the regulatory role of Rho GTPases in cytoskeleton and gene expression. * vs IL-1 β : p value < 0.01, ** vs IL-1 β : p value < 0.001; and \$ vs IL-1 β + simvastatin: p value < 0.01.

4.3.3 Statin Can Directly Regulate the Expression of Rho GTPase-related Genes in Chondrocytes

We performed RNA sequencing (RNAseq) to assess the whole genomic gene expression changes of cartilage under simvastatin treatment. After 48-hour treatment, the expression of 1,048 genes was differentially expressed (DEGs) in the chondrocytes (Fig. 4.3a). Among these DEGs, 650 genes were significantly downregulated and 398 genes were upregulated in the group treated with IL-1 β plus simvastatin compared to that of the IL-1 β alone group. The expression changes of anabolic genes were minor, such as aggrecan (ACAN, fold change: 1.32, FDR: 0.6), type II and VI collagen (COL2A1, fold change: 1.43, FDR: 0.59; and COL6A1, fold change: 1.41, FDR: 0.41), and bone morphogenetic proteins (BMP2, fold change: 1.58; and BMP6, fold change: 1.67, FDR < 0.01 for both) (Fig. 4.3b). In contrast, the expression of catabolic genes was significantly suppressed in the simvastatin-treated group, such as the MMP-13 (fold change: -6.68, FDR < 0.001), ADAMTS-5 (fold change: -4.47, FDR < 0.001) and IL1B (fold change: -9.84236, FDR < 0.001) (Fig. 4.3b). These data suggested that, under inflammatory stimulation, the protective effects of statins on cartilage ECM integrity might be main through preventing the chondrocytes from entering a catabolic, degradative process rather than promoting cellular anabolic activates for self-repair.

According to enrichment analysis using 1,048 DEGs, Rho GTPase signaling was also identified as one of the significantly altered pathways in the statin-treated cartilage explant compared to IL-1 β alone group (Fig. 4.3c). In total, 42 DEGs from our total DEGs were shown to be involved in Rho GTPase signaling, and the expression of some well-studied genes was listed, *e.g.* Rac GTPase Activating Protein 1 (RACGAP1, fold change: -2.47, FDR < 0.001) and Rho GTPase Activating Protein

genes (ARHGAP11A, fold change: -4.19, FDR < 0.001) (Fig. 4.3d). Similarly, overrepresentation analysis also identified 22 significant Gene Ontology terms of biological process using the DEGs list, 5 of which are related to cell morphology including cell differentiation, cytoskeleton organization, regulation of cell cycle, cell proliferation, and cell growth (Fig. 4.3e). Taken together, RNAseq analysis indicated the protective effects of statin on cartilage ECM and cell phenotypic stability is associated with its direct, systematic regulation on gene expression in chondrocytes. More importantly, Rho GTPase signaling may play an important role in the chondrocytes gene expression regulation by statins.

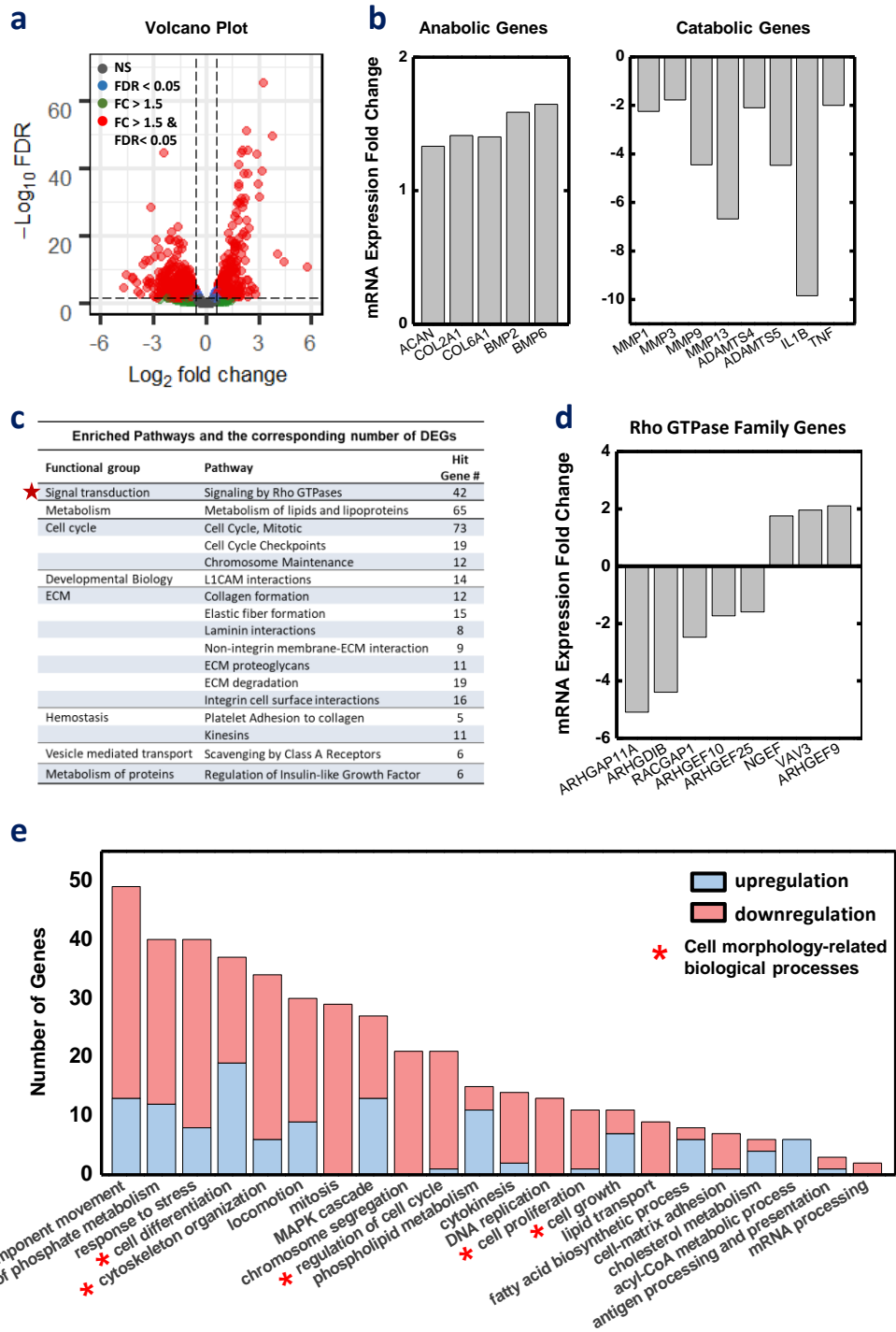


Figure 4.3 RNA sequencing analysis. (a) Total number of Differentially Expressed Genes (DEGs, absolute fold change > 1.5 and FDR < 0.05). (b) Expression changes of well-studied anabolic genes and catabolic genes in chondrocytes treated by IL-1 β + simvastatin compared to that of IL-1 β alone group. (c) Enrichment analysis using DEGs for identifying significantly altered pathways (FDR < 0.05). (d) Overrepresented biological processes in the simvastatin-treated cartilage (FDR < 0.05). The pathways denoted by red star are involved in the regulation of chondrocytes phenotype stability.

4.3.4 Another Mevalonate Inhibitor, Bisphosphonate, Presented Similar Chondro-protective Effects as Statins Did

Bisphosphonates, a class of drugs to treat osteoporosis, is also a potent inhibitor of mevalonate pathway, which can disable the ruffled border formation of osteoclast for bone resorption (Fig. 4.4a). In this study, we aimed to assess whether zoledronic acid (ZA), a member of bisphosphonate family, would present similar protection effect on cartilage as statins did. Using the inflammatory cartilage explant *in vitro* model, ZA significantly inhibited the loss of sGAG compared to IL-1 β alone group during 8-day culture, $36.3 \pm 1.24\%$ of IL-1 β -treated samples vs $21.3 \pm 2.27\%$ of IL-1 β plus ZA rescued samples (Fig. 4.3b). The expression of ECM-degrading genes, including MMP-1, 9 and ADAMTS-4, -5 was significantly suppressed in the ZA-rescued samples compared to that of the IL-1 β alone group (Fig. 4.3c). Safranin O and IHC staining images confirmed the inhibitory effects of ZA on sGAG loss and type II collagen loss particularly in the surface of cartilage explant (Fig. 4.3d). The mechanical integrity of ZA-rescued cartilage explants was significantly higher than IL-1 β alone group, both Young's modulus and dynamic modulus ($p = 0.01$ for both); while adding GGOH in combination with ZA masked the protective function of ZA by reducing the modulus compared to the ZA treated group ($p = 0.01$ for both) (Fig. 4.3e).

We further verified the favorable effects of ZA using another *in vitro* model, serum-damaged cartilage explant model. Joint trauma often leads to intra-articular bleeding, which is widely believed to be a potential cause of cartilage degradation. In previous studies, we exposed the cartilage explants to a serum-supplemented (10% FBS) medium for 7 days, which significantly compromised the mechanical integrity and ECM integrity of cartilage tissues. In this study, we aimed to check whether ZA can rescue the adverse effects of serum exposure. The cartilage explants were first treated in serum-containing medium for 7 days and then rescued with ZA for 4 weeks (Fig. 4.3f). As results, ZA treatment preserved the ECM integrity of cartilage explant by preserving the sGAG content of cartilage explant ($7.36 \pm 1.57\%$ vs. $4.67 \pm 1.75\%$ for the non-ZA group) and the collagen content ($9.76 \pm 2.90\%$ vs. $7.04 \pm 2.21\%$ for the non-ZA group) (Fig. 4.3g). Mechanism testing result confirmed the protective actions of ZA on cartilage ECM, ZA-rescued group presented significantly higher Young's Modulus at day 15 and day 29 ($p < 0.01$ for both) (Fig. 4.3h). Addition of GGOH reversed the protective effects of ZA during this long-term culture, which was reflected by Young's modulus (Fig. 4.3h). Therefore, another inhibitor for mevalonate pathway, Bisphosphonate, also present chondro-protection property as statin did. The disease-modifying role of both statins and bisphosphonates are related to the inhibition of mevalonate pathway and the subsequent deactivation of Rho GTPase signaling.

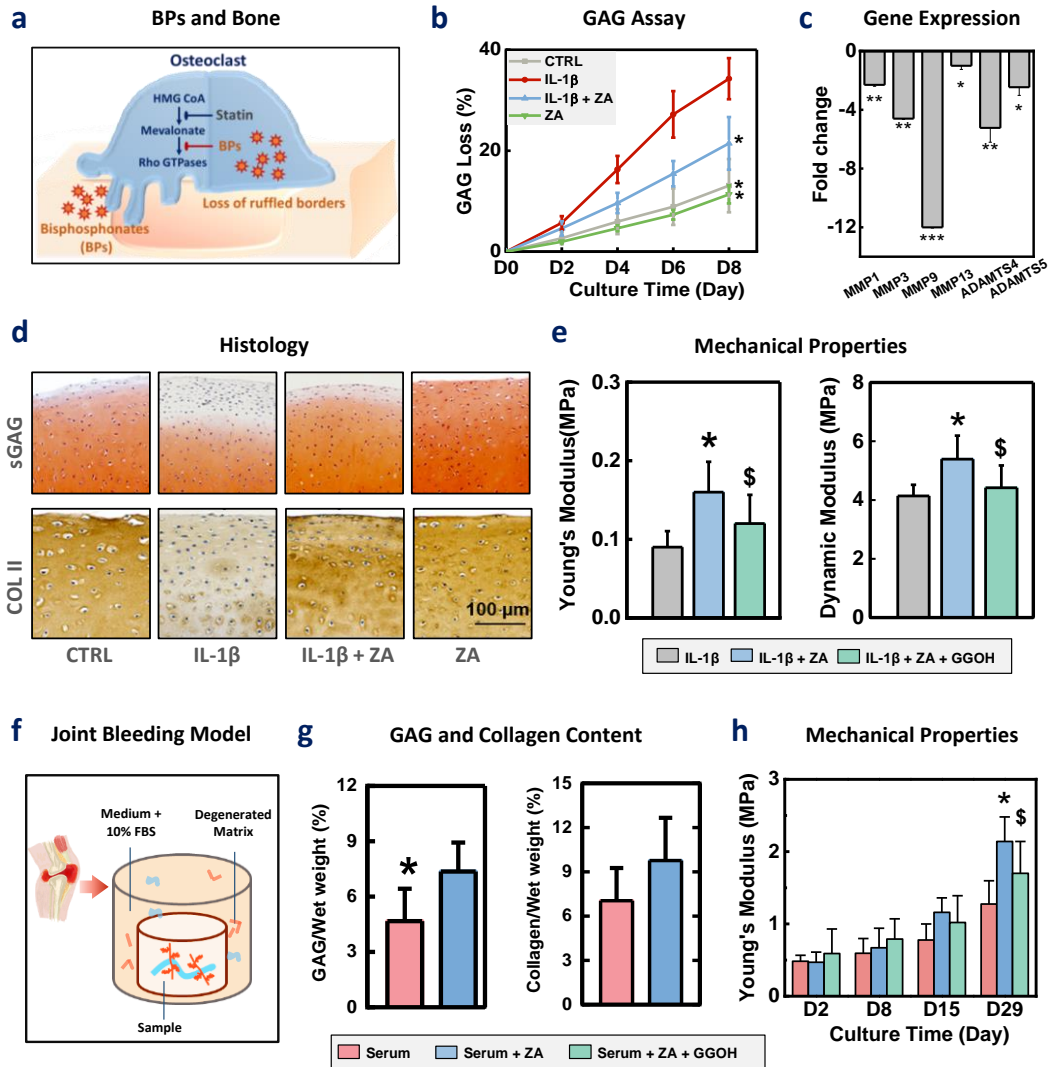


Figure 4.4 Zoledronic acid, another mevalonate inhibitor, presented similar protective effects on cartilage explants as statins did. (a) Osteoclasts mediated bone resorption is inhibited by bisphosphonates and undergo apoptosis. ZA treatment suppressed the (b) loss of GAG and (c) catabolic gene expression of IL-1 β -treated cartilage explant. (d) Safranin O histological and immune-histological staining of sGAG and type II collagen respectively. (e) Mechanical property of cartilage explant was preserved by ZA treatment after 8-day culture. (f) Serum damaged cartilage explant model. ZA treatment rescued the cartilage explant in terms of (g) ECM content and (h) mechanical property. Co-treatment of ZA and GGOH overrides the beneficial effects of ZA. All data were shown as mean \pm 95% CI. * vs IL-1 β : p value < 0.01, ** vs IL-1 β : p value < 0.001; and \$ vs IL-1 β + simvastatin: p value < 0.01.

4.4 Discussion

This study reveals a mechanism by which statin and bisphosphonate can prevent cartilage degeneration under various OA-inducing factors. Statin- or bisphosphonate-induced inhibition of mevalonate pathway and the subsequent Rho GTPases activities prevent the chondrocytes from responding to OA-inducing stimulations, which further prevents the degeneration of cartilage ECM (Fig. 4.5). This newly identified chondro-protective mechanism of statin might resolve the “contradiction” in previous cohort studies regarding the role of statins in OA patients and joint function. The European studies report a beneficial effect of statins; while others suggest that statins might be associated with worsening joint function probably through negative effects on subchondral bone formation angiogenesis²⁰² or through adverse effects on muscle or soft tissue related pain²⁰⁸. This discrepancy, in fact, could be, at least partially, explained by the early protection mechanism of statin on cartilage revealed in our study. The aberrant activation of Rho GTPases in chondrocytes occurs in acute phase of OA, *e.g.* immediately after the joint injuries; and thus the protective effects of statin on cartilage through inhibiting cellular Rho

activities could be most effective in early stage as compared with later stage of OA ²². In the European studies, eligible patients were selected from general population based on statin use, *i.e.*, patients with statin prescription and OA free history; while the U.S. studies focused on the patients who are radiographically suspected or confirmed knee OA. Future research should include participants without history of OA diagnosis and examine the role of statins on preventing the onset of OA.

The protective mechanisms of statin on cartilage have been under investigation, and many studies attributed to its control of cholesterol metabolism ²¹⁰. A previous study using *in vitro* cartilage explant report that addition of squalene, the precursor for the synthesis of cholesterol, is unable to reverse the beneficial effects of simvastatin on cartilage ²¹¹; and removal of cholesterol from chondrocytes could not favorably affect the cartilage structure integrity ²¹¹. Similarly, another study reported that 36-hour treatment of IL-1 β significantly increased the cholesterol level in primary chondrocytes, while this trend is not changed by simvastatin treatment ²¹⁰. This indicates that cholesterol-modifying function of statin is not associated with its protective mechanisms in chondrocytes.

Another important property of statin, anti-inflammation, has been proven by a large body of clinical and experimental evidence ²⁰⁶. The most compelling clinical studies derived from large-scale population data indicate that statins can lower an inflammatory biomarker C-reactive protein by 15-30% in a manner largely independent of plasma lipid reduction ²¹²⁻²¹⁴. Also, experimental observations from animal and *in vitro* studies strongly support the anti-inflammatory role for statins. For instance, statins exhibit dosage-dependent effects in suppressing IL-1-induced MAPK signaling pathway via downregulating the activation of ERK, p38, and JNK in

chondrocytes²¹¹. This observation is also reinforced by our RNAseq analysis which suggested the decreased expression of cytokines, chemokines, and NF- κ B genes and altered MAPK pathway in simvastatin-treated cartilage explant. It's of note that many anti-inflammation drugs are dedicated to ease joint inflammation but unable to exert protective functions as effective as statins. Meanwhile, the compounds with little regulatory effects on inflammation, such as bisphosphonates, geranylgeranylation inhibitor, and specific Rho GTPase inhibitors, still demonstrated potent chondro-protection functions in our study. Therefore, we believe that anti-inflammation property of statin alone cannot justify the clinical usage of statins for OA prevention.

Recent studies have suggested that statins have cholesterol-independent, “pleiotropic” effects, that is, they are capable of simultaneously suppressing multiple pathogenic pathways and thus producing more than one benefit²¹⁵. Indeed, a growing body of evidence indicate that statins are involved in endothelial function improvement, atherosclerotic plaques stabilization, oxidative stress suppression, and thrombogenic response inhibition. More importantly, statins have been suggested to have been implied to have disease-modifying effects on skeletal dysplasia²¹⁶, cardiac rejection²¹⁷, and transplant arteriopathy²¹⁸. Many of these pleiotropic effects are mediated by inhibition of the downstream of mevalonate pathway, specifically, inhibition of isoprenoids, which plays an essential role in regulating the prenylation of Rho GTPase proteins. Rho GTPases, as molecular switches, play prominent role in controlling a wide variety of signal transduction pathways in all eukaryotic cells²¹⁹.

During OA progression, Rho GTPase proteins are believed to play pathological roles in shift chondrocytes toward a hypertrophic, degradative state. RhoA has been shown to be involved in actin cytoskeletal reorganization in response to OA-inducing

factors, such as mechanical insult ⁹⁰ and cytokine IL-1 β stimulation ¹¹⁸. The regulatory effects of RhoA are partially through interacting with OA-associated growth factors, including epidermal growth factor receptor signaling factors ⁹¹, insulin-like growth factor-1 (IGF-1) ⁹² and fibroblast growth factor ⁹³, suggesting a universal role of RhoA in OA progression. With regards to the pathological role of Rac1/Cdc42 signaling pathway, a majority of the evidences are focusing on their indispensable role in disturbing metabolic balance of chondrocytes. Rac1 is involved in MMP-13, ADAMTS-5, COLX and Runx2 overexpression ^{97,117}, probably through regulating of the transforming growth factor- β signaling ²²⁰. Cdc42 has been shown to be required for ECM degeneration by inducing the overexpression of MMP-13 and collagen X in articular cartilage of mouse OA model with surgical destabilization of the medial meniscus ⁹⁸. Taken together, it's well established that Rho GTPases play specific but complementary roles in OA progression; and blocking the activity of some member of Rho GTPase proteins might be a promising approach to delay OA development.

Although sharing similarity in some aspects of biological functions, the specific role of RhoA, Rac1, and Cdc42 on chondrocytes may be of distinction. In this study, unlike the inhibitor for Rac1 or Cdc42, RhoA inhibitor (Y27632) didn't present significant protection effects on cartilage ECM integrity. In fact, Y27632 induces the loss of RhoA activity by inhibiting a major downstream effector, Rho-associated protein kinase (ROCK), which is one of the major regulators of the cytoskeleton ²²¹. According to previous studies, RhoA/ROCK and Rac1/Cdc42 signaling have antagonistic effects in controlling the proliferation and differentiation of chondrocytes ^{18,80,89} and other cell types ^{222,223}. The effects of RhoA regulating chondrogenesis seem context-dependent, monolayer cultured or three-dimensional cultured cells ⁸⁷. For

monolayer ATDC5 cells, over-expression of RhoA resulted in delayed hypertrophic differentiation with reduced COLX and MMP13 expression⁸⁸. However, the inhibitory effects of RhoA on chondrocyte differentiation are not observed in a three-dimensional micromass culture system⁸⁷. In response to ROCK inhibition, the gel-cultured cells display a decrease in chondrogenesis marker gene expression, including collagen II, aggrecan, and Sox9⁸⁹. Furthermore, inhibition of RhoA by Y27632 treatment can only partially rescue the effects of RhoA overexpression¹⁸, signifying that RhoA may signal through ROCK-independent pathways in regulating chondrocytes morphology²²¹. Future study is necessary to explore the other effector pathways of RhoA, which are potential candidates for mediating RhoA effects in chondrocytes²²⁴. Despite the complex interactions among Rho GTPase members, both statin and bisphosphonates can effectively halt the OA initiation through regulating Rho GTPases activities in chondrocytes. It's of note that the timing of administrating statin or bisphosphonate is critical to achieve optimal therapeutic effect for OA treatment. Statin or bisphosphonate would be used immediately after the trauma injuries to prevent the cells from responding to catabolic stimuli; in contrast, the drug may have little effect for the cessation or reversal of late OA progression, when most chondrocytes are gone or have experienced phenotypic changes.

There were some limitations of this study. First, although the statin concentrations used in this study are identical to previous studies, it must be considered that the concentrations are higher than clinically prescribed plasma concentrations which range between 0.01 and 0.1 μM for simvastatin. One potential solution would be direct intraarticular injection of a statin in combination with a sustained release technology in order to ensure sufficient exposure of chondrocytes to

the statin while minimizing systemic exposures. Second, animal studies are still required to confirm the effect of inhibition of Rho GTPases in chondrocytes for preventing OA progression. However, given previous in vivo animal studies using statins and Rac1 inhibitors, we expect the results will be highly consistent with the results presented in this study.

To the best of our knowledge, this is a first study to report that statins can prevent cartilage ECM breakdown and chondrocytes phenotypic shift by directly regulating the Rho GTPases activities. Two selective Rho GTPases inhibitors showed the similar protection effects as statin did; while addition of GGOH in cartilage reversed the effects of statin, indicating that the protective effect of statin on cartilage is mainly through the prevention of Rho GTPases geranylgeranylation. These findings suggest that statins can directly protect against cartilage damage and, given their well-established anti-inflammatory role, have potential as therapeutic agents for OA.

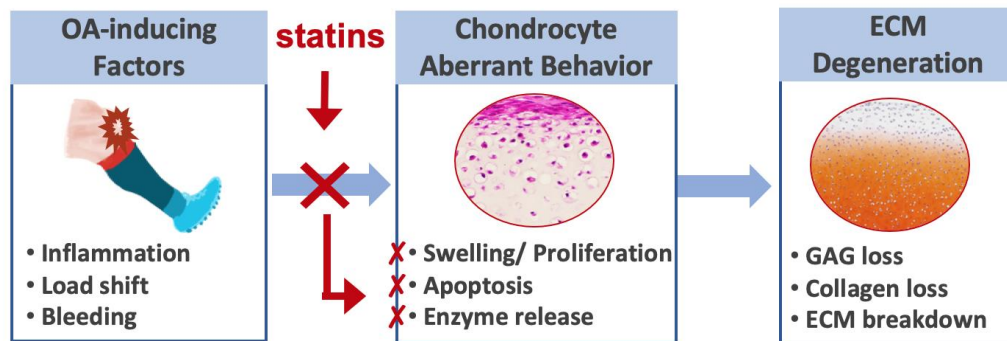


Figure 4.5 Statins and bisphosphonates inhibit the Rho activities in chondrocytes and prevent the aberrant phenotypic shift of chondrocytes under catabolic stimuli.

Table 4.1 Summary of statins' effects on the cartilage: clinical cohort studies.

Authors	Study Population	Follow-up Time	Outcome Assessment	Main Findings
Beattie et al ²⁰² .	Prospective observational cohort study of 5,674 women with OA	8 years	Radiographic hip OA	<p>> Statin presented very modest but significant ($p = 0.045$) increase in the risk of developing new-onset severe hip OA.</p> <p>> Statin users showed consistent but not significant trend toward a decreased risk of OA</p>
Peeters et al ²⁰³ .	Cohort study of 6,966 middle-aged women and 4,806 older women	10 years	Self-report of joint pain/stiffness, physical function, and self-rated health	<p>> No demonstrated association between statin use and reduced onset of joint pain.</p> <p>> Statin use in middle-aged women was weakly associated with poor physical functioning, but not with new joint</p>
Riddle et al ²⁰⁴ .	Prospective cohort study of 2207 persons with radiographically suspected or confirmed knee OA	4 years	WOMAC Physical Function scale	<p>> Increased duration of statin use was associated with worsening in WOMAC Physical Function scores over the study period ($p = 0.005$).</p> <p>> Statin use was not associated with improvements in knee pain, function or structural progression trajectories.</p>
Kadam et al ²²⁵ .	Cohort study of 16,609 adults with cardiovascular disease	10 years	OA defined on the basis of any coded clinical entry instead of radiographic OA	Higher therapeutic dose of statin, with a treatment duration of at least 2 years was associated with a significant reduction in clinical OA compared to non-users.
Clockaerts et al ²⁰⁰ .	prospective cohort study of 2921 patients aged 55 years and older	6.5 years	Radiographic OA	Statin use is associated with more than a 50% reduction in overall progression of osteoarthritis of the knee, but not of the hip.
Valdes et al ²⁰¹ .	Cohort of 3,800 patients with large joint OA who underwent total joint replacement	4 years	Radiographic OA	Use of statins is associated with a lower prevalence of only a specific OA phenotype, e.g. generalized nodal OA.

Sheng et al ²²⁶ .	Cohort study of 1269 patients with OA	3.6 year	All-cause mortality	Statins were associated with reduced mortality in OA in primary prevention.
------------------------------	---------------------------------------	----------	---------------------	---

Table 4.2 Summary of statins' effects on the cartilage: animal studies.

Authors	Animal Model	Administration	Statins	Daily Dose	Main Findings of Statin Effects
Leung et al ²²⁷ .	Monosodium iodoacetate injection, mouse	Intraperitoneal	Simvastatin	10 to 40 mg/kg	Reduced histological evidence of cartilage damage
Funk et al ²²⁸ .	Streptococcal cell wall injection, rat	Subcutaneous	Simvastatin	20 mg/kg	Inhibition of cartilage destruction (47%)
Akasaki et al ²²⁹ .	Experimental OA, rabbit	Intra-articular	Mevastatin	0.02 to 1 mg/kg *	> Inhibition of morphologic and histologic signs of cartilage degradation > Reduction in MMP-3
Zhang et al ²³⁰ .	IVD degeneration model, rat	Intra-discal	Simvastatin	0.01 mg **	> Improvement in histologic changes and <i>in vivo</i> alterations detected by MRI imaging > increase in BMP-2 and collagen type II mRNA levels, and collagen type II/type I ratio (differentiation index)
El-Seweidy et al ²³¹ .	Monosodium iodoacetate injection, rat	Intra-articular	Atorvastatin	10 mg/kg	> Decreased inflammatory cytokines and cholesterol > Increased MMP2 tissue inhibitor
Bayyurt et al ²³² .	ACLT model, rat	Intra-articular	Atorvastatin	0.4 mg/kg for 3 weeks *	> Prevention of OA development, with more normal cartilage surface, and less damaged cells over time

*: weekly injection dose **: Single injection dose

Chapter 5

STATIN USE AND REDUCED RISK OF OSTEOARTHRITIS FOR DELAWARE POPULATION: A RETROSPECTIVE COHORT STUDY WITH PROPENSITY SCORE-MATCHING

5.1 Introduction

Osteoarthritis (OA), a degenerative joint disorder disease, is the most common cause of long-term disability, affecting nearly 27 million (12%) adult population of the United States³⁹. While the etiology of OA remains controversial, researchers commonly believe that it's multifactorial, including aging, female gender, sports participation, injury to the joint, obesity, and genetic susceptibility³⁹. In addition, lower educational level, repetitive use of joint, bone density, muscle weakness, and joint laxity are also shown to play roles in the development of joint OA³⁹. Current treatment options for OA include modification of mechanical loading patterns, improvement of psychosocial factors, or replacement of intra-articular cartilage²³³. However, these treatments achieved minimal outcomes and are only able to delay the costly total joint replacement⁴⁴. Thus, a significant unmet clinical need exists for early clinical interventions that can be applied to slow or stop OA progression.

Statins are a class of FDA-approved lipid-lowering medications, which are commonly prescribed for the prevention and treatment of cardiovascular diseases (CVDs). Recently, a growing body of evidences suggest the disease-modifying effects of statins on joint disorders, *e.g.* skeletal dysplasia²¹⁶, cardiac rejection²¹⁷, and transplant arteriopathy²¹⁸. In fact, the joint-favoring effects of statins have been

observed in various animal models decades ago. However, the results from several longitudinal clinical studies present conflicting results, which hinders the clinical application of statins on OA treatment. The clinical studies from Europe report that the use of statin is associated with significantly lower OA occurrence during long-term follow up period ^{200,201,225}. In contrast, two clinical studies focusing on the U.S. population observe a positive association of statin use with worsening physical function of knee joint for patients with radiographically suspected or confirmed knee OA ^{202,204}. The discrepancies between publications aroused heated debates regarding the methodological factors ^{205,209}. For example, the baseline characteristics of statin user groups often systematically differ from those non-user group. Such unbalanced baseline characteristic is a common confounding issue within observational study and can induce severely biased estimation of predictors ²³⁴. Historically, researchers have been relied on the use of regression adjustment to account for confounding differences between two groups. Nowadays, there has been increasing interest in incorporating propensity score-based methods into a regression model to reduce or eliminate the confounding effects ²³⁵. Therefore, future investigations are still needed to apply and compare multiple propensity score methods to reduce the effects of confounding in observational studies.

In addition to classic regression model, a variety of artificial intelligence models have been developed for predicting clinical outcomes, such as artificial neural networks (ANNs) ²³⁶. As to date, the classic regression model and artificial neural networks are the most widely used models in biomedicine, as measured by the number of publications indexed in Medline: 28,500 for logistic regression, 8500 for neural networks, and 2400 for other artificial intelligence models ²³⁶. In fact, ANN can be

considered as a generalization of the logistic regression model; and these two models share common roots in recognizing statistical patterns²³⁶. It is widely believed that artificial intelligence models are more accurate and less subjected to outliers.

In this study, our central hypothesis was that statin use will yield the clinically meaningful absolute and relative increase in OA-free life expectancy and reductions in OA occurrence rate. A retrospective cohort study was conducted using patients' electronic medical records from the database of Christiana Care Health System (Newark, DE, U.S.), among which OA is a common disease and the use of statin is routine. Classic regression model and ANN model will be implemented and compared in terms of each predictor's effects on total OA occurrence. The results of this study will enable us to assess the comparative effectiveness of statin use in the prevention or delay of OA occurrence.

5.2 Materials and Methods

5.2.1 Cohort Population

We collected the patients' information from the database of Christiana Health Care System, Newark, Delaware, U.S.A. All the patients who were diagnosed with cardiovascular diseases (CVD) during our observation window (January 2008 to December 2015) were considered. The patients are those who are >18 years old and have > 2-year medical record in the database were selected and followed up until January 2018. This study was given full ethics approval by the Institutional Review Board of both the Christiana Care Health System and University of Delaware.

5.2.2 Definition of OA Case and Statin User

In the cohort, patients identified as OA case must satisfy the following 2 criteria: (1) with a first-time recorded ICD-9 code of OA diagnosis (715.x) during the follow-up period; and (2) with ≥ 2 years of OA-free history prior to the first recorded OA diagnosis. Considering that a certain duration of statin treatment is required to achieve a significant beneficial effect on joint health, we only included the patients who have been diagnosed with OA ≥ 1 after first date of statins prescription/CVD diagnosis. The patients diagnosed with OA prior to or within 1 year after the statin use prescription /CVD diagnosis were excluded.

Statin user was defined as with at least one prescription record of statins (simvastatin, atorvastatin, lovastatin, pravastatin, or rosuvastatin) during our observation window (2008-2018). The patients without any statin prescription at any time of the observation window were defined as non-statin users.

5.2.3 Baseline Covariates

The cofounding factors from 4 categories were collected as below. *Basic information*: age, gender, and race; *healthcare utilization*: number of general practice visits per year, and number of drugs prescribed per year; *Disease history*: peripheral artery disease (PAD), diabetes, CVD type and diagnosis year, and mortality; *life style*: smoke status, body mass index (BMI; weight (kg)/height (m²)), diastolic blood pressure (DBP) (mm Hg), and systolic blood pressure (SBP) (mm Hg). Subjects with missing value in continuous covariates were excluded from the cohort. The missing values in categorical covariates were specified as a new category named “unknown”.

5.2.4 Propensity Score Estimation

The propensity score is the conditional probability of a subject being assigned to the treatment group given the observed covariates. It is true that we do not know the true propensity score of each individual; however, we could observe that which individuals were assigned to treatment, along with a number of measured covariates for each individual. Accordingly, we can develop a model to predict the probability of treatment (propensity score) using the covariates. The propensity score is often used to reduce the bias due to confounding variables in the statistical analysis of observational study. In this study, the propensity score for each individual was estimated using a logistic regression model with all the covariates available:

$$p(x) = p(T = \text{statin prescription} \mid X = x),$$

which estimates the effect of statin treatment by accounting for the covariates that predict receiving the statin.

Inverse Probability Weighting: To balance the baseline characteristics, we first used inverse probability weighting (IPW) method to assign each observation a weight as shown as below,

$$w(x) = \begin{cases} \frac{1}{p(x)} & \text{for OA case,} \\ \frac{1}{1 - p(x)} & \text{for control.} \end{cases}$$

As results, IPW weights the outcome measures by the inverse of the probability of the individual with a given set of covariates being assigned to their treatment. One common issue with IPW is that individuals with a propensity score very close to 0, *i.e.* those are not likely to be treated, will end up with an extremely large weight, potentially making the weighted estimator highly unstable. We therefore

further stabilized the weight using the marginal probability of statin treatment instead of 1 in the weight numerator.

$$w(x) = \begin{cases} \frac{P(T = 1)}{p(x)} = \frac{P(T = 1)}{P(T = 1 | X = x)} & \text{for OA case,} \\ \frac{1 - P(T = 1)}{1 - p(x)} = \frac{1 - P(T = 1)}{1 - P(T = 1 | X = x)} & \text{for control.} \end{cases}$$

Note that whereas the original weights essentially double the sample size, the stabilized weights preserve the sample size.

Propensity Score Matching: Propensity score matching technique was used in many previous statin-OA cohort studies to reduce the bias of raw data. In this study, we adopted a latest modified matching method. The propensity score was estimated using a logistic regression model within each half-year cohort accrual block, *i.e.*, 14 blocks from January 2008 to December 2015 to address the potential secular trends in statin prescription and OA occurrence. Within each accrual block, we matched each statin user with a non-user using a 1-to-1 ‘nearest matching’ algorithm with caliper as 0.0007. We elaborated more details in Result section (Fig. 5.3).

5.2.5 Statistical Analysis:

Descriptive Analysis: A descriptive analysis of all the 15 covariates was performed and summarized as mean for continuous variables and percentage for categorical variables. To compare the baseline characteristics between statin users and non-users, we used Student’s t test for continuous variables and Pearson’s χ^2 test for categorical variables.

Cox proportional hazard model: The cox proportional hazard models, with survival time to OA incidence, was used to estimate the hazard ratio between the statin user vs non-user groups. Survival plots were generated as estimates of cumulative risk

to identify time trends in the OA occurrence. We repeated the same analysis using raw data, IPW weighted data and propensity score matched data. We conducted subgroup analysis stratified by age (< 45, 45 – 55, or > 55 years old), gender (female or male), smoking status (never smoking or others status), and diabetes (yes or no).

Logistic regression model: To assess the association between statin use and common musculoskeletal diseases, we performed a logistic regression model composed of statin use and all the variables. The odds ratio (OR) in statin users vs non-users, 95% CI and p values were calculated for each musculoskeletal disease.

Artificial neural network: Artificial neural network (ANN) belongs to a class of neural networks called multilayer perceptrons. We trained the model method using a supervised backpropagation algorithm with logarithmic loss function to minimize the misclassification between the ANN's output and the true OA case of the cohort. After hyperparameter tuning, we designed an ANN composed of 17 input neurons, 10 hidden neurons, and 1 output neuron designed to predict the occurrence of OA. The decay size was set as 15 to regularize the cost function for avoiding overfitting problem.

5.3 Results

5.3.1 Cohort Population

We included all the patients diagnosed with CVD during January 2008 to December 2015. The patients who were diagnosed OA before first statin prescription (N = 4,068, 6.5%) and the patients without complete covariate information (N =5,000, 8.0%) were excluded from this cohort population (Fig. 5.1a).

Demographic information of the cohort (N = 53,452) was summarized in Fig. 5.1b. The average age of the cohort is 56 ± 15 years old, following a normal distribution. 43% population are female. White population represents 54% of the cohort, 18% non-white, and 28% without race information. 63% patients were diagnosed with hypertension, 32% with dyslipidemia, and 5% with other CVD, such as heart failure. A majority (87%) were residents of Delaware state, followed by Pennsylvania (5%), New Jersey (4%), and Maryland (4%) (Fig. 5.1c).

All eligible patients (N = 53,452) are followed from the date of their first CVD diagnosis date until the end of January 2018, which is referred as observation window in this study (Fig. 5.1d). During the observation window, all the patients who are diagnosed with OA is defined as case, and all the others are defined as non-OA case.

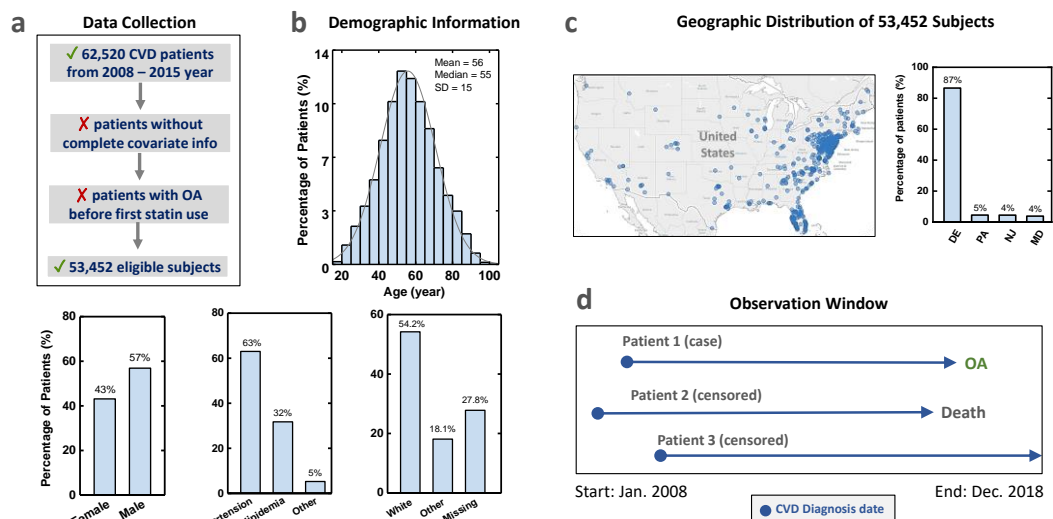


Figure 5.1 The cohort information. (a) Collecting of patients with CVD during the observation window from January 1, 2008 to December 31, 2015. (b) Demographic information including age, gender, CVD type, and race. (C) The geographic information. (d) The definition of OA case and censored patients within our observation window.

Within the overall study population, there were 25,677(48%) statin users who had been prescribed at least one form of statin within the observation window, and 27,775 (52%) are non-statin users. The baseline characteristics were compared and showed significant difference between statin user and non-user group (Fig. 5.2 and Table 1). The demographic features between the users and non-users are disparate, including age (60 vs 51 years old, $p < 0.001$), gender (58% vs 52% as female, $p < 0.001$), and race (26% vs 28% as white, $p < 0.001$). In addition, despite minimal difference in BMI value between two groups (31.60 vs 31.60, $p = 0.96$), statins users present significantly worse health status in terms of higher diastolic blood pressure (80.74 vs 78.57, $p < 0.001$), systolic blood pressure (132.73 vs 131.97, $p < 0.001$), mortality rate (6.6% vs 3.5%, $p < 0.001$), PAD rate (3.9% vs 1.2%, $p < 0.001$), and diabetes (40.9% vs 16.5%, $p < 0.001$) compared to those of non-users. Finally, statin users visit hospital office more often than non-users (21 vs 15 times in 10 years, $p < 0.001$). Taken together, statin user and non-user group have significantly, systematically difference in baseline characteristics. The worse health status of statin users may predispose them to a higher risk of OA development and impedes cohort analysis from detecting true association between statin use and OA occurrence.

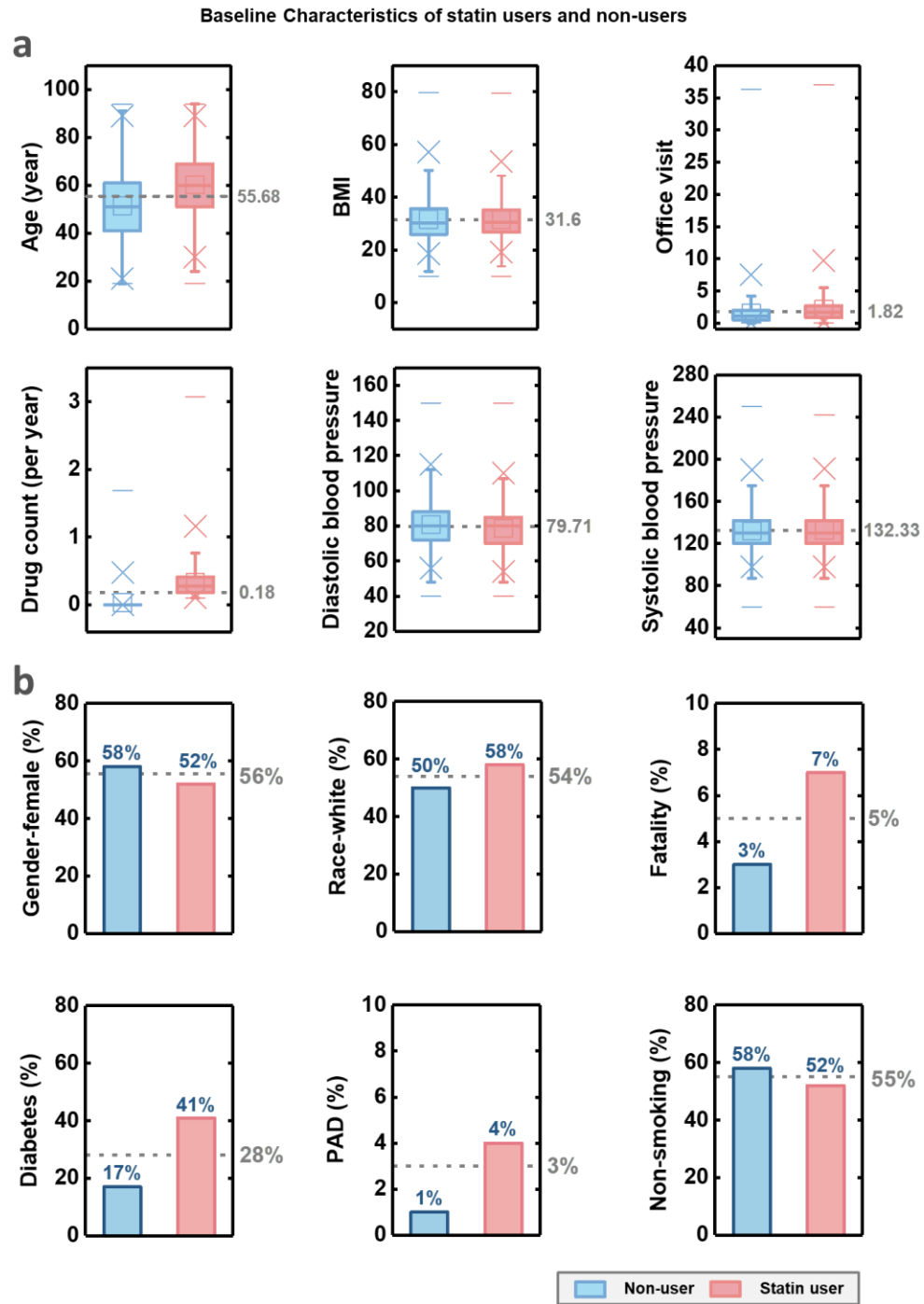


Figure 5.2 The baseline characteristics of 53,452 patients in the raw cohort. The baseline difference between statin-users and non-users on (a) The continuous variates, and (b) the categorical variates.

5.3.2 Propensity Score Methods to Reduce Confounding Effects

To reduce the confounding effects due to unbalanced baseline covariates, we used a logistic regression model to estimate the propensity score as the conditional probability of a patient receiving statin treatment given a vector of all covariates. In our raw cohort, the distribution of estimated score presented obvious divergence between the statin user and non-user group, reflecting the unbalance in baseline characteristics (Fig. 5.3b, left).

We used two different propensity score methods to remove the confounding effects before estimating the effects of statin use on outcome, propensity score matching and inverse probability weighting. Standardized differences of the baseline parameters were calculated between two groups. For the data weighted by the inverse probability of statin treatment, some predictors, such as gender, blood pressure, PAD and smoking status, in the statin user group became comparable to those of non-user group (standardized difference < 10%), indicating some improvement in the bias elimination (Fig. 5.3c). Compared to inverse probability weight, the propensity score matching method significantly improved the data balance, the standardized differences of all predictors except drug count were well within the standard guideline (10%) (Fig. 5.3b-c). The scored matched data presented great similarity in baseline characteristics between two groups, such as age (57 vs 57 years old, $p = 0.77$), gender as female (54.3% vs 55.0%, $p = 0.37$), and mortality (4.7% vs 4.6%, $p = 0.82$) (Table 1).

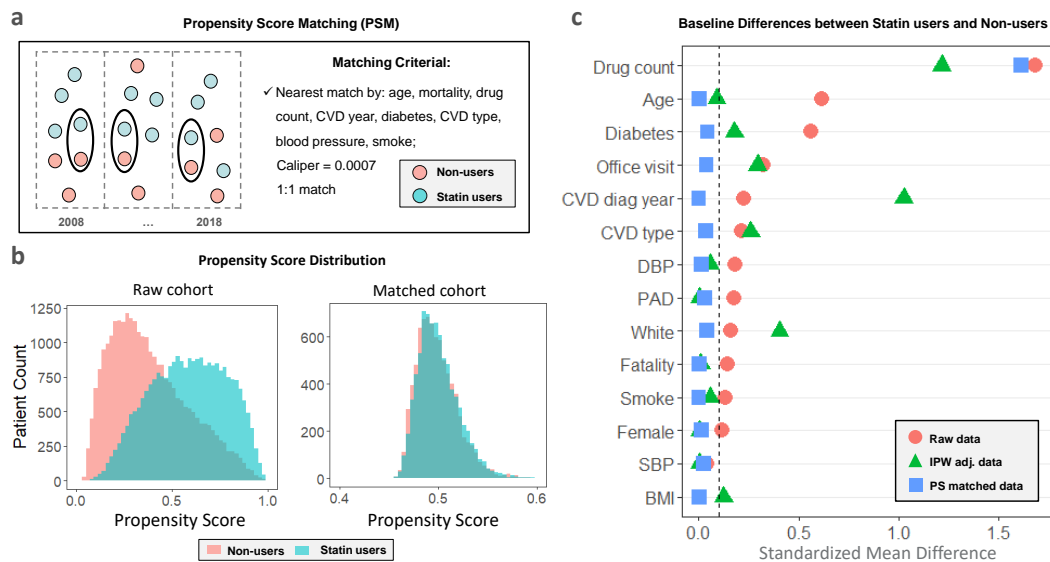


Figure 5.3 The propensity score matching process. (a) The matching criterial. (b) The propensity score distribution of statin-users and non-users before and after matching. (c) The Standardized Mean Difference between statin-users and non-users.

5.3.3 Survival Analysis by Cox Proportional Hazard Model

Correlation matrix of Pearson coefficients indicated minimal risk of multicollinearity issue within either raw data or matched data cohort for downstream statistical analysis (Fig. 5.4a). We analyzed the matched cohort data using a cox proportional hazards model adjusting for all covariates described above. As result, the adjusted hazard ratio for OA occurrence in the statin user group is 0.61 (95% CI: 0.48 - 0.79, $p < 0.001$) compared to non-user group, which means statin use is associated with a 39% reduction in risk of OA development. (Fig. 5.4b). Other covariates that were significantly associated with increasing risk of OA rate included age (HR: 1.45, $p < 0.001$), BMI (HR: 1.04, $p < 0.001$), office visit frequency (HR: 1.21, $p < 0.001$), gender as female vs male (HR: 1.28, $p < 0.001$), hypertension vs other CVDs (HR: 1.88, $p < 0.001$), dyslipidemia vs other CVDs (HR: 2.01, $p < 0.001$), and number of

drug prescriptions (HR: 2.58, p value < 0.001) (Fig. 5.4c). It's interesting to note that the hazard ratio in the patients with diabetes, a well-established risk factors for OA development, is 0.76 (p = 0.002), indicating it reducing OA rate compared to patients without diabetes. This counterfactual result suggests the possible existence of lurking variable that affects the interpretation of relationship between variables or a non-linear trends between diabetes and OA development²³⁷. Using raw data, we repeated the analysis and observed a consistent trend, the hazard ratio for OA rate in the statin user group is 0.74 (95% CI: 0.67 - 0.82, p < 0.01), less strong but still significant inverse association between statin use and OA occurrence (Fig. 5.4d).

We further investigated the association between statin use and OA rate across subgroups. The raw cohort population was separated on the basis of age, gender, smoking status, and diabetes history (Table 5.2). As results, the magnitude of inverse association between statin use and OA reduction was more significant for the sub-population of younger patients (age \leq 45 years old), female, non-smokers and patients without history of diabetes when compared to the corresponding counterpart subgroup (Table 5.2). The results also suggested there is no meaningful heterogeneity of the inverse association between statin use and OA development in our data set. This subgroup analysis can not only be able to ensure a proper interpretation of positive study findings in the overall population but also provide guidance on how the statin treatment should be used for OA management.

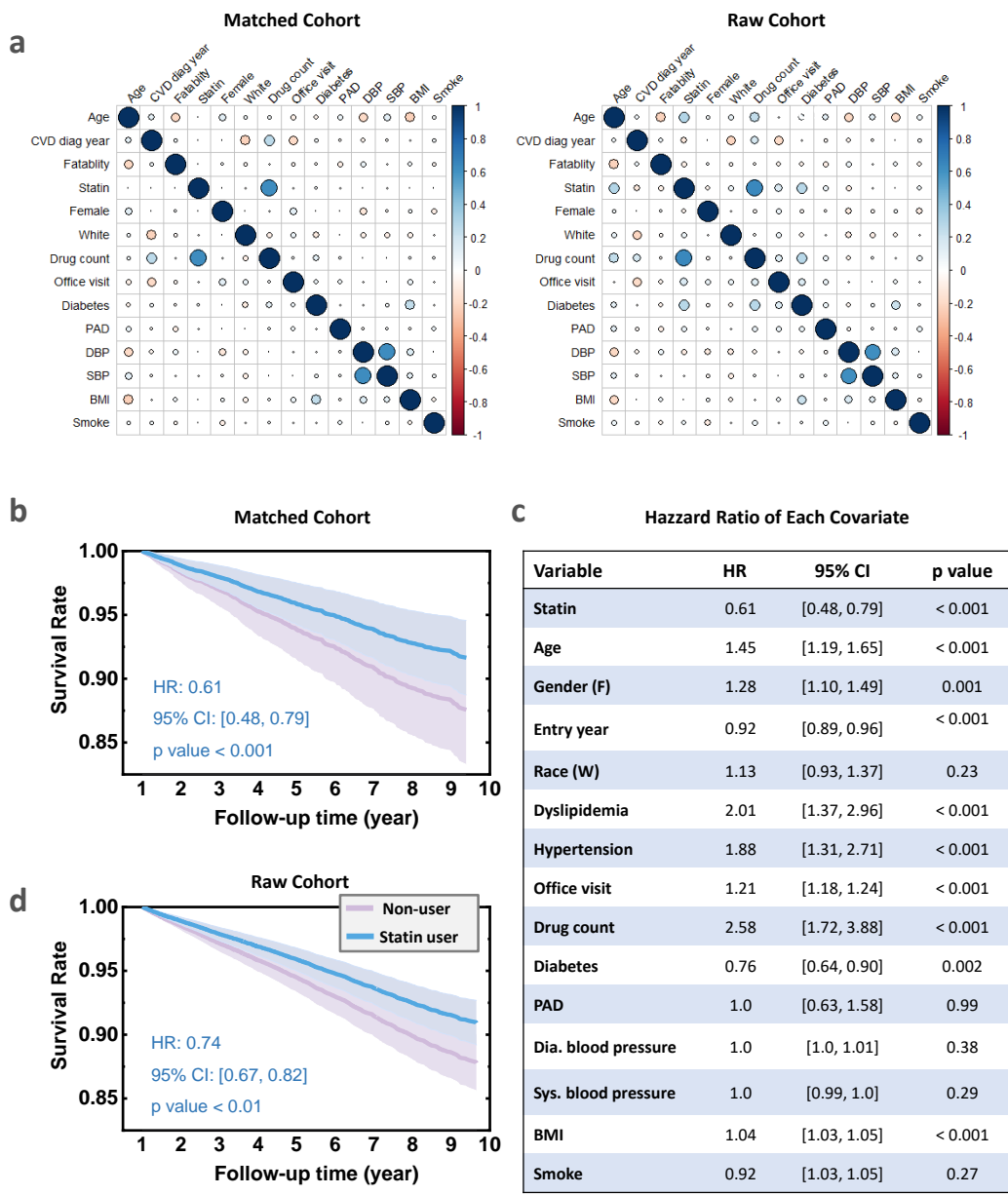


Figure 5.4 Cox proportional hazard model analysis. (a) Correlation of the covariates for the raw and propensity score-matched data. Time to OA for the (b) propensity score-matched and (c) raw patients. (d) The hazard ratio for OA occurrence in statin users compared to non-users.

5.3.4 Association between Statin use and Other Common Joint Diseases

Of our cohort population, their common musculoskeletal disease history was collected and the prevalence of each disease was calculated. Eight reported diseases with prevalence $\geq 2\%$ were listed, including joint pain (14%), limb pain (6%), low back pain (5%), OA (5%), bone and cartilage disorder (3%), neck pain (3%), muscle ligament disorder (2%), and arthropathy (2%) (Fig. 5.5a). The association between statin use and occurrence of joint diseases was estimated using logistic regression. As results, statin use was significantly associated with lower occurrence of the muscle ligament disorder (Odds Ratio: 0.65), low back pain (OR: 0.80), limb pain (OR: 0.80), and joint pain (OR: 0.84) (Fig. 5.5b).

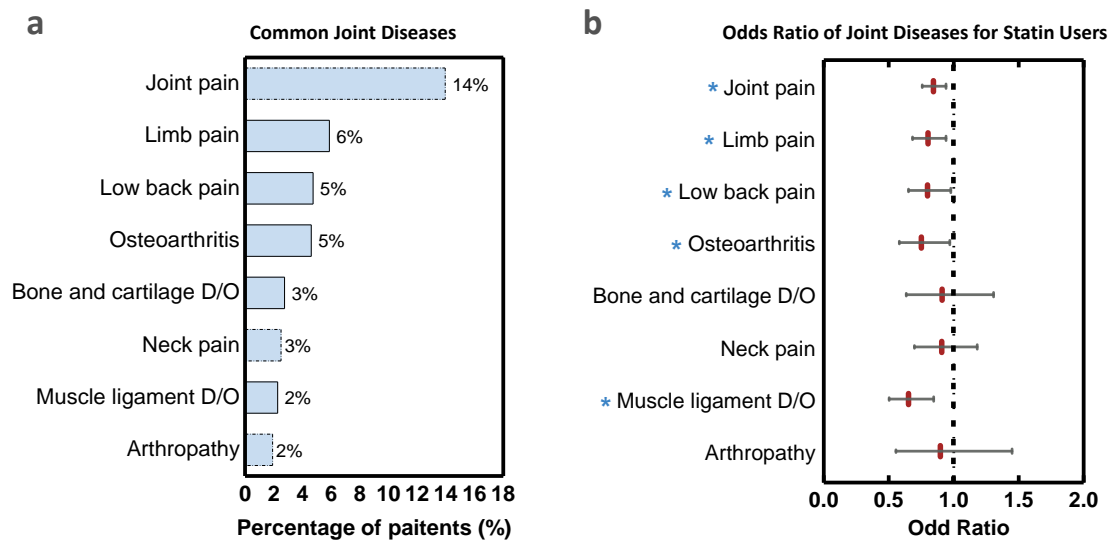
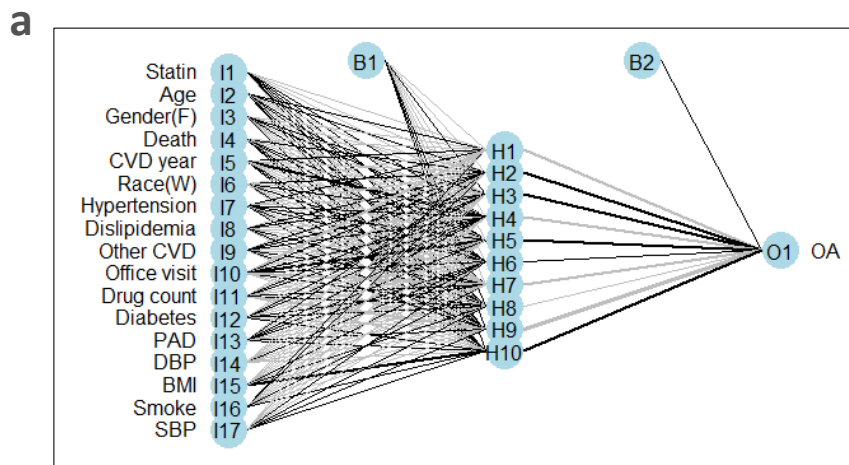


Figure 5.5 Logistic regression analysis. (a) Top eight common musculoskeletal disorders in the cohort of our study. (b) The odds ratio for specific joint disease in statin user population compared to the non-user population.

5.3.5 Artificial Intelligence for Cohort Analysis

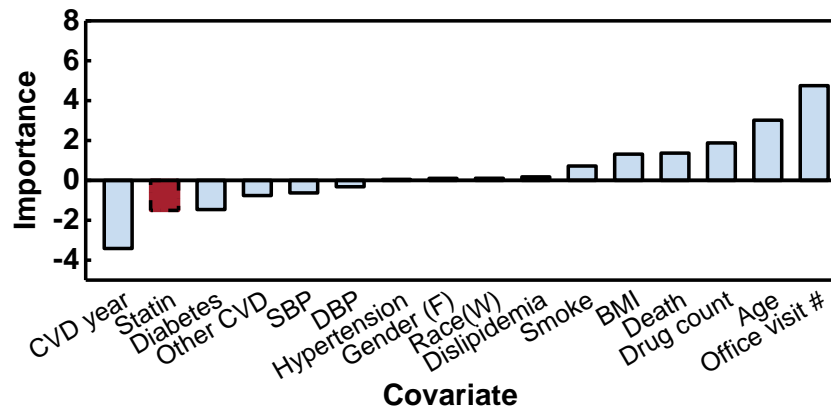
Finally, we implemented a modern machine learning method, ANN, to analyze the patient data. In total, 15 features including 14 covariates and statin use were used as input of the ANN model; and a binary outcome, OA case or non-case, was used as output for the model. Model overfitting is a common problem when training neural network, which comprises the generalization and predictive capability of the model. To avoid overfitting, two hyperparameters, number of nodes and weight decay, were carefully pruned through grid search. As results, we chose the optimized parameters, weight decay as 20 and number of nodes as 10, to build the final model as they achieved the optimal accuracy and minimal risk of overfitting (Fig. 5.6a).

To facilitate the clinical interpretation, we used a randomization approach to statistically assess the relative importance of each variable in the ANN model²³⁸. As results, statin use was identified to be the second most important predictors contributing to prediction of non-OA case, confirming its effect in reducing OA rate (Fig. 5.6b). We further assessed the correlation between feature importance values of the ANN model and the coefficient estimates of the logistic regression model. The results generated from these two methods were highly consistent (Pearson's r : 0.85), confirming the validity of our logistic regression results (Fig. 5.6c). Taken together, the ANN model was of greater complexity and flexibility compared to logistic regression model, which probably has better capability in recognizing nonlinear and interaction patterns within patient data. Meanwhile, the estimated effect of each predictor on predicting OA outcome generated by the ANN model and logistic regression model were comparable, further confirming the accuracy and validity of our previous model results.



b

$$Impact\ Score(X) = \sum_{Y=A}^E Weight_{XH} * Weight_{HY}$$



c

Correlation: Pearson's $r = 0.85$

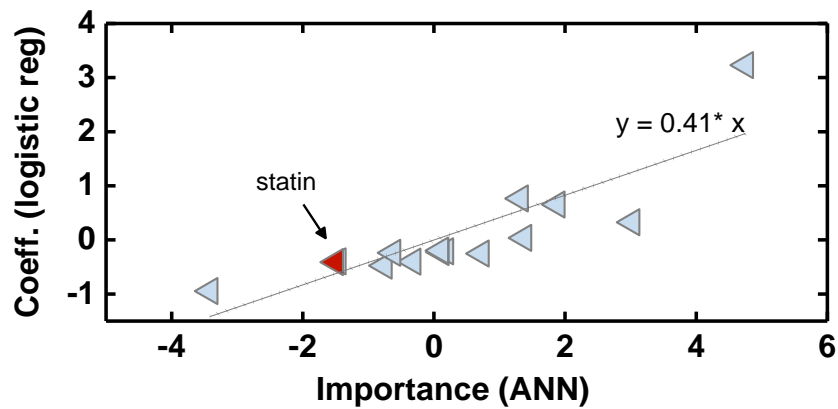


Figure 5.6 The Artificial Intelligence model. (a) The artificial neuron network (ANN) with the optimized number of nodes as 10 and the decay as 15. (b) The ordered importance score of all covariates. (c) Correlation between the importance score determined by ANN and the coefficient determined by logistic regression model.

Table 5.1 The baseline characteristics between statin users and non-users for raw and propensity score matched cohort. * office visit denotes total number of hospital office visits in 10 years, and drug count denotes total number of prescribed drug in 10 years.

Variable	Raw cohort			Matched cohort		
	Non-users N = 27,747	Statin users N = 25,663	p value	Non users N = 8,017	Statin users N = 8,017	p value
Age	51	60	<0.001	57	57	0.77
Office visit*	15	21	<0.001	17	14	0.02
Drug count*	0	3	<0.001	0	3	<0.001
BMI	31.6	31.6	0.96	31.34	31.36	0.82
DBP	78.57	80.74	<0.001	79.71	79.87	0.42
SBP	131.97	132.73	<0.001	132.06	132.58	0.09
Entry year	2012	2011	<0.001	2012	2012	1
Female (%)	58.3	52.5	<0.001	54.3	55.0	0.37
Fatality (%)	3.5	6.6	<0.001	4.7	4.6	0.82
CVD (%)			<0.001			0.1
ICD-401	67.9	57.7		61.3	62.9	
ICD-272	27.8	36.0		33.2	31.8	
ICD-other	4.3	6.3		5.5	5.3	

Race (%)	<0.001			0.01		
White	50.3	58.3		56.1	54.2	
Other	49.7	41.7		43.9	45.8	
Diabetes (%)	16.5	40.9	<0.001	24.2	26.0	0.006
PAD (%)	1.2	3.9	<0.001	1.6	2.0	0.06
Smoke (%)	<0.001			1		
None	41.7	48.2		55.2	55.2	
Other	58.3	51.8		44.8	44.8	

Table 5.2 Association between statin initiation and OA occurrence according to different populations.

Subpopulation		Patient number	HR	95% CI	p value
Age	Age < 45	11, 243	0.57	[0.53, 0.92]	0.01
	45 < Age < 55	11, 412	0.62	[0.48, 0.73]	<0.001
	Age ≥ 55	27, 075	0.77	[0.67, 0.85]	<0.001
Gender	Female	29, 402	0.74	[0.64, 0.82]	<0.001
	Male	22, 690	0.77	[0.65, 0.91]	<0.001
Smoking	Never	28, 868	0.68	[0.60, 0.78]	<0.001
	Other	23, 224	0.86	[0.72, 0.98]	0.03
Diabetes	Yes	14, 902	0.77	[0.64, 0.93]	0.01
	No	37, 190	0.71	[0.63, 0.81]	<0.001

5.4 Discussion

This population-based, retrospective study demonstrates that the use of statins is associated with a 39% lower risk of overall OA occurrence among Delaware population. This association was apparently observed using raw patient's data, inverse probability weighted-data, and matched data. Furthermore, this inverse association was observed after adjusting for age, gender, race, relevant comorbidities, cardiovascular conditions, and basic health status. Finally, this positive association was also consistent according to our subgroup analyses according to essential covariates including age, gender, smoking status, and diabetes disease history, which may be able to provide the basis of future guidelines to clinicians for future prescription of statin.

In our study, the magnitude of inverse association between statin use and OA occurrence was similar compared to those of previous European studies using various general populations^{200,201,225}. Among these studies, the UK study using 16,609 CVD cohorts aged over 40 years reports the association between statin use and 40% reduction in OA occurrence, whose cohort baseline characteristics and results are very close to our study using CVD cohorts aged 56 years old on average and reporting 39% reduction in OA outcome. Such consistence provides us extra confidence in the external validity of our study. Indeed, the compositions and features of Delaware population are highly consistent with those of the U.S. nation, in terms of median age, race share, household income, and Medicare reimbursements per enrollee. Another European study including 10,75 Rotterdam participants aged 55 years and older observes more significant joint-favoring effects of statins. This Rotterdam study concludes that statin use is associated with more than 50% reduction in OA progression of knee joints. This finding is not surprising as our patients all have

cardiovascular conditions when entering into study and are expected to be at a higher risk for OA than the general population of Rotterdam study. Finally, the disease-modifying effects of statins have been implied to be OA phenotypes dependent ^{189,213}. Statins may be more effective for metabolism disorder-associated OA induced by cytokines or other pathological acute factors rather than primary OA due to long-term cartilage wear and tear ^{189,213}. This observation from cohort studies agrees well with our molecular mechanism study revealing that statin can directly regulate the cellular activities and prevent cells from responding to OA-inducing factors, which will be discussed in more details in next paragraph.

In contrast to promising European cohort studies, two longitudinal cohort studies suggest that statin use is associated with worsening physical function, pain and structural progression of OA joints among U.S. population ^{203,204}. Such discrepancies between published studies on statins and OA have aroused heat debate on methodological factors ²⁰⁵ but remain unsolved due to lack of knowledge of its underlying mechanism. As results, the clinical application of statins on OA treatment is hindered. The modifying role of statin on cartilage has been postulated to be through two mechanisms, lowering the cholesterol level ²¹⁰ or anti-inflammatory action ²⁰⁶. However, neither reducing cholesterol level in chondrocyte ²¹¹ or inhibition of joint inflammation ²³⁹ can achieve comparable protective effects as statin did. According to our lab's recent finding, we proposed a novel mechanism that statin can directly prevent the chondrocytes from entering a degradative, hypertrophic state at the acute phase of OA, *e.g.* trauma joint injury-induced inflammation and hemorrhage; and thus inhibits the cartilage degeneration. This mechanism implies that statin could effectively prevent the initiation of OA but have little effect for the cessation or

reversal of late-stage OA, as the phenotype of chondrocytes has already been changed with significant amount of cartilage loss. This newly identified chondro-protective mechanism of statin might resolve the “contradiction” between the European and U.S. cohort studies regarding the role of statins in OA patients and joint function. In the European studies, eligible patients were selected from general population based on statin use, *i.e.*, patients with statin prescription and OA free history; while the U.S. studies include the patients who are with suspected and confirmed knee OA, which may substantially decrease probability of observing the immediate, early effects of statin on preventing OA onset. Future research should include participants without history of OA diagnosis and examine the role of statins on preventing the early-stage OA development.

The strengths of our study are worthy of discussion. First, statins have already been a class of FDA approved drugs that are historically being prescribed for cardiovascular disease. Repurposing of statins for OA treatment would be cost- and time-effective compared to other brand new chemicals. In fact, a large randomized clinical trial (TRACE-RA) have proven that atorvastatin 40mg daily intake is a safe therapy in patients with rheumatoid arthritis²⁴⁰; and there is a undergoing clinical trial of statin for reducing the events of disability among elderly population in U.S., which can provide more clinical guidance in the near future. Second, this is a large-population study conducted with a substantial number of statin users and a sufficient number of outcome events to produce meaningful estimates. Large-scale observational study has minimal risk of being underpowered and generates more precise estimation of the effects of statin use and other confounding factors. Third, to reduce bias, we successfully used propensity score matching approaches to minimize confounding bias

due to the systematic difference in the baseline characteristics between statin user group and non-user group. We applied score matching within every 6-month block allowing for time course changes in the relative importance of covariates to be accounted. In raw cohort, the statin users seem to have more severe health conditions and comorbidities, which may impede us from detecting statistically significant association between statin use and OA rate reduction. After matching, ~30% of the total patients were successfully paired, of which the balance in baseline features was significantly improved. It's true that matching may result in less generalizability; however, both analysis using raw data and matched data showed significant inverse association between statin use and OA occurrence, making generalizability less of a concern.

The findings of this study should be considered in the light of several limitations, primarily related to its retrospective design. First, our study was performed at a single institution and was retrospective. Potentially, some Delaware residents were treated at other hospitals without our knowledge, or one patient could visit different hospitals based upon his/her disease conditions, causing key information missing or follow-up interruption. Such missing data could cause significant bias. However, it should not be a critical concern in this study as Christiana Care Health System is the largest community hospital in Delaware state; and our patients' data are comparable to other previous studies in terms of statin use and OA occurrence rate. Secondly, although our study found a lower risk of OA development associated with statin use, we were unable to examine cause-specific OA and dosage-dependent effects of statins, as these data are generally incomplete within our database. We hypothesize that the lower OA rate associated with statin use mainly stems from the reduction in OA of

patients with trauma injuries; and the protective effects of statins on joint health is expected to be time- and dosage-dependent. All these speculation calls for future studies that examine cause specific OA outcomes. Nevertheless, the conclusion generated in this study regarding the overall lower OA risk associated with statin use per se is critically significant for future OA study.

In conclusion, we found that statin initiation was associated with a 39% lower risk of OA occurrence among patients after adjustment for potential confounding variables. This finding can not only provide evidence that statin could be a promising therapy for OA management, but also increase the statin adherence for existing patients as cardiovascular disease and joint disorder may share same preventative approaches.

Chapter 6

SUMMARY AND FUTURE WORK

6.1 Summary

The first part of my Ph.D. work is focus on the mechanotransduction of *in situ* chondrocytes under mechanical loading stimulation. Articular cartilage is subjected to a various range of physical stimuli during daily activities. Under the physical stimuli, one of the earliest response in chondrocytes is the intracellular calcium ($[Ca^{2+}]_i$) signaling, which is believed to play an essential role in regulating chondrocyte metabolism and maintaining cartilage hemostasis. In this study, I developed a novel bi-directional microscopy loading device that enables the record of transient $[Ca^{2+}]_i$ responses of *in situ* chondrocytes in loaded cartilage. The role of seven related calcium signaling pathways that are involved in the mechanotransduction of chondrocytes were systematically investigated. This study provided new knowledge about the $[Ca^{2+}]_i$ signaling and mechanobiology of chondrocytes in its natural residing environment.

In addition to cartilage mechanotransduction, a main motivation of my Ph.D. research is to understand pathological process of PTOA and to find effective therapeutics for early-stage PTOA prevention. The second project of my research is the identification of the genes and pathways in chondrocytes in response to acute joint inflammation. Traumatic joint injuries often result in elevated proinflammatory cytokine levels in the joint cavity, which can increase the catabolic activities of chondrocytes and damage cartilage. By RNA sequencing of gene expression from

cartilage tissue, we systematically investigated the early genetic responses of healthy in situ chondrocytes under IL-1 β attack, with a focus on cell cycle and calcium signaling pathways. This study provided a comprehensive list of differentially expressed genes involved in the acute phase of joint injury, which represents a useful reference to verify and guide future cartilage studies related to the acute inflammation after joint trauma.

Furthermore, I successfully elucidated the potential mechanisms by which two classes of FDA-approved drugs, statins and bisphosphonate, can exert direct, concentration-dependent, and time-dependent protective effects on chondrocytes for cartilage protection. Both statins- and bisphosphonate-induced inhibition of mevalonate pathway can suppress the activation of Rho GTPases in chondrocytes, which prevent the cells from entering the phenotypic shift and thus prevent the cartilage degeneration under the OA-inducing factors stimuli. These *in vitro* results were further confirmed in our large-population, longitudinal cohort clinical study. Using the electronic medical records of 54,362 patients, we proved that use of statins is associated with a significant reduction in long-term occurrence of clinically defined OA in the Delaware population. My findings in this study can provide: 1) critical justifications regarding the application of statins for PTOA prevention, 2) guidance for future clinical trials of the mevalonate inhibitors in OA prevention, including the targeted population, design of delivery methods, and timing of drug administration, and 3) a new target pathway in chondrocytes, *i.e.*, Rho GTPases, for the inhibition of osteoarthritis initiation after joint injuries.

Collectively, this dissertation provides a fundamental and novel understanding on the pathological changes of cartilage following a traumatic joint injury on the

tissue, cellular, and molecular level. Additionally, my work provides the foundation for future studies to leverage statin use for PTOA prevention. Most importantly, this work has the potential to help accelerate the translation of a novel, safe, and inexpensive strategy for PTOA disease-modification based upon the treatment of statins to acutely injured joints.

6.2 Future Directions

Working in Dr. Lu's lab provided me with the precious and fortunate opportunity to work on interdisciplinary research projects. In the future, my colleagues at the Lucas lab will continue to discover and investigate the potential therapies for the treatment of OA. My Ph.D. projects have yielded many interesting questions to be investigated in the future.

First is the *in vivo* effectiveness of statin and bisphosphonate for PTOA prevention. My thesis work has proved that statin or bisphosphonate can prevent the cells from responding to OA-inducing factors in a Rho-signaling-dependent manner using *in vitro* cartilage explant model. In future study, we hypothesize that immediate administration of statin or bisphosphonate after joint injuries can suppress the development of PTOA. Using experimental OA rat model, we will evaluate the therapeutic potentials of the mevalonate and specific Rho GTPases inhibitors for the PTOA prevention through systemic administration. Activities of Rho GTPases in chondrocytes during PTOA development will be also investigated.

Secondly, we aim to fabricate an intra-articular delivery system of statin in joint cavity, *e.g.* HA hydrogel containing nano-sized statin depots. A promising route of drug administration during the early phase after joint injury is intraarticular injection. The statin release profiles will first be optimized *in vitro*, and then the

PTOA prevention effectiveness of the hydrogel in experimental OA rat model will be evaluated and compared with those from systemic administration. This has the advantages of reaching high drug concentrations at the lesion site with low systemic drug exposure, and thus reduced risk for systemic adverse events.

Lastly, an important unanswered question for our lab is whether use of statins can reduce the long-term occurrence of clinically defined OA among U.S. nation population. We aim to conduct a case-control study for examining the association between the OA occurrence and statin usage. Patients data will be collected from the database of Veterans Affairs at U.S. Department and Chronic Conditions Data Warehouse at Centers for Medicare and Medicaid Services. The combined patient data will leverage the completeness and quality of existing datasets for larger clinical data analysis, which supports future randomized clinical trials of statin for patients after joint injuries.

REFERENCES

1. Mow, V. C., Ratcliffe, A. & Robin Poole, A. Cartilage and diarthrodial joints as paradigms for hierarchical materials and structures. *Biomaterials* (1992). doi:10.1016/0142-9612(92)90001-5
2. Carballo, C. B., Nakagawa, Y., Sekiya, I. & Rodeo, S. A. Basic Science of Articular Cartilage. *Clinics in Sports Medicine* (2017). doi:10.1016/j.csm.2017.02.001
3. Lu, X. L., Mow, V. C. & Guo, X. E. Proteoglycans and mechanical behavior of condylar cartilage. *J. Dent. Res.* (2009). doi:10.1177/0022034508330432
4. Buckwalter, Mow & Ratcliffe. Restoration of Injured or Degenerated Articular Cartilage. *J. Am. Acad. Orthop. Surg.* (1994).
5. Ateshian, G. A. & Mow, V. C. Basic Orthopaedic Biomechanics and Mechano-Biology. *Friction, lubrication, and wear of articular cartilage and diarthrodial joints* (2005). doi:10.1080/14614103.2017.1377405
6. Fox, A. J. S., Wanivenhaus, F. & Rodeo, S. A. The basic science of the patella: structure, composition, and function. *The journal of knee surgery* (2012). doi:10.1055/s-0032-1313741
7. Francis SL, Di Bella C, Wallace GG, C. P. Cartilage Tissue Engineering Using Stem Cells and Bioprinting Technology-Barriers to Clinical Translation. *Front. Surg.* **5**, (2018).
8. Alford, J. W. & Cole, B. J. Cartilage restoration, part 1: Basic science, historical perspective, patient evaluation, and treatment options. *American Journal of Sports Medicine* (2005). doi:10.1177/0363546504273510
9. Archer, C. W. & Francis-West, P. The chondrocyte. *International Journal of Biochemistry and Cell Biology* (2003). doi:10.1016/S1357-2725(02)00301-1
10. Akkiraju, H. & Nohe, A. Role of Chondrocytes in Cartilage Formation, Progression of Osteoarthritis and Cartilage Regeneration. *J. Dev. Biol.* (2015). doi:10.3390/jdb3040177

11. Shen, G. The role of type X collagen in facilitating and regulating endochondral ossification of articular cartilage. *Orthod. Craniofacial Res.* (2005). doi:10.1111/j.1601-6343.2004.00308.x
12. Leong, D. J., Hardin, J. A., Cobelli, N. J. & Sun, H. B. Mechanotransduction and cartilage integrity. *Annals of the New York Academy of Sciences* (2011). doi:10.1111/j.1749-6632.2011.06301.x
13. Szafranski, J. D. *et al.* Chondrocyte mechanotransduction: Effects of compression on deformation of intracellular organelles and relevance to cellular biosynthesis. *Osteoarthr. Cartil.* (2004). doi:10.1016/j.joca.2004.08.004
14. Bader, D. L., Salter, D. M. & Chowdhury, T. T. Biomechanical Influence of Cartilage Homeostasis in Health and Disease. *Arthritis* (2011). doi:10.1155/2011/979032
15. Bian, L. *et al.* Dynamic Mechanical Loading Enhances Functional Properties of Tissue-Engineered Cartilage Using Mature Canine Chondrocytes. *Tissue Eng. Part A* **16**, 1781–1790 (2010).
16. Lv, M. *et al.* Identification of Chondrocyte Genes and Signaling Pathways in Response to Acute Joint Inflammation. *Sci. Rep.* **9**, 93 (2019).
17. Li, J. & Dong, S. The Signaling Pathways Involved in Chondrocyte Differentiation and Hypertrophic Differentiation. *Stem Cells Int.* (2016). doi:10.1155/2016/2470351
18. Wang, G. *et al.* RhoA/ROCK Signaling Suppresses Hypertrophic Chondrocyte Differentiation. *J. Biol. Chem.* (2004). doi:10.1074/jbc.M311427200
19. Zhu, S. *et al.* Wnt and Rho GTPase signaling in osteoarthritis development and intervention: implications for diagnosis and therapy. *Arthritis Res. Ther.* **15**, 217 (2013).
20. Li, Y. *et al.* Effects of insulin-like growth factor-1 and dexamethasone on cytokine-challenged cartilage: Relevance to post-traumatic osteoarthritis. *Osteoarthr. Cartil.* **23**, 266–274 (2015).
21. Bush, J., Bérubé, N. & Beier, F. A new prescription for growth? Statins, cholesterol and cartilage homeostasis. *Osteoarthr. Cartil.* **23**, 503–506 (2015).
22. Clapham, D. E. Calcium Signaling. *Cell* (2007). doi:10.1016/j.cell.2007.11.028
23. Pingguan-Murphy, B., El-Azzeh, M., Bader, D. L. & Knight, M. M. Cyclic

- compression of chondrocytes modulates a purinergic calcium signalling pathway in a strain rate- and frequency-dependent manner. *J. Cell. Physiol.* (2006). doi:10.1002/jcp.20747
24. Madden, R. M. J., Han, S. K. & Herzog, W. The effect of compressive loading magnitude on in situ chondrocyte calcium signaling. *Biomech. Model. Mechanobiol.* (2015). doi:10.1007/s10237-014-0594-4
 25. Han, S. K., Wouters, W., Clark, A. & Herzog, W. Mechanically induced calcium signaling in chondrocytes in situ. *J. Orthop. Res.* (2012). doi:10.1002/jor.21536
 26. Edlich, M., Yellowley, C. E., Jacobs, C. R. & Donahue, H. J. Oscillating fluid flow regulates cytosolic calcium concentration in bovine articular chondrocytes. *J. Biomech.* (2001). doi:10.1016/S0021-9290(00)00158-5
 27. Browning, J. A., Saunders, K., Urban, J. P. G. & Wilkins, R. J. The influence and interactions of hydrostatic and osmotic pressures on the intracellular milieu of chondrocytes. *Biorheology* (2004).
 28. Chao, P.-H. G., West, A. C. & Hung, C. T. Chondrocyte intracellular calcium, cytoskeletal organization, and gene expression responses to dynamic osmotic loading. *Am. J. Physiol. Cell Physiol.* **291**, C718–C725 (2006).
 29. O’Conor, C. J., Leddy, H. A., Benefield, H. C., Liedtke, W. B. & Guilak, F. TRPV4-mediated mechanotransduction regulates the metabolic response of chondrocytes to dynamic loading. *Proc. Natl. Acad. Sci.* **111**, 1316–1321 (2014).
 30. Zhou, Y. *et al.* Effects of Osmolarity on the Spontaneous Calcium Signaling of In Situ Juvenile and Adult Articular Chondrocytes. *Ann. Biomed. Eng.* **44**, 1138–1147 (2016).
 31. Xu, J., Wang, W., Clark, C. C. & Brighton, C. T. Signal transduction in electrically stimulated articular chondrocytes involves translocation of extracellular calcium through voltage-gated channels. *Osteoarthr. Cartil.* (2009). doi:10.1016/j.joca.2008.07.001
 32. Zhou, Y. *et al.* Effects of Osmolarity on the Spontaneous Calcium Signaling of In Situ Juvenile and Adult Articular Chondrocytes. *Ann. Biomed. Eng.* **44**, 1138–1147 (2016).
 33. Kono, T. *et al.* Spontaneous oscillation and mechanically induced calcium waves in chondrocytes. *Cell Biochem. Funct.* (2006). doi:10.1002/cbf.1304

34. Zhou, Y., Park, M., Cheung, E., Wang, L. & Lu, X. L. The effect of chemically defined medium on spontaneous calcium signaling of in situ chondrocytes during long-term culture. *J. Biomech.* **48**, 990–996 (2015).
35. Lv, M. *et al.* Calcium signaling of in situ chondrocytes in articular cartilage under compressive loading: Roles of calcium sources and cell membrane ion channels. *Journal of Orthopaedic Research* 730–738 (2017). doi:10.1002/jor.23768
36. Lai, W. M., Hou, J. S. & Mow, V. C. A Triphasic Theory for the Swelling and Deformation Behaviors of Articular Cartilage. *J. Biomech. Eng.* (1991). doi:10.1115/1.2894880
37. Maldonado, M. & Nam, J. The role of changes in extracellular matrix of cartilage in the presence of inflammation on the pathology of osteoarthritis. *Biomed Res. Int.* **2013**, 284873 (2013).
38. R&D System Inc. Overview of Articular Cartilage Extracellular Matrix. (2012). doi:10.1055/b-0034-87249
39. Kwoh, C. K. Epidemiology of osteoarthritis. in *The Epidemiology of Aging* (2012). doi:10.1007/978-94-007-5061-6_29
40. Loeser, R. F., Goldring, S. R., Scanzello, C. R. & Goldring, M. B. Osteoarthritis: A disease of the joint as an organ. *Arthritis and Rheumatism* (2012). doi:10.1002/art.34453
41. Zhang, W. *et al.* EULAR evidence-based recommendations for the diagnosis of knee osteoarthritis. *Ann. Rheum. Dis.* (2010). doi:10.1136/ard.2009.113100
42. Lotz, M. K. New developments in osteoarthritis. Posttraumatic osteoarthritis: Pathogenesis and pharmacological treatment options. *Arthritis Research and Therapy* (2010). doi:10.1186/ar3046
43. Kramer, W. C., Hendricks, K. J. & Wang, J. Pathogenetic mechanisms of posttraumatic osteoarthritis: Opportunities for early intervention. *International Journal of Clinical and Experimental Medicine* (2011).
44. Stiebel, M., Miller, L. & Block, J. Post-traumatic knee osteoarthritis in the young patient: therapeutic dilemmas and emerging technologies. *Open Access J. Sport. Med.* (2014). doi:10.2147/OAJSM.S61865
45. Blagojevic, M., Jinks, C., Jeffery, A. & Jordan, K. P. Risk factors for onset of osteoarthritis of the knee in older adults: a systematic review and meta-analysis.

- Osteoarthr. Cartil.* (2010). doi:10.1016/j.joca.2009.08.010
46. Thomas, A. C., Hubbard-Turner, T., Wikstrom, E. A. & Palmieri-Smith, R. M. Epidemiology of Posttraumatic Osteoarthritis. *J. Athl. Train.* (2016). doi:10.4085/1062-6050-51.5.08
 47. Punzi, L. *et al.* Post-traumatic arthritis: Overview on pathogenic mechanisms and role of inflammation. *RMD Open* (2016). doi:10.1136/rmdopen-2016-000279
 48. Pritchard, S. & Guilak, F. Effects of interleukin-1 on calcium signaling and the increase of filamentous actin in isolated and in situ articular chondrocytes. *Arthritis Rheum.* **54**, 2164–2174 (2006).
 49. Pritchard, S., Votta, B. J., Kumar, S. & Guilak, F. Interleukin-1 inhibits osmotically induced calcium signaling and volume regulation in articular chondrocytes. *Osteoarthr. Cartil.* **16**, 1466–73 (2008).
 50. Bush, P. G. & Hall, A. C. The volume and morphology of chondrocytes within non-degenerate and degenerate human articular cartilage. *Osteoarthr. Cartil.* (2003). doi:10.1016/S1063-4584(02)00369-2
 51. Fernandes, J. C., Martel-Pelletier, J. & Pelletier, J. P. The role of cytokines in osteoarthritis pathophysiology. *Biorheology* **39**, 237–246 (2002).
 52. Dreier, R. Hypertrophic differentiation of chondrocytes in osteoarthritis: The developmental aspect of degenerative joint disorders. *Arthritis Research and Therapy* **12**, (2010).
 53. Van der Kraan, P. M. & Van den Berg, W. B. Chondrocyte hypertrophy and osteoarthritis: Role in initiation and progression of cartilage degeneration? *Osteoarthritis and Cartilage* (2012). doi:10.1016/j.joca.2011.12.003
 54. Ryd, L. *et al.* Pre-Osteoarthritis: Definition and Diagnosis of an Elusive Clinical Entity. *Cartilage* (2015). doi:10.1177/1947603515586048
 55. Madry, H. *et al.* Early osteoarthritis of the knee. *Knee Surgery, Sports Traumatology, Arthroscopy* (2016). doi:10.1007/s00167-016-4068-3
 56. Von Der Mark, K. *et al.* Type x collagen synthesis in human osteoarthritic cartilage. indication of chondrocyte hypertrophy. *Arthritis Rheum.* (1992). doi:10.1002/art.1780350715
 57. Appleton, C. T. G., Pitelka, V., Henry, J. & Beier, F. Global analyses of gene

- expression in early experimental osteoarthritis. *Arthritis Rheum.* **56**, 1854–68 (2007).
58. Fukui, N. *et al.* Zonal gene expression of chondrocytes in osteoarthritic cartilage. *Arthritis Rheum.* (2008). doi:10.1002/art.24036
 59. Zenmyo, M. *et al.* Morphological and biochemical evidence for apoptosis in the terminal hypertrophic chondrocytes of the growth plate. *J. Pathol.* (1996). doi:10.1002/(SICI)1096-9896(199612)180:4<430::AID-PATH691>3.0.CO;2-H
 60. D’Lima, D., Hermida, J., Hashimoto, S., Colwell, C. & Lotz, M. Caspase inhibitors reduce severity of cartilage lesions in experimental osteoarthritis. *Arthritis Rheum.* (2006). doi:10.1002/art.21874
 61. Srinivas, V. & Shapiro, I. M. Chondrocytes embedded in the epiphyseal growth plates of long bones undergo autophagy prior to the induction of osteogenesis. *Autophagy* (2006). doi:10.4161/auto.2649
 62. Saitoh, T. *et al.* Loss of the autophagy protein Atg16L1 enhances endotoxin-induced IL-1 β production. *Nature* (2008). doi:10.1038/nature07383
 63. Harris, J. *et al.* Autophagy controls IL-1 β secretion by targeting Pro-IL-1 β for degradation. *J. Biol. Chem.* (2011). doi:10.1074/jbc.M110.202911
 64. Furman, B. D., Olson, S. A. & Guilak, F. The development of posttraumatic arthritis after articular fracture. in *Journal of Orthopaedic Trauma* (2006). doi:10.1097/01.bot.0000211160.05864.14
 65. Marks, P. H. & Donaldson, M. L. C. Inflammatory cytokine profiles associated with chondral damage in the anterior cruciate ligament-deficient knee. *Arthrosc. - J. Arthrosc. Relat. Surg.* (2005). doi:10.1016/j.arthro.2005.08.034
 66. Chandrasekhar, S., Harvey, A. K. & Hrubey, P. S. Intra-Articular Administration of Interleukin-1 Causes Prolonged Suppression of Cartilage Proteoglycan Synthesis in Rats. *Matrix* (1992). doi:10.1016/S0934-8832(11)80099-5
 67. Van Den Berg, W. B., Joosten, L. A. B. & Van De Loo, F. A. J. TNF α and IL-1 β are separate targets in chronic arthritis. *Clin. Exp. Rheumatol.* (1999).
 68. Aizawa, T., Kon, T., Einhorn, T. A. & Gerstenfeld, L. C. Induction of apoptosis in chondrocytes by tumor necrosis factor-alpha. *J. Orthop. Res.* (2001). doi:10.1016/S0736-0266(00)00078-4

69. Webb, G. R., Westacott, C. I. & Elson, C. J. Chondrocyte tumor necrosis factor receptors and focal loss of cartilage in osteoarthritis. *Osteoarthr. Cartil.* (1997). doi:10.1016/S1063-4584(97)80047-7
70. López-Armada, M. J. *et al.* Cytokines, tumor necrosis factor- α and interleukin-1 β , differentially regulate apoptosis in osteoarthritis cultured human chondrocytes. *Osteoarthr. Cartil.* (2006). doi:10.1016/j.joca.2006.01.005
71. Caramés, B. *et al.* Differential effects of tumor necrosis factor- α and interleukin-1 β on cell death in human articular chondrocytes. *Osteoarthr. Cartil.* (2008). doi:10.1016/j.joca.2007.10.006
72. Haslauer, C. M. *et al.* Loss of extracellular matrix from articular cartilage is mediated by the synovium and ligament after anterior cruciate ligament injury. *Osteoarthr. Cartil.* (2013). doi:10.1016/j.joca.2013.09.003
73. Lieberthal, J., Sambamurthy, N. & Scanzello, C. R. Inflammation in joint injury and post-traumatic osteoarthritis. *Osteoarthritis and Cartilage* **23**, 1825–1834 (2015).
74. Zwierzchowski, T. J., Stasikowska-Kanicka, O., Danilewicz, M. & Fabiś, J. Assessment of apoptosis and MMP-1, MMP-3 and TIMP-2 expression in tibial hyaline cartilage after viable medial meniscus transplantation in the rabbit. *Arch. Med. Sci.* (2012). doi:10.5114/aoms.2012.30947
75. Burrage, P. S. Matrix Metalloproteinases: Role In Arthritis. *Front. Biosci.* (2007). doi:10.2741/1817
76. Wang, M. *et al.* MMP13 is a critical target gene during the progression of osteoarthritis. *Arthritis Res. Ther.* (2013). doi:10.1186/ar4133
77. Bonnans, C., Chou, J. & Werb, Z. Remodelling the extracellular matrix in development and disease. *Nature Reviews Molecular Cell Biology* (2014). doi:10.1038/nrm3904
78. McCulloch, D. R. *et al.* ADAMTS Metalloproteases Generate Active Versican Fragments that Regulate Interdigital Web Regression. *Dev. Cell* (2009). doi:10.1016/j.devcel.2009.09.008
79. Woods, A., Wang, G. & Beier, F. Regulation of chondrocyte differentiation by the act in cytoskeleton and adhesive interactions. *Journal of Cellular Physiology* (2007). doi:10.1002/jcp.21110
80. Wang, G. & Beier, F. Rac1/Cdc42 and RhoA GTPases Antagonistically

Regulate Chondrocyte Proliferation, Hypertrophy, and Apoptosis. *J. Bone Miner. Res.* **20**, 1022–1031 (2005).

81. Suzuki, D. *et al.* Essential mesenchymal role of small GTPase Rac1 in interdigital programmed cell death during limb development. *Dev. Biol.* (2009). doi:10.1016/j.ydbio.2009.09.014
82. Aizawa, R. *et al.* Cdc42 is required for chondrogenesis and interdigital programmed cell death during limb development. *Mech. Dev.* (2012). doi:10.1016/j.mod.2012.02.002
83. Wang, G. *et al.* Genetic ablation of Rac1 in cartilage results in chondrodysplasia. *Dev. Biol.* (2007). doi:10.1016/j.ydbio.2007.03.520
84. Wang, G. *et al.* Inducible nitric oxide synthase-nitric oxide signaling mediates the mitogenic activity of Rac1 during endochondral bone growth. *J. Cell Sci.* (2011). doi:10.1242/jcs.076026
85. Wu, X. *et al.* Rac1 Activation Controls Nuclear Localization of β -catenin during Canonical Wnt Signaling. *Cell* (2008). doi:10.1016/j.cell.2008.01.052
86. Zhu, S. *et al.* Wnt and Rho GTPase signaling in osteoarthritis development and intervention: implications for diagnosis and therapy. *Arthritis Res. Ther.* **15**, 217 (2013).
87. Woods, A. & Beier, F. RhoA/ROCK Signaling Regulates Chondrogenesis in a Context-dependent Manner. *J. Biol. Chem.* **281**, 13134–13140 (2006).
88. Woods, A., Wang, G. & Beier, F. RhoA/ROCK signaling regulates Sox9 expression and actin organization during chondrogenesis. *J. Biol. Chem.* (2005). doi:10.1074/jbc.M409158200
89. Kumar, D. & Lassar, A. B. The Transcriptional Activity of Sox9 in Chondrocytes Is Regulated by RhoA Signaling and Actin Polymerization. *Mol. Cell. Biol.* (2009). doi:10.1128/MCB.01779-08
90. Haudenschild, D. R., Nguyen, B., Chen, J., D’Lima, D. D. & Lotz, M. K. Rho kinase-dependent CCL20 induced by dynamic compression of human chondrocytes. *Arthritis Rheum.* **58**, 2735–2742 (2008).
91. Appleton, C. T. G., Usmani, S. E., Mort, J. S. & Beier, F. Rho/ROCK and MEK/ERK activation by transforming growth factor- α induces articular cartilage degradation. *Lab. Invest.* **90**, pages 20–30 (2010).

92. Novakofski, K., Boehm, A. & Fortier, L. The small GTPase Rho mediates articular chondrocyte phenotype and morphology in response to interleukin-1alpha and insulin-like growth factor-I. *J. Orthop. Res.* **27**, 58–64 (2009).
93. Ellman, M. B. *et al.* Fibroblast growth factor control of cartilage homeostasis. *Journal of Cellular Biochemistry* (2013). doi:10.1002/jcb.24418
94. Shi, D. *et al.* Association of single-nucleotide polymorphisms in RHOB and TXNDC3 with knee osteoarthritis susceptibility: Two case-control studies in East Asian populations and a meta-analysis. *Arthritis Res. Ther.* (2008). doi:10.1186/ar2423
95. N., T. *et al.* Alleviating effects of AS1892802, a rho kinase inhibitor, on osteoarthritic disorders in rodents. *J. Pharmacol. Sci.* (2011).
96. Fortier, L. A. & Miller, B. J. Signaling through the small G-protein Cdc42 is involved in insulin-like growth factor-I resistance in aging articular chondrocytes. *J. Orthop. Res.* (2006). doi:10.1002/jor.20185
97. Long, D. L., Willey, J. S. & Loeser, R. F. Rac1 is required for matrix metalloproteinase 13 production by chondrocytes in response to fibronectin fragments. *Arthritis Rheum.* (2013). doi:10.1002/art.37922
98. Hu, X. *et al.* Cdc42 Is Essential for Both Articular Cartilage Degeneration and Subchondral Bone Deterioration in Experimental Osteoarthritis. *J. Bone Miner. Res.* **33**, 945–958 (2018).
99. Russell, R. G. G. Bisphosphonates: The first 40 years. *Bone* (2011). doi:10.1016/j.bone.2011.04.022
100. Ebetino, F. H. *et al.* The relationship between the chemistry and biological activity of the bisphosphonates. *Bone* (2011). doi:10.1016/j.bone.2011.03.774
101. Ridley, A. J. & Hall, A. The small GTP-binding protein rho regulates the assembly of focal adhesions and actin stress fibers in response to growth factors. *Cell* (1992). doi:10.1016/0092-8674(92)90163-7
102. Hayami, T. *et al.* The Role of Subchondral Bone Remodeling in Osteoarthritis: Reduction of Cartilage Degeneration and Prevention of Osteophyte Formation by Alendronate in the Rat Anterior Cruciate Ligament Transection Model. *Arthritis Rheum.* (2004). doi:10.1002/art.20124
103. Strassle, B. W. *et al.* Inhibition of osteoclasts prevents cartilage loss and pain in a rat model of degenerative joint disease. *Osteoarthr. Cartil.* (2010).

doi:10.1016/j.joca.2010.06.007

104. Nishitani, K. *et al.* Positive Effect of Alendronate on Subchondral Bone Healing and Subsequent Cartilage Repair in a Rabbit Osteochondral Defect Model. *Am. J. Sports Med.* (2009). doi:10.1177/0363546509350984
105. Bingham, C. O. *et al.* Risedronate decreases biochemical markers of cartilage degradation but does not decrease symptoms or slow radiographic progression in patients with medial compartment osteoarthritis of the knee: Results of the two-year multinational knee osteoarthritis st. *Arthritis Rheum.* (2006). doi:10.1002/art.22160
106. Saag, K. G. Bisphosphonates for osteoarthritis prevention: "Holy Grail" or not? *Ann. Rheum. Dis.* **67**, 1358–9 (2008).
107. Carbone, L. D. *et al.* The relationship of antiresorptive drug use to structural findings and symptoms of knee osteoarthritis. *Arthritis Rheum.* (2004). doi:10.1002/art.20627
108. Salami, J. A. *et al.* National Trends in Statin Use and Expenditures in the US Adult Population From 2002 to 2013. *JAMA Cardiol.* **2**, 56 (2017).
109. Reinholz, G. G. *et al.* Distinct mechanisms of bisphosphonate action between osteoblasts and breast cancer cells: Identity of a potent new bisphosphonate analogue. *Breast Cancer Res. Treat.* (2002). doi:10.1023/A:1014418017382
110. Plotkin, L. I., Bivi, N. & Bellido, T. A bisphosphonate that does not affect osteoclasts prevents osteoblast and osteocyte apoptosis and the loss of bone strength induced by glucocorticoids in mice. *Bone* (2011). doi:10.1016/j.bone.2010.08.011
111. Orriss, I. R., Key, M. L., Colston, K. W. & Arnett, T. R. Inhibition of osteoblast function in vitro by aminobisphosphonates. *J. Cell. Biochem.* (2009). doi:10.1002/jcb.21983
112. Evans, K. D. & Oberbauer, a M. Alendronate inhibits VEGF expression in growth plate chondrocytes by acting on the mevalonate pathway. *Open Orthop. J.* (2009). doi:10.2174/1874325000903010083
113. Dombrecht, E. J. *et al.* Antioxidant effect of bisphosphonates and simvastatin on chondrocyte lipid peroxidation. *Biochem. Biophys. Res. Commun.* (2006). doi:10.1016/j.bbrc.2006.07.075
114. Van Offel, J. F., Schuerwegh, A. J., Bridts, C. H., Stevens, W. J. & De Clerck,

- L. S. Effect of bisphosphonates on viability, proliferation, and dexamethasone-induced apoptosis of articular chondrocytes. *Ann. Rheum. Dis.* (2002). doi:10.1136/ard.61.10.925
115. Duque, G., Li, W., Adams, M., Xu, S. & Phipps, R. Effects of risedronate on bone marrow adipocytes in postmenopausal women. *Osteoporos. Int.* (2011). doi:10.1007/s00198-010-1353-8
116. Goldstein, J. L. & Brown, M. S. Regulation of the mevalonate pathway. *Nature* (1990). doi:10.1038/343425a0
117. Zhu, S. *et al.* Wnt and Rho GTPase signaling in osteoarthritis development and intervention: Implications for diagnosis and therapy. *Arthritis Research and Therapy* **15**, 217 (2013).
118. Novakofski, K., Boehm, A. & Fortier, L. The small GTPase Rho mediates articular chondrocyte phenotype and morphology in response to interleukin-1?? and insulin-like growth factor-1. *J. Orthop. Res.* (2009). doi:10.1002/jor.20717
119. Fortier, L. A., Deak, M. M., Semevolos, S. A. & Cerione, R. A. Insulin-like growth factor-I diminishes the activation status and expression of the small GTPase Cdc42 in articular chondrocytes. *J. Orthop. Res.* (2004). doi:10.1016/j.orthres.2003.08.021
120. Hu, X. *et al.* Cdc42 Is Essential for Both Articular Cartilage Degeneration and Subchondral Bone Deterioration in Experimental Osteoarthritis. *J. Bone Miner. Res.* **33**, 945–958 (2018).
121. Zhu, S. *et al.* Inhibition of Rac1 activity by controlled release of NSC23766 from chitosan microspheres effectively ameliorates Osteoarthritis development in vivo. *Ann. Rheum. Dis.* (2015). doi:10.1136/annrheumdis-2013-203901
122. Guilak, F., Butler, D. L., Goldstein, S. A. & Baaijens, F. P. T. Biomechanics and mechanobiology in functional tissue engineering. *Journal of Biomechanics* (2014). doi:10.1016/j.jbiomech.2014.04.019
123. Mow, V. C., Zhu, W. & Ratcliffe, A. Structure and function of articular cartilage and meniscus. in *Basic Orthopaedic Biomechanics*. Raven Press. New York. (1991).
124. Chen, X. *et al.* Determining Tension–Compression Nonlinear Mechanical Properties of Articular Cartilage from Indentation Testing. *Ann. Biomed. Eng.* **44**, 1148–1158 (2016).

125. Varady, N. H. & Grodzinsky, A. J. Osteoarthritis year in review 2015: mechanics. *Osteoarthr. Cartil.* **24**, 27–35 (2016).
126. Lee, W. *et al.* Synergy between Piezo1 and Piezo2 channels confers high-strain mechanosensitivity to articular cartilage. *Proc. Natl. Acad. Sci.* **111**, E5114–E5122 (2014).
127. Srinivasan, P. P. *et al.* Inhibition of T-Type Voltage Sensitive Calcium Channel Reduces Load-Induced OA in Mice and Suppresses the Catabolic Effect of Bone Mechanical Stress on Chondrocytes. *Catabolic Eff. Bone Mech. Stress Chondrocytes. PLoS ONE* **10**, (2015).
128. Millward-Sadler, S. J., Wright, M. O., Flatman, P. W. & Salter, D. M. ATP in the mechanotransduction pathway of normal human chondrocytes. *Biorheology* (2004).
129. Vandenburg, H. H., Shansky, J., Karlisch, P. & Solerssi, R. L. Mechanical stimulation of skeletal muscle generates lipid-related second messengers by phospholipase activation. *J. Cell. Physiol.* (1993). doi:10.1002/jcp.1041550109
130. Qusous, A., Parker, E., Ali, N., Mohmand, S. G. & Kerrigan, M. J. P. The effects of REV5901 on intracellular calcium signalling in freshly isolated bovine articular chondrocytes. *Gen. Physiol. Biophys.* (2012). doi:10.4149/gpb-2012-035
131. Guilak, F. *et al.* Mechanically induced calcium waves in articular chondrocytes are inhibited by gadolinium and amiloride. *J. Orthop. Res.* **17**, 421–429 (1999).
132. Kerrigan, M. J. P. & Hall, A. C. Control of chondrocyte regulatory volume decrease (RVD) by $[Ca^{2+}]_i$ and cell shape. *Osteoarthr. Cartil.* (2008). doi:10.1016/j.joca.2007.07.006
133. Kerrigan, M. J. P., Hook, C. S. V., Qusous, A. & Hall, A. C. Regulatory volume increase (RVI) by in situ and isolated bovine articular chondrocytes. *J. Cell. Physiol.* (2006). doi:10.1002/jcp.20758
134. Gao, Y. *et al.* The ECM-cell interaction of cartilage extracellular matrix on chondrocytes. *BioMed Research International* (2014). doi:10.1155/2014/648459
135. Bian, L. *et al.* Effects of dexamethasone on the functional properties of cartilage explants during long-term culture. *Am. J. Sports Med.* **38**, 78–85 (2010).
136. Lu, X. L., Huo, B., Park, M. & Guo, X. E. Calcium response in osteocytic

- networks under steady and oscillatory fluid flow. *Bone* **51**, 466–473 (2012).
137. Lu, X. L., Huo, B., Chiang, V. & Guo, X. E. Osteocytic network is more responsive in calcium signaling than osteoblastic network under fluid flow. *J. Bone Miner. Res.* **27**, 563–574 (2012).
 138. Hung, C. T., Allen, F. D., Mansfield, K. D. & Shapiro, I. M. Extracellular ATP modulates $[Ca^{2+}]_i$ in retinoic acid-treated embryonic chondrocytes. *Am. J. Physiol. Physiol.* **272**, C1611–C1617 (1997).
 139. Lambrecht, G. *et al.* PPADS, a novel functionally selective antagonist of P2 purinoceptor-mediated responses. *Eur. J. Pharmacol.* (1992). doi:10.1016/0014-2999(92)90877-7
 140. Wilusz, R. E., Zauscher, S. & Guilak, F. Micromechanical mapping of early osteoarthritic changes in the pericellular matrix of human articular cartilage. *Osteoarthr. Cartil.* (2013). doi:10.1016/j.joca.2013.08.026
 141. Korhonen, R. K. & Herzog, W. Depth-dependent analysis of the role of collagen fibrils, fixed charges and fluid in the pericellular matrix of articular cartilage on chondrocyte mechanics. *J. Biomech.* (2008). doi:10.1016/j.jbiomech.2007.09.002
 142. Madden, R., Han, S. K. & Herzog, W. Chondrocyte deformation under extreme tissue strain in two regions of the rabbit knee joint. *J. Biomech.* (2013). doi:10.1016/j.jbiomech.2012.09.021
 143. Zimmerman, B. K. *et al.* Role of interstitial fluid pressurization in TMJ lubrication. *J. Dent. Res.* (2015). doi:10.1177/0022034514553626
 144. Ateshian, G. A., Costa, K. D. & Hung, C. T. A theoretical analysis of water transport through chondrocytes. *Biomech. Model. Mechanobiol.* (2007). doi:10.1007/s10237-006-0039-9
 145. Garon, M., Légaré, A., Guardo, R., Savard, P. & Buschmann, M. D. Streaming potentials maps are spatially resolved indicators of amplitude, frequency and ionic strength dependant responses of articular cartilage to load. *J. Biomech.* (2002). doi:10.1016/S0021-9290(01)00197-X
 146. Lai, W. M., Mow, V. C., Sun, D. D. & Ateshian, G. A. On the Electric Potentials Inside a Charged Soft Hydrated Biological Tissue: Streaming Potential Versus Diffusion Potential. *J. Biomech. Eng.* (2000). doi:10.1115/1.1286316

147. Roberts, S. R., Knight, M. M., Lee, D. A. & Bader, D. L. Mechanical compression influences intracellular Ca²⁺ signaling in chondrocytes seeded in agarose constructs. *J. Appl. Physiol.* (2001). doi:10.1152/jappl.2001.90.4.1385
148. Huo, B., Lu, X. L., Costa, K. D., Xu, Q. & Guo, X. E. An ATP-dependent mechanism mediates intercellular calcium signaling in bone cell network under single cell nanoindentation. *Cell Calcium* (2010). doi:10.1016/j.ceca.2009.12.005
149. Huo, B. B., Lu, X. L. & Guo, X. E. Intercellular calcium wave propagation in linear and circuit-like bone cell networks. *Philos. Trans. R. Soc. A Math. Phys. Eng. Sci.* (2010). doi:10.1098/rsta.2009.0221
150. Phan, M. N. *et al.* Functional characterization of TRPV4 as an osmotically sensitive ion channel in porcine articular chondrocytes. *Arthritis Rheum.* **60**, 3028–3037 (2009).
151. Hurd, L. *et al.* A mutation in TRPV4 results in altered chondrocyte calcium signaling in severe metatropic dysplasia. *Am. J. Med. Genet. Part A* (2015). doi:10.1002/ajmg.a.37182
152. Kanju, P. *et al.* Small molecule dual-inhibitors of TRPV4 and TRPA1 for attenuation of inflammation and pain. *Sci. Rep.* **6**, (2016).
153. Servin-Vences, M. R., Moroni, M., Lewin, G. R. & Poole, K. Direct measurement of TRPV4 and PIEZO1 activity reveals multiple mechanotransduction pathways in chondrocytes. *Elife* (2017). doi:10.7554/eLife.21074
154. Plant, T. D. & Strotmann, R. TRPV4: A Multifunctional Nonselective Cation Channel with Complex Regulation. in *TRP Ion Channel Function in Sensory Transduction and Cellular Signaling Cascades* (2007).
155. Nilius, B., Talavera, K. & Verkhatsky, A. T-type calcium channels: The never ending story. *Cell Calcium* (2006). doi:10.1016/j.ceca.2006.04.011
156. Swärd, P., Frobell, R., Englund, M., Roos, H. & Struglics, A. Cartilage and bone markers and inflammatory cytokines are increased in synovial fluid in the acute phase of knee injury (hemarthrosis) - a cross-sectional analysis. *Osteoarthr. Cartil.* **20**, 1302–1308 (2012).
157. Irie, K., Uchiyama, E. & Iwaso, H. Intraarticular inflammatory cytokines in acute anterior cruciate ligament injured knee. *Knee* **10**, 93–96 (2003).

158. Lewis, J. S. *et al.* Genetic and cellular evidence of decreased inflammation associated with reduced incidence of posttraumatic arthritis in MRL/MpJ mice. *Arthritis Rheum.* **65**, 660–670 (2013).
159. Fan, Z., Bau, B., Yang, H., Soeder, S. & Aigner, T. Freshly isolated osteoarthritic chondrocytes are catabolically more active than normal chondrocytes, but less responsive to catabolic stimulation with interleukin-1. *Arthritis Rheum.* **52**, 136–143 (2005).
160. Towle, C. A., Han Hwa Hung, Bonassar, L. J., Treadwell, B. V. & Mangham, D. C. Detection of interleukin-1 in the cartilage of patients with osteoarthritis: A possible autocrine/paracrine role in pathogenesis. *Osteoarthr. Cartil.* **5**, 293–300 (1997).
161. Goldring, M. B. Osteoarthritis and cartilage: The role of cytokines. *Curr. Rheumatol. Rep.* **2**, 459–465 (2000).
162. Johnson, C. I., Argyle, D. J. & Clements, D. N. In vitro models for the study of osteoarthritis. *Veterinary Journal* (2016). doi:10.1016/j.tvjl.2015.07.011
163. Hoemann, C. D. Molecular and biochemical assays of cartilage components. *Methods Mol. Med.* **101**, 127–156 (2004).
164. Schneider, C. A., Rasband, W. S. & Eliceiri, K. W. NIH Image to ImageJ: 25 years of image analysis. *Nature Methods* **9**, 671–675 (2012).
165. Nover, A. B. *et al.* Long-term storage and preservation of tissue engineered articular cartilage. *J. Orthop. Res.* **34**, 141–148 (2016).
166. Lu, X. L. *et al.* Indentation determined mechano-electrochemical properties and fixed charge density of articular cartilage. *Ann. Biomed. Eng.* **32**, 370–379 (2004).
167. Chen, X., Zimmerman, B. K. & Lu, X. L. Determine the equilibrium mechanical properties of articular cartilage from the short-term indentation response. *J. Biomech.* (2015). doi:10.1016/j.jbiomech.2014.10.036
168. Ruettger, A., Neumann, S., Wiederanders, B. & Huber, R. Comparison of different methods for preparation and characterization of total RNA from cartilage samples to uncover osteoarthritis in vivo. *BMC Res. Notes* **3**, 7 (2010).
169. Hart, S. N., Therneau, T. M., Zhang, Y., Poland, G. A. & Kocher, J.-P. Calculating sample size estimates for RNA sequencing data. *J. Comput. Biol.* **20**, 970–8 (2013).

170. Gallego Romero, I., Pai, A. A., Tung, J. & Gilad, Y. RNA-seq: Impact of RNA degradation on transcript quantification. *BMC Biol.* **12**, (2014).
171. Robinson, M. D., McCarthy, D. J. & Smyth, G. K. edgeR: a Bioconductor package for differential expression analysis of digital gene expression data. *Bioinformatics* **26**, 139–40 (2010).
172. Mi, H., Muruganujan, A., Casagrande, J. T. & Thomas, P. D. Large-scale gene function analysis with the panther classification system. *Nat. Protoc.* **8**, 1551–1566 (2013).
173. Wu, G., Feng, X. & Stein, L. A human functional protein interaction network and its application to cancer data analysis. *Genome Biol* **11**, R53 (2010).
174. Luo, W. & Brouwer, C. Pathview: An R/Bioconductor package for pathway-based data integration and visualization. *Bioinformatics* **29**, 1830–1831 (2013).
175. Kanehisa, M., Furumichi, M., Tanabe, M., Sato, Y. & Morishima, K. KEGG: New perspectives on genomes, pathways, diseases and drugs. *Nucleic Acids Res.* (2017). doi:10.1093/nar/gkw1092
176. Aigner, T. *et al.* Gene expression profiling of serum- and interleukin-1 beta-stimulated primary human adult articular chondrocytes - a molecular analysis based on chondrocytes isolated from one donor. *Cytokine* **31**, 227–240 (2005).
177. Chang, J. C. *et al.* Global molecular changes in a tibial compression induced ACL rupture model of post-traumatic osteoarthritis. *J. Orthop. Res.* **35**, 474–485 (2017).
178. Carl R. Flannery, Chris B. Little Bruce, C. E. H. and C. Expression of matrix metalloproteinases (MMPs) and disintegrin metalloproteinases (ADAMs) in experimental systems of cartilage matrix degradation. *Int. J. Exp. Pathol.* **81**, 1–29 (2000).
179. Le Goff, C. *et al.* Regulation of procollagen amino-propeptide processing during mouse embryogenesis by specialization of homologous ADAMTS proteases: insights on collagen biosynthesis and dermatosparaxis. *Development* **133**, 1587–96 (2006).
180. Brandl, A. *et al.* Influence of the growth factors PDGF-BB, TGF- β 1 and bFGF on the replicative aging of human articular chondrocytes during in vitro expansion. *J. Orthop. Res.* **28**, 1002–1007 (2009).
181. Nakaseko, Y. & Yanagida, M. Cytoskeleton in the cell cycle. *Nature* **412**, 291–

- 292 (2001).
182. Bobacz, K. *et al.* Toll-like receptors and chondrocytes: The lipopolysaccharide-induced decrease in cartilage matrix synthesis is dependent on the presence of toll-like receptor 4 and antagonized by bone morphogenetic protein 7. *Arthritis Rheum.* **56**, 1880–1893 (2007).
 183. Su, S.-L., Tsai, C.-D., Lee, C.-H., Salter, D. M. & Lee, H.-S. Expression and regulation of Toll-like receptor 2 by IL-1beta and fibronectin fragments in human articular chondrocytes. *Osteoarthr. Cartil.* **13**, 879–86 (2005).
 184. James, C. G., Appleton, C. T. G., Ulici, V., Underhill, T. M. & Beier, F. Microarray analyses of gene expression during chondrocyte differentiation identifies novel regulators of hypertrophy. *Mol. Biol. Cell* **16**, 5316–33 (2005).
 185. Ramos, Y. F. M. *et al.* Genes involved in the osteoarthritis process identified through genome wide expression analysis in articular cartilage; the RAAK study. *PLoS One* **9**, (2014).
 186. Dunn, S. L. *et al.* Gene expression changes in damaged osteoarthritic cartilage identify a signature of non-chondrogenic and mechanical responses. *Osteoarthr. Cartil.* **24**, 1431–1440 (2016).
 187. Aigner, T. *et al.* Large-scale gene expression profiling reveals major pathogenetic pathways of cartilage degeneration in osteoarthritis. *Arthritis Rheum.* **54**, 3533–3544 (2006).
 188. Rodova, M. *et al.* Nfat1 regulates adult articular chondrocyte function through its age-dependent expression mediated by epigenetic histone methylation. *J. Bone Miner. Res.* **26**, 1974–86 (2011).
 189. Jia, H. *et al.* EGFR signaling is critical for maintaining the superficial layer of articular cartilage and preventing osteoarthritis initiation. *Proc. Natl. Acad. Sci.* **113**, 14360–14365 (2016).
 190. Posever, J., Phillips, F. M. & Pottenger, L. A. Effects of basic fibroblast growth factor, transforming growth factor-1, insulin-like growth factor-1, and insulin on human osteoarthritic articular cartilage explants. *J. Orthop. Res.* **13**, 832–837 (1995).
 191. Bock, H. C. *et al.* The small proteoglycans decorin and biglycan in human articular cartilage of late-stage osteoarthritis. *Osteoarthr. Cartil.* (2001). doi:10.1053/joca.2001.0420

192. Berenbaum, F. Osteoarthritis as an inflammatory disease (osteoarthritis is not osteoarthrosis!). *Osteoarthritis and Cartilage* (2013). doi:10.1016/j.joca.2012.11.012
193. Zhang, Z. Chondrons and the Pericellular Matrix of Chondrocytes. *Tissue Eng. Part B Rev.* (2015). doi:10.1089/ten.teb.2014.0286
194. Allen, J. M. *et al.* WARP is a novel multimeric component of the chondrocyte pericellular matrix that interacts with perlecan. *J. Biol. Chem.* (2006). doi:10.1074/jbc.M513746200
195. Appleton, C. T. G., James, C. G. & Beier, F. Regulator of G-protein signaling (RGS) proteins differentially control chondrocyte differentiation. *J. Cell. Physiol.* **207**, 735–745 (2006).
196. Kamiyama, M. *et al.* Contribution of Rho A and Rho kinase to platelet-derived growth factor-BB-induced proliferation of vascular smooth muscle cells. *J. Atheroscler. Thromb.* **10**, 117–23 (2003).
197. Barendse, W. *et al.* A genetic linkage map of the bovine genome. *Nat. Genet.* **6**, 227–235 (1994).
198. Anderson, D. D. *et al.* Post-traumatic osteoarthritis: Improved understanding and opportunities for early intervention. *J. Orthop. Res.* **29**, 802–809 (2011).
199. Salami, J. A. *et al.* National Trends in Statin Use and Expenditures in the US Adult Population From 2002 to 2013. *JAMA Cardiol.* **2**, 56 (2017).
200. Clockaerts, S. *et al.* Statin use is associated with reduced incidence and progression of knee osteoarthritis in the Rotterdam study. *Ann. Rheum. Dis.* (2012). doi:10.1136/annrheumdis-2011-200092
201. Valdes, A. M. *et al.* Use of statins is associated with a lower prevalence of generalised osteoarthritis. *Annals of the Rheumatic Diseases* (2014). doi:10.1136/annrheumdis-2013-204382
202. Beattie, M. S., Lane, N. E., Hung, Y.-Y. & Nevitt, M. C. Association of statin use and development and progression of hip osteoarthritis in elderly women. *J. Rheumatol.* (2005).
203. Peeters, G., Tett, S. E., Conaghan, P. G., Mishra, G. D. & Dobson, A. J. Is Statin Use Associated With New Joint-Related Symptoms, Physical Function, and Quality of Life? Results From Two Population-Based Cohorts of Women. *Arthritis Care Res. (Hoboken)*. (2015). doi:10.1002/acr.22389

204. Riddle, D. L., Moxley, G. & Dumenci, L. Associations between Statin use and changes in pain, function and structural progression: A longitudinal study of persons with knee osteoarthritis. *Ann. Rheum. Dis.* (2013). doi:10.1136/annrheumdis-2012-202159
205. Clockaerts, S., Van Osch, G. J. V. M. & Bierma-Zeinstra, S. M. Comment on ‘Associations between statin use and changes in pain, function and structural progression: a longitudinal study of persons with knee osteoarthritis’. *Ann. Rheum. Dis.* **72**, e9–e9 (2013).
206. Jain, M. K. & Ridker, P. M. Anti-inflammatory effects of statins: Clinical evidence and basic mechanisms. *Nature Reviews Drug Discovery* (2005). doi:10.1038/nrd1901
207. Bonetti, P. O., Lerman, L. O., Napoli, C. & Lerman, A. Statin effects beyond lipid lowering - Are they clinically relevant? *European Heart Journal* (2003). doi:10.1016/S0195-668X(02)00419-0
208. Riddle, D. L., Moxley, G. & Dumenci, L. Associations between Statin use and changes in pain, function and structural progression: a longitudinal study of persons with knee osteoarthritis. *Ann. Rheum. Dis.* **72**, 196–203 (2013).
209. Riddle, D. L., Moxley, G. & Dumenci, L. Response to comments in: Statin use is associated with reduced incidence and progression of knee osteoarthritis in the Rotterdam study by Clockaerts *et al.* *Ann. Rheum. Dis.* **72**, e12–e12 (2013).
210. Chun, J.-S. *et al.* The CH25H–CYP7B1–ROR α axis of cholesterol metabolism regulates osteoarthritis. *Nature* (2019). doi:10.1038/s41586-019-0920-1
211. Barter, M. J. *et al.* Lipophilic statins prevent matrix metalloproteinase-mediated cartilage collagen breakdown by inhibiting protein geranylgeranylation. *Ann. Rheum. Dis.* (2010). doi:10.1136/ard.2010.129197
212. Ridker, P. M., Rifai, N., Pfeffer, M. A., Sacks, F. & Braunwald, E. Long-term effects of pravastatin on plasma concentration of C-reactive protein. The Cholesterol and Recurrent Events (CARE) Investigators. *Circulation* (1999). doi:10.1161/01.cir.100.3.230
213. Ridker, P. M. *et al.* Measurement of C-reactive protein for the targeting of statin therapy in the primary prevention of acute coronary events. *N. Engl. J. Med.* (2001). doi:10.1056/NEJM200106283442601
214. Albert, M. A., Danielson, E., Rifai, N., Ridker, P. M. & for the PRINCE Investigators. Effect of Statin Therapy on C-Reactive Protein Levels. *JAMA*

- (2001). doi:10.1001/jama.286.1.64
215. Pella, D., Rybar, R. & Mechirova, V. Pleiotropic effects of statins. *Acta Cardiologica Sinica* (2005). doi:10.1097/FTD.0b013e31817b1a95
 216. Yamashita, A. *et al.* Statin treatment rescues FGFR3 skeletal dysplasia phenotypes. *Nature* (2014). doi:10.1038/nature13775
 217. Kobashigawa, J. A. *et al.* Effect of Pravastatin on Outcomes after Cardiac Transplantation. *N. Engl. J. Med.* (1995). doi:10.1056/NEJM199509073331003
 218. Wenke, K. *et al.* Simvastatin reduces graft vessel disease and mortality after heart transplantation: A four-year randomized trial. *Circulation* (1997). doi:10.1161/01.CIR.96.5.1398
 219. Etienne-Manneville, S. & Hall, A. Rho GTPases in cell biology. *Nature* (2002). doi:10.1038/nature01148
 220. Nishida, T. *et al.* Regeneration of defects in articular cartilage in rat knee joints by CCN2 (connective tissue growth factor). *J. Bone Miner. Res.* (2004). doi:10.1359/JBMR.040322
 221. Riento, K. & Ridley, A. J. Rocks: Multifunctional kinases in cell behaviour. *Nature Reviews Molecular Cell Biology* (2003). doi:10.1038/nrm1128
 222. Yuan, X. B. *et al.* Signalling and crosstalk of Rho GTPases in mediating axon guidance. *Nature Cell Biology* (2003). doi:10.1038/ncb895
 223. Clerk, A. *et al.* Regulation of Mitogen-Activated Protein Kinases in Cardiac Myocytes through the Small G Protein Rac1. *Mol. Cell. Biol.* **21**, 1173–1184 (2001).
 224. Hodge, R. G. & Ridley, A. J. Regulating Rho GTPases and their regulators. *Nature Reviews Molecular Cell Biology* (2016). doi:10.1038/nrm.2016.67
 225. Kadam, U. T., Blagojevic, M. & Belcher, J. Statin use and clinical osteoarthritis in the general population: a longitudinal study. *J. Gen. Intern. Med.* **28**, 943–9 (2013).
 226. Sheng, X., Murphy, M. J., Macdonald, T. M. & Wei, L. Effectiveness of statins on total cholesterol and cardiovascular disease and all-cause mortality in osteoarthritis and rheumatoid arthritis. *J. Rheumatol.* (2012). doi:10.3899/jrheum.110318
 227. Leung, B. P. *et al.* A Novel Anti-Inflammatory Role for Simvastatin in

- Inflammatory Arthritis. *J. Immunol.* (2003). doi:10.4049/jimmunol.170.3.1524
228. Funk, J. L., Chen, J., Downey, K. J. & Clark, R. A. Bone protective effect of simvastatin in experimental arthritis. *J. Rheumatol.* (2008).
229. Akasaki, Y. *et al.* Mevastatin reduces cartilage degradation in rabbit experimental osteoarthritis through inhibition of synovial inflammation. *Osteoarthr. Cartil.* **17**, 235–243 (2009).
230. Zhang, H. *et al.* Intradiscal injection of simvastatin retards progression of intervertebral disc degeneration induced by stab injury. *Arthritis Res. Ther.* (2009). doi:10.1186/ar2861
231. El-Seweidy, M. M., Ali, S. I., Elsewify, S. E., Ali, A. A. & Mashhour, M. M. Omega3 Fatty Acids Intake Versus Diclofenac in Osteoarthritis Induced in Experimental rats. *Funct. Foods Heal. Dis.* **7**, 291–302 (2017).
232. Bayyurt, S. *et al.* The chondroprotective effects of intraarticular application of statin in osteoarthritis. *Indian J. Orthop.* (2015). doi:10.4103/0019-5413.168751
233. Zhang, W. *et al.* OARSI recommendations for the management of hip and knee osteoarthritis, Part II: OARSI evidence-based, expert consensus guidelines. *Osteoarthr. Cartil.* (2008). doi:10.1016/j.joca.2007.12.013
234. Austin, P. C. An introduction to propensity score methods for reducing the effects of confounding in observational studies. *Multivariate Behav. Res.* (2011). doi:10.1080/00273171.2011.568786
235. Schoenfeld, S. R. *et al.* Statin use and mortality in rheumatoid arthritis: A general population-based cohort study. *Ann. Rheum. Dis.* (2016). doi:10.1136/annrheumdis-2015-207714
236. Dreiseitl, S. & Ohno-Machado, L. Logistic regression and artificial neural network classification models: A methodology review. *J. Biomed. Inform.* (2002). doi:10.1016/S1532-0464(03)00034-0
237. Bellamy, L., Casas, J. P., Hingorani, A. D. & Williams, D. Type 2 diabetes mellitus after gestational diabetes: a systematic review and meta-analysis. *Lancet* (2009). doi:10.1016/S0140-6736(09)60731-5
238. Olden, J. D. & Jackson, D. A. Illuminating the ‘black box’: A randomization approach for understanding variable contributions in artificial neural networks. *Ecol. Modell.* (2002). doi:10.1016/S0304-3800(02)00064-9

239. da Costa, B. R. *et al.* Effectiveness of non-steroidal anti-inflammatory drugs for the treatment of pain in knee and hip osteoarthritis: a network meta-analysis. *Lancet* (2017). doi:10.1016/S0140-6736(17)31744-0
240. Kitas, G. D. *et al.* SAT0105 Trial of Atorvastatin for the Primary Prevention of Cardiovascular Events in Patients with Rheumatoid Arthritis (TRACE RA). *Ann. Rheum. Dis.* **74**, 688.1-688 (2015).

Appendix A

PERMISSION FOR USING COPYRIGHTED MATERIALS

3D bioprinting of cartilage for orthopedic surgeons: reading between the lines

Claudia Di Bella^{1,2*}, Amanda Fosang³, Davide M. Donati⁴, Gordon G. Wallace⁵ and Peter F. M. Choong^{1,2}

¹ Department of Orthopaedic, St Vincent's Hospital, Melbourne, VIC, Australia, ² Department of Surgery, University of Melbourne, Melbourne, VIC, Australia, ³ Murdoch Childrens Research Institute, University of Melbourne, Parkville, VIC, Australia, ⁴ Unit of Orthopaedic Pathology and Osteoarticular Tissue Regeneration, Rizzoli Orthopaedic Institute, Bologna, Italy, ⁵ ARC Centre of Excellence for Electromaterials Science, AIFM Facility, Intelligent Polymer Research Institute, University of Wollongong, Wollongong, NSW, Australia

Chondral and osteochondral lesions represent one of the most challenging and frustrating scenarios for the orthopedic surgeon and for the patient. The lack of therapeutic strategies capable to reconstitute the function and structure of hyaline cartilage and to halt the progression toward osteoarthritis has brought clinicians and scientists together, to investigate the potential role of tissue engineering as a viable alternative to current treatment modalities. In particular, the role of bioprinting is emerging as an innovative technology that allows for the creation of organized 3D tissue constructs via a "layer-by-layer" deposition process. This process also has the capability to combine cells and biomaterials in an ordered and predetermined way. Here, we review the recent advances in cartilage bioprinting and we identify the current challenges and the directions for future developments in cartilage regeneration.

Keywords: bioprinting, osteochondral injuries, cartilage, additive manufacturing, tissue engineering

OPEN ACCESS

Edited by:

William Robert Walsh,
UNSW Australia, Australia

Reviewed by:

Konstantinos Markatos,
University of Athens, Greece
Angad Malhotra,
Maastricht University, Netherlands

*Correspondence:

Claudia Di Bella,
Department of Orthopaedic, St
Vincent's Hospital, Level 3 Daly Wing,
41 Victoria Pde, Fitzroy, VIC 3065,
Australia
claudia.dibella@svha.org.au

Specialty section:

This article was submitted to
Orthopedic Surgery, a section of the
journal *Frontiers in Surgery*

Received: 17 June 2015

Accepted: 31 July 2015

Published: 13 August 2015

Citation:

Di Bella C, Fosang A, Donati DM,
Wallace GG and Choong PFM (2015)
3D bioprinting of cartilage for
orthopedic surgeons: reading
between the lines.
Front. Surg. 2:39.
doi: 10.3389/fsurg.2015.00039

Introduction

Orthopedic surgeons commonly face clinical and surgical challenges for which current therapeutic strategies are not able to provide a satisfactory result. An example are young patients with large osteochondral defects due to injury or osteochondritis dissecans, which represents a difficult and frustrating clinical scenario for both the patient and the surgeon. Previous hyaline cartilage damage has been reported to predispose individuals to osteoarthritis, possibly due to the limited capacity of hyaline cartilage to repair itself (1).

The inability to halt degenerative changes in the articular surface in patients with chondral and osteochondral lesions has brought scientists, clinicians, and surgeons together to tackle the difficulties in cartilage tissue engineering. The goal of such collaboration is to produce mature hyaline cartilage that can maintain its physical and functional properties in the long term, without accelerated degeneration that may lead to arthritic changes.

Microfractures, mosaicplasty, and osteochondral allografts are the most common solutions for a young patient with an osteochondral defect. Options like membrane autologous chondrocyte implantation (MACI) and other autologous chondrocytes implantation techniques have failed to demonstrate sufficient superiority over the former techniques (2–6) leading to a loss of support from important jurisdictional advisory committees because of the large cost differential (7).

Copyright © 2015 Di Bella, Fosang, Donati, Wallace and Choong. This is an open-access article distributed under the terms of the Creative Commons Attribution License (CC BY). The use, distribution or reproduction in other forums is permitted, provided the original author(s) or licensor are credited and that the original publication in this journal is cited, in accordance with accepted academic practice. No use, distribution or reproduction is permitted which does not comply with these terms.

**BMJ PUBLISHING GROUP LTD. LICENSE
TERMS AND CONDITIONS**

Apr 19, 2019

This Agreement between University of Delaware -- Mengxi Lv ("You") and BMJ Publishing Group Ltd. ("BMJ Publishing Group Ltd.") consists of your license details and the terms and conditions provided by BMJ Publishing Group Ltd. and Copyright Clearance Center.

License Number	4572560161775
License date	Apr 19, 2019
Licensed Content Publisher	BMJ Publishing Group Ltd.
Licensed Content Publication	RMD Open: Rheumatic and Musculoskeletal Diseases
Licensed Content Title	Post-traumatic arthritis: overview on pathogenic mechanisms and role of inflammation
Licensed Content Author	Leonardo Punzi,Paola Galozzi,Roberto Luisetto,Marta Favero,Roberta Ramonda,Francesca Oliviero,Anna Scanu
Licensed Content Date	Sep 1, 2016
Licensed Content Volume	2
Licensed Content Issue	2
Type of Use	Dissertation/Thesis
Requestor type	Individual
Format	Print and electronic
Portion	Figure/table/extract
Number of figure/table/extracts	1
Description of figure/table/extracts	Figure 1
Will you be translating?	No
Circulation/distribution	1
Title of your thesis / dissertation	STATIN FOR THE PREVENTION OF OSTEOARTHRITIS – A CLINICAL COHORT STUDY AND ITS CELLULAR MECHANISMS
Expected completion date	May 2019
Estimated size(pages)	186
Requestor Location	University of Delaware 130 academy street NEWARK, DE 19716 United States Attn: Mengxi Lv
Publisher Tax ID	GB674738491
Total	0.00 USD
Terms and Conditions	

BMJ Group Terms and Conditions for Permissions

When you submit your order you are subject to the terms and conditions set out below. You will also have agreed to the Copyright Clearance Center's ("CCC") terms and conditions regarding billing and <https://s100.copyright.com/CustomerAdmin/PLF.jsp?ref=34e7584d-c907-482c-865f-86572f2d8f82>

1/4

**ELSEVIER LICENSE
TERMS AND CONDITIONS**

Apr 19, 2019

This Agreement between University of Delaware -- Mengxi Lv ("You") and Elsevier ("Elsevier") consists of your license details and the terms and conditions provided by Elsevier and Copyright Clearance Center.

License Number	4572561033263
License date	Apr 19, 2019
Licensed Content Publisher	Elsevier
Licensed Content Publication	Osteoarthritis and Cartilage
Licensed Content Title	Chondrocyte hypertrophy and osteoarthritis: role in initiation and progression of cartilage degeneration?
Licensed Content Author	P.M. van der Kraan,W.B. van den Berg
Licensed Content Date	Mar 1, 2012
Licensed Content Volume	20
Licensed Content Issue	3
Licensed Content Pages	10
Start Page	223
End Page	232
Type of Use	reuse in a thesis/dissertation
Intended publisher of new work	other
Portion	figures/tables/illustrations
Number of figures/tables/illustrations	1
Format	both print and electronic
Are you the author of this Elsevier article?	No
Will you be translating?	No
Original figure numbers	Figure 1
Title of your thesis/dissertation	STATIN FOR THE PREVENTION OF OSTEOARTHRITIS – A CLINICAL COHORT STUDY AND ITS CELLULAR MECHANISMS
Expected completion date	May 2019
Estimated size (number of pages)	186
Requestor Location	University of Delaware 130 academy street NEWARK, DE 19716 United States Attn: Mengxi Lv
Publisher Tax ID	98-0397604
Total	0.00 USD

**JOHN WILEY AND SONS LICENSE
TERMS AND CONDITIONS**

Apr 19, 2019

This Agreement between University of Delaware -- Mengxi Lv ("You") and John Wiley and Sons ("John Wiley and Sons") consists of your license details and the terms and conditions provided by John Wiley and Sons and Copyright Clearance Center.

License Number	4572620147866
License date	Apr 19, 2019
Licensed Content Publisher	John Wiley and Sons
Licensed Content Publication	Journal of Orthopaedic Research
Licensed Content Title	Calcium signaling of in situ chondrocytes in articular cartilage under compressive loading: Roles of calcium sources and cell membrane ion channels
Licensed Content Author	Mengxi Lv, Yilu Zhou, Xingyu Chen, et al
Licensed Content Date	Nov 3, 2017
Licensed Content Volume	36
Licensed Content Issue	2
Licensed Content Pages	9
Type of use	Dissertation/Thesis
Requestor type	Author of this Wiley article
Format	Print and electronic
Portion	Full article
Will you be translating?	No
Title of your thesis / dissertation	STATIN FOR THE PREVENTION OF OSTEOARTHRITIS – A CLINICAL COHORT STUDY AND ITS CELLULAR MECHANISMS
Expected completion date	May 2019
Expected size (number of pages)	186
Requestor Location	University of Delaware 130 academy street NEWARK, DE 19716 United States Attn: Mengxi Lv
Publisher Tax ID	EU826007151
Total	0.00 USD
Terms and Conditions	

TERMS AND CONDITIONS

This copyrighted material is owned by or exclusively licensed to John Wiley & Sons, Inc. or one of its group companies (each a "Wiley Company") or handled on behalf of a society with which a Wiley Company has exclusive publishing rights in relation to a particular work (collectively "WILEY"). By clicking "accept" in connection with completing this licensing transaction, you agree that the following terms and conditions apply to this transaction

SCIENTIFIC REPORTS

OPEN

Identification of Chondrocyte Genes and Signaling Pathways in Response to Acute Joint Inflammation

Received: 23 July 2018

Accepted: 21 November 2018

Published online: 14 January 2019

Mengxi Lv^{1,2}, Yilu Zhou¹, Shawn W. Polson², Leo Q. Wan³, Meiqing Wang⁴, Lin Han⁵, Liyun Wang¹ & X. Lucas Lu^{1,2}

Traumatic joint injuries often result in elevated proinflammatory cytokine (such as IL-1 β) levels in the joint cavity, which can increase the catabolic activities of chondrocytes and damage cartilage. This study investigated the early genetic responses of healthy *in situ* chondrocytes under IL-1 β attack with a focus on cell cycle and calcium signaling pathways. RNA sequencing analysis identified 2,232 significantly changed genes by IL-1 β , with 1,259 upregulated and 973 downregulated genes. Catabolic genes related to ECM degeneration were promoted by IL-1 β , consistent with our observations of matrix protein loss and mechanical property decrease during 24-day *in vitro* culture of cartilage explants. IL-1 β altered the cell cycle (108 genes) and Rho GTPases signaling (72 genes) in chondrocytes, while chondrocyte phenotypic shift was observed with histology, cell volume measurement, and MTT assay. IL-1 β inhibited the spontaneous calcium signaling in chondrocytes, a fundamental signaling event in chondrocyte metabolic activities. The expression of 24 genes from 6 calcium-signaling related pathways were changed by IL-1 β exposure. This study provided a comprehensive list of differentially expressed genes of healthy *in situ* chondrocytes in response to IL-1 β attack, which represents a useful reference to verify and guide future cartilage studies related to the acute inflammation after joint trauma.

Interleukin 1 β (IL-1 β) is an essential mediator of acute joint inflammation after traumatic injuries, one of the potential causes of post-traumatic osteoarthritis (PTOA). Within 24 hours after trauma injuries, the concentration of IL-1 β in synovial fluid can increase up to 70 times to 140 pg/mL in human^{1,2} and 7 times to 6 ng/mL in mice³. Overexpression of IL-1 β protein is also observed in chondrocytes of early osteoarthritic cartilage^{4,5}. High level of IL-1 β aggravates the catabolic activities of synovial cells and chondrocytes^{6,7} and stimulates chondrocytes to enter an abnormal phenotypic shift, such as proliferation of pre-chondrocytes, swelling of mature chondrocytes, and hypertrophic differentiation of cells in deep zone^{8,9}. Associated with these changes are the increased release of enzymes from chondrocytes, such as the MMP (matrix metalloproteinases) and ADAMTS (a disintegrin and metalloproteinase with thrombospondin motifs) families. Thus acute inflammatory attack often results in the degeneration of healthy cartilage^{7,10}.

Due to its important role in OA pathology, IL-1 β -treated articular cells or tissues have been widely adopted as *in vitro* models to study OA initiation or PTOA^{6,11}. For both isolated and *in situ* chondrocytes, IL-1 β has been observed to induce transient concentration changes of intracellular calcium ([Ca²⁺]_i) and small GTPases. The coordination of Rho GTPases signaling and [Ca²⁺]_i signaling plays a fundamental role in cytoskeleton organization, regulating the chondrocyte phenotypic shift and cartilage ECM homeostasis^{8,9}. Many of these studies focused on specific genes/pathways in chondrocytes. A systematic study to clarify the effects of IL-1 β on the entire gene expression profile and signaling transduction coordination remains lacking. In this study, we put special

¹Department of Mechanical Engineering, University of Delaware, Newark, DE, United States. ²Center for Bioinformatics and Computational Biology, University of Delaware, Newark, DE, United States. ³Department of Biomedical Engineering, Rensselaer Polytechnic Institute, Troy, NY, United States. ⁴Department of Oral Anatomy and Physiology and TMD, the Fourth Military Medical University, Xi'an, Shanxi, China. ⁵School of Biomedical Engineering, Science, and Health Systems, Drexel University, Philadelphia, PA, United States. Correspondence and requests for materials should be addressed to X.L.L. (email: xlu@udel.edu)



Open Access This article is licensed under a Creative Commons Attribution 4.0 International License, which permits use, sharing, adaptation, distribution and reproduction in any medium or format, as long as you give appropriate credit to the original author(s) and the source, provide a link to the Creative Commons license, and indicate if changes were made. The images or other third party material in this article are included in the article's Creative Commons license, unless indicated otherwise in a credit line to the material. If material is not included in the article's Creative Commons license and your intended use is not permitted by statutory regulation or exceeds the permitted use, you will need to obtain permission directly from the copyright holder. To view a copy of this license, visit <http://creativecommons.org/licenses/by/4.0/>.

© The Author(s) 2019